2019

Stimulation of PGC-1α to attenuate Duchenne muscular dystrophy disease pathology and activate autophagy

Hannah Spaulding
Iowa State University

Stimulation of PGC-1α to attenuate Duchenne muscular dystrophy disease pathology and activate autophagy

by

Hannah Rose Spaulding

A dissertation submitted to the graduate faculty

in partial fulfillment of the requirements for the degree of

DOCTOR OF PHILOSOPHY

Major: Molecular Cellular and Developmental Biology

Program of Study Committee:
Joshua Selsby, Major Professor
Elisabeth Lonergan
Jason Ross
Kenneth Stalder
Rudy Valentine

The student author, whose presentation of the scholarship herein was approved by the program of study committee, is solely responsible for the content of this dissertation. The Graduate College will ensure this dissertation is globally accessible and will not permit alterations after a degree is conferred.

Iowa State University

Ames, Iowa

2019

TABLE OF CONTENTS

ACKNOWLEDGMENTS

I would like to thank my major professor, Dr. Joshua Selsby, for his guidance, support, and endless patience. He provided the structure for me to achieve my goals and the space to grow into the person and scientist I am today. I will always cherish his mentorship. Additionally, I would like to thank my committee members, Dr. Elisabeth Lonergan, Dr. Jason Ross, Dr. Kenneth Stalder, and Dr. Rudy Valentine for their expertise and advisement throughout the course of this research.

I would also like to thank my current and former colleagues, Alex Brownstein, Olga Volodina, Shanthi Ganesan, and Melissa Roths for making my time at Iowa State University a wonderful experience. Thank you to the Keating and Ross lab groups for providing practical knowledge and endless laughs. I am especially grateful for Adrianne Kaiser-Vry for her assistance in all aspects of my life and research as well as her friendship since my first day. Thank you to my undergraduate researchers, Sydney Hill, Katerina Herzberg, Rose Robuccio, Stuart Lien, Amanda Ludwig, Kayleen Hammer, Clara Young and Megan Gard for contributing to this work and bringing liveliness to the lab.

This journey would not have been possible without the friends I gained through my experience at Iowa State University, including Bhavika Patel, Ellen Hansen, Remy Carmichael, Mackenzie Dickson, Sarah Hartman, Katie Bidne, Wesley Wierson, Lexi Rose, Kendra Clark and Najiba Mammadova. You endured mundane complaints of research and encouraged me to continue striving for greatness. Without all of you I would have succumbed to the stress of graduate school and failed to celebrate successes, both big and small.

A special thank you to Jenny (Lohmiller) Shaw for encouraging me to pursue a graduate degree and for sharing her journey with me. Further, thank you to my lifelong friend, Sarah Marti, for sticking with me the last two decades and her mother, Rebecca Marti, for fostering my love for science long before I discovered my love of biology.

Finally, I am most grateful to my family. Thank you to my parents, Scott and Lori Ann, my siblings, Megan, Christopher and Leighton, my nephews, Cooper and Carter, and brother-in-law, Matt, for their endless love and encouragement through this process. You have encouraged me to work hard in every aspect of my life and to never forget to step back and enjoy the special moments.

ABSTRACT

Duchenne muscular dystrophy (DMD) is a fatal muscle wasting disease caused by the absence of functional dystrophin protein. Dystrophin-deficiency results in numerous cellular dysfunctions and increased muscle injury leading to progressive muscle weakness and ultimately death due to cardiomyopathy or respiratory insufficiency. Overexpression of the transcriptional coactivator, PGC-1α, has been shown to provide therapeutic benefits for dystrophic muscle. In a preliminary experiment, quercetin, a nutraceutical that can drive PGC-1α through SIRT1, protected dystrophin-deficient skeletal muscle following 6 months of treatment. Therapies for DMD must demonstrate long-term efficacy, therefore in the first research chapter we evaluated the effect of 12 months of quercetin treatment on dystrophin-deficient skeletal muscle. To improve the lasting efficacy of quercetin, in the second and third research chapters we fed dystrophic mice quercetin in combination with several agents intended to potentiate or augment the effects of quercetin. We found that these quercetin-based cocktails failed to protect muscle from injury or preserve respiratory or muscle function. Collectively, these studies suggest that quercetin and these quercetin-based cocktails do not attenuate disease pathology long-term.

Stemming from our biochemical experiments from the first research chapter, we began to investigate the role of autophagy in dystrophic muscle. During autophagy a membrane is formed around protein aggregates or dysfunctional organelles, which then fuses with a lysosome for degradation. To better understand autophagy in the context of DMD and identify new therapeutic targets, in the fourth research chapter we evaluated autophagy at 7 weeks and 17 months of age in healthy and dystrophic mice. We

discovered that autophagy was impaired in dystrophic muscle. Additionally, we discovered that lysosome abundance was decreased with advanced disease and Transcription Factor EB (TFEB), a transcription factor that drives lysosome biogenesis, was partially excluded from dystrophic myonuclei. In the fifth research chapter we used an adeno-associated virus (AAV) vector to drive PGC-1α expression, which is known to increase TFEB protein abundance in healthy tissue. The data suggest that PGC-1α overexpression increased TFEB nuclear localization and subsequently lysosome abundance and autophagosome degradation.

CHAPTER 1: DISSERTATION ORGANIZATION

This dissertation begins with an introduction and a review of the literature addressing key knowledge helpful in appreciating the impact of the following research chapters. The review of the literature includes three sections. The first provides an overview of DMD. The second section discusses the use of exercise as a therapy for DMD and was recently published in *Medicine & Science in Sports & Exercise.* The third section provides an overview of autophagy signaling, autophagy within the context of DMD, and the relationship between autophagy and transcriptional coactivator, PGC-1α. The review of literature is followed by five research chapters. The first research chapter explores the effect of long-term quercetin treatment on dystrophic limb muscles, which led to the second and third research chapters evaluating the use of quercetin in combination with nutraceuticals and pharmaceuticals that have shown promise in attenuating disease pathology. The second research chapter specifically assesses limb muscle function and injury while the third research chapter evaluates respiratory and diaphragm function and muscle injury. During the course of my work we began to suspect that dysfunctional autophagy played a role in diseased pathology. In the fourth research chapter we investigated the effect of disease progression on autophagy in dystrophin deficient skeletal muscle. This led to a fifth research chapter evaluating the effect of PGC-1α overexpression on transcription factor EB nuclear localization, lysosome abundance and autophagic degradation in dystrophic skeletal muscle. The final research chapter is followed by a general discussion of these data as a whole and comments about future directions of this work.

CHAPTER 2: GENERAL INTRODUCTION

Duchenne Muscular Dystrophy

Duchenne muscular dystrophy (DMD) is an X-linked, progressive muscle wasting disease affecting 1:3500-5000 boys (124). DMD is characterized by the absence of functional dystrophin protein due to mutations in the dystrophin gene. It is estimated that about 20% of disease-causing mutations are small mutations (smaller than 1 exon) resulting in small deletions, insertions, missense mutations, and nonsense mutations, and the remaining 80% are large mutations (1 exon or larger), of which 86% are deletions and 14% are duplications (23). Ultimately, these mutations disrupt the reading frame and prevent translation of full-length dystrophin protein. Dystrophin is a vital structural protein and the anchor of the dystroglycoprotein (DGC) complex, which connects the cytoskeleton to the extracellular matrix through the sarcolemma (65, 153). The DGC is composed of a variety of extracellular, cytoplasmic and transmembrane proteins including dystrophin, sarcoglycans, dystroglycans, sacrospan, dystrobrevin, laminin (79). Together these proteins function to tether dystrophin to the sarcolemma, provide structure to the sarcolemma, participate in force transmission, and act as a platform for signaling.

Dystrophin is a 427 kDa protein composed of four distinct domains including an actin-binding domain (ABD1), a central rod-like domain, a cysteine-rich domain, and a carboxyl terminal domain (77, 112). The ABD1 has 2 calponin homolog domains, which facilitate the binding of dystrophin directly to F-actin (208). ABD1 also interacts with cytokeratin 19, an abundant intermediate filament protein, to attach dystrophin to the costamere and ultimately the contractile apparatus of muscle, the sarcomere (194). The central rod-like domain also has an actin-binding motif (ABD2), which allows for lateral

association of dystrophin with actin filaments (77, 168). As the name describes, the central rod-like domain is made up of 24 spectrin-like repeats, which fold together as a triple α-helix into a rod shape (30, 112). This region provides structure along with increased actin binding, microtubule binding, and microtubule organization (18, 156). Within the central rod-like domain there are four "hinges" which are proline-rich spacers that provide elasticity to the dystrophin protein (1, 111). Additionally, α-syntrophin interacts with dystrophin at spectrin-like repeat 16/17 to facilitate nNOS signaling (1).

The cysteine-rich domain and first portion of the C-terminal domain of dystrophin binds β-dystrogylcan (64, 77). β-dystrogylcan is a single-pass transmembrane protein that is glycosylated and binds α-dystroglycan to anchor α-dystroglycan to the exterior of the sarcolemma. Glycosylation of α-dystroglycan is required for this binding of laminin to α-dystroglycan (64), and other extracellular matrix ligands, such as perlecan and agrin. Additionally, β-dystrogylcan interacts with the sarcoglycan complex, which is made up of four subunits: α, β, γ and δ. The sarcoglycan complex facilitates stabilization of β-dystrogylcan at the sarcolemma (96, 134). Interestingly, the mutation of even one of these four sarcoglycan subunits prevents the proper formation and localization of the sarcoglycan proteins to the (126) membrane, which is known to cause limb girdle muscular dystrophy (96). The sarcoglycans are glycosylated transmembrane proteins that bind sarcospan, a transmembrane protein that interacts with multiple sarcoglycan subunits (48), generating a subcomplex. Sarcospan interacts with not only β-dystrogylcan, but also binds integrins to further stabilize the sarcolemma (126).

On the cytosolic face of the dystroglycoprotein complex, dystrophin binds directly to syntrophin and α-dystrobrevin (171). To assist in muscle stability, α-

dystrobrevin binds to intermediate filaments and works together with syntrophin and dystrophin to localize nNOS at the DGC (141). Syntrophin further acts a signaling platform for proteins involved in signaling transduction, ion transport and calcium homeostasis (46, 141).

Boys are typically diagnosed with DMD between 2-5 years of age due to delayed time to walking, waddling gait, struggling to stand (Gower's movement), and other missed movement milestones (62, 196). Typically, boys are treated with glucocorticoids, prednisone and more recently, deflazacort (182), to preserve muscle function, prolong ambulation, and decrease inflammation (17). As muscle weakness progresses, boys will first rely on assisted walking and eventually lose ambulation resulting in part-time and then full-time wheelchair assistance. Ultimately their respiratory muscles will weaken and require respiratory support. Due to the progress in respiratory care, the natural history of the disease has evolved to include more frequent mortality due to cardiomyopathy making therapies to protect the heart important for consideration (61). Commonly, once left ventricle ejection fraction falls to less than 55% patients are started on angiotensin converting enzyme inhibitors (ACEi), such as Lisinopril, to delay cardiomyopathy (155).

As a multifaceted disease, DMD disease pathology does not only affect muscle function and injury, but a variety of physiological systems and can have psychological impacts. As muscle wasting progresses, muscle injury accumulates resulting in degradation of muscle fibers and subsequent infiltration of adipose tissue and fibrotic tissue (164). Increased fibrosis and adipose combined with reduced mobility can lead to an increased risk of obesity, hyperinsulinemia and insulin resistance (165, 175). As muscle continues to deteriorate, joint contractures resulting in further reduced mobility

and decreased ability to perform daily tasks (187). Similarly, patients also experience anxiety and depression due, at least in part, to stress from social and physical hardship endured throughout disease progression (170). Lastly, muscle wasting, chronic inflammation and immobility further contribute to reduced bone density in patients with DMD leading to bone fractures and immobility (32).

Mouse Models

Duchenne muscular dystrophy is most often modeled by the mdx mouse. The mdx mouse has been used for decades to investigate fundamental dysfunctions of dystrophic muscle and evaluate potential therapies for DMD (183). The mdx mouse is on the C57BL/10 (B10) mouse background and has an exon 23 point mutation (C-T) within the dystrophin gene resulting in a nonsense mutation (186, 93). The mdx mouse was discovered in the 1984 due to increased creatine kinase, a marker of muscle damage, and histological lesions similar to those found in muscular dystrophies (33).

At 2-weeks of age mdx mice are indistinguishable from their healthy controls, but by 3-8 weeks mdx muscle undergoes an intense bout of necrosis followed by remarkable regeneration (132). The only muscle to escape this pathology is the diaphragm, which displays progressive muscle injury and weakness similar to DMD patients (193). These mdx mice also experience limb muscle weakness. By 28 weeks of age, forelimb grip strength is reduced 25% (45). At 12-14 months of age, solus, extensor digitorum longus, and diaphragm *in vitro* specific force decreased by 18-40% and EDL fatigue resistance fell to less than 50% of healthy control (122, 190). At this same time point, respiratory function measured by whole body plethysmography was also largely decreased (180).

Though mdx mice have been an invaluable model to investigate DMD, many argue that the phenotype of mdx limb muscles and the heart are too mild. For example, cardiac dysfunction and the onset of scoliosis are delayed relative to human disease and mice live a nearly normal lifespan compared to the profound reduction in human disease (41, 116). To increase disease severity in a mouse model, the mdx mutation was bred onto a variety of genetic backgrounds. Ultimately, it was discovered that when introgressed into the DBA/2J background, the exon 23 mutation caused an earlier onset of disease and a more severe phenotype compared to the C57 line (45). Fibrosis and inflammation are increased in D2-mdx (D2.B10-Dmd^{mdx}/J) compared to DBA controls and increased compared to traditional mdx mice due to a 12-amino acid deletion in the latent TGF-β-binding protein gene 4 (Ltbp4) (45, 74). DMD patients also have increased fibrosis and a relationship is emerging between mutations in the Ltbp4 gene and time to loss of ambulation such that the Ltbp4 gene mutation accelerates loss of ambulation (69). Additionally, when dystrophic DBA mice were compared to mdx, Evan's blue dye uptake, a marker of membrane instability, was further increased 30% at 8 weeks of age suggestive of increased muscle fiber damage in the D2-mdx model (45). When ejection fraction was directly compared between D2-mdx and age-matched mdx mice, ejection fraction was decreased 10% and shortening fraction was reduced by 7% as early as 28 weeks of age suggestive of an early onset of cardiac dysfunction (45). Further, signs of cardiomyopathy were already present at 7 weeks in D2-mdx hearts compared to mdx and DBA demonstrated by histopathological changes (45).

Exercise as a therapy for DMD

Exercise may be able to counter some DMD-associated effects, such as muscle weakness, kyphosis, obesity, and depression (24, 50). In healthy muscle, exercise elevated a transcriptional coactivator, peroxisome proliferator-activated receptor-gamma coactivator (PGC-1α), able to promote mitochondrial biogenesis and utrophin abundance, a protein able to compensate for the absence of dystrophin (145, 172). Indeed, increased PGC-1α, mitochondrial biogenesis, and utrophin have all been shown to decrease dystrophin pathology (89, 94, 181, 202, 203). DMD patients also develop kyphosis and endure vertebral and leg fractures (131). In non-DMD patients, exercise increased bone density (24), which may prevent fractures that coincide with premature loss of ambulation in DMD patients (131). The following review was undertaken to compile the current literature evaluating exercise as a treatment for DMD and assess the effect of exercise intensity, modality and duration on functional outcome in dystrophic muscle.

Is Exercise the Right Medicine for Dystrophic Muscle?

Hannah R. Spaulding and Joshua T. Selsby

Department of Animal Science, Iowa State University, Ames, IA 50011

Modified from a review published in

Medicine & Science in Sports & Exercise, September 2018 Volume 50, Issue 9, pages 1723-1732.

Abstract

Introduction: Duchenne muscular dystrophy (DMD) is a neuromuscular disease caused by a dystrophin protein deficiency. Dystrophin functions to stabilize and protect the muscle fiber during muscle contraction, thus the absence of functional dystrophin protein leads to muscle injury. DMD patients experience progressive muscle necrosis, loss of function, and ultimately succumb to respiratory failure or cardiomyopathy. Exercise is known to improve muscle health and strength in healthy individuals as well as positively impact other systems. Because of this, exercise has been investigated as a potential therapeutic approach for DMD. Methods: This review aims to provide a concise presentation of the exercise literature with a focus on dystrophin deficient muscle. Our intent was to identify trends and gaps in knowledge with an appreciation of exercise modality. Results: After compiling data from mouse and human studies it became apparent that endurance exercises such as a swimming and voluntary wheel running have therapeutic potential in limb muscles of mice and respiratory training was beneficial in

humans. However, in the comparatively few long-term investigations the effect of low intensity training on cardiac and respiratory muscles was contradictory. In addition, the effect of exercise on other systems is largely unknown. Conclusion: In order to safely prescribe exercise as a therapy to DMD patients, multi-systemic investigations are needed including the evaluation of respiratory and cardiac muscle.

Key words: mdx, DMD, dystrophin, running, swimming

Introduction

Duchenne muscular dystrophy (DMD) affects one in every 5,000 boys (124) and is caused by a deficiency of the protein, dystrophin. It is a muscle wasting disease that leads to impaired mobility, wheel chair confinement, and ultimately patients succumb to respiratory or cardiac failure. Diagnoses of DMD typically occur around 4-5 years of age, driven largely by parental concerns about missed or delayed achievement of developmental milestones, frequent falls, and in some instances a distinct gait. Dystrophin is a 2.3 Mb gene with 79 exons that is translated into a 427 kDa protein (2). Mutations to the dystrophin gene resulting in a frame shift or nonsense mutation cause a deficiency of functional dystrophin protein. Dystrophin acts as the anchor for the dystrophin-glycoprotein complex, functions in related signaling, and serves a critical role in membrane stability during muscle contraction and eccentric contractions, in particular. In the absence of dystrophin, muscle cells are sensitive to eccentric injury resulting in physical disruption of the sarcolemma, loss of Ca^{2+} homeostasis, increased proteolysis, free radical injury, and widespread cellular dysfunction, among other maladies (3, 82, 138, 177). DMD is most commonly modeled by the mdx mouse which has a nonsense

mutation in exon 23. On the whole, the disease phenotype is relatively mild with only slight reductions in longevity (41) and impaired cardiac function only apparent after approximately 8 months (158, 218) likely due to increased utrophin protein abundance (128), increased capacity for repair (26), and differences in locomotion (99). Limb muscles experience an acute necrotic bout from approximately 3-8 weeks of age followed by relative stability before declining again following 12 months of age (166). The diaphragm undergoes a progressive disease and most accurately recapitulates many aspects of disease progression including impaired function, fibrosis, and necrosis, among others (193).

The absence of functional dystrophin not only affects skeletal and cardiac muscle cells, but also the skeletal, endocrine, and central nervous systems (36). Kyphosis, due in part to osteoporosis, is prevalent in DMD patients. Indeed, vertebral and leg fractures are common in DMD patients and resultant immobilization from leg fractures can lead to permanent loss of ambulation (131). The use of glucocorticoids, which is the standard of care for DMD patients, may exacerbate bone loss and contribute to fractures directly and indirectly, and it prolongs ambulation, which increases the opportunity for fractures due to falls (107). DMD patients tend to be obese with excess weight gain beginning early in disease progression due to decreased mobility and weight gain is further driven by increased appetite with steroid treatments (50). Obesity and increased weight gain result in increased rate of hyperinsulinemia and insulin resistance leading to increased occurrence of type 2 diabetes and cardiovascular disease for DMD patients (165). In addition, and perhaps due, at least in part, to these physical effects, DMD patients suffer increased risk of depression and anxiety (189). Importantly, in healthy populations

exercise has been widely shown to counter many of these DMD-associated effects. At the very core of endurance training is increased cardiorespiratory function while overload training increases hypertrophy serving to combat two significant problems encountered by DMD patients. In addition, exercise has been shown to decrease the severity of depression, maintain bone density, and increase overall muscle health, among other benefits (24). Thus, exercise would appear to be a well-suited intervention for DMD patients. Indeed, exercise serves as the basis of physical therapy and utilizes multiple exercise modalities to maintain muscle flexibility and health in DMD patients.

As a premise of this review it is assumed that patients are receiving appropriate nutritional support and effective physical therapy. This review will focus on exercise beyond that what is generally performed during physical therapy. The role of exercise on DMD has been previously reviewed, i.e. Gianola et al. (80), Grange et al. (85) and Markert et al. (125), though in many of these previous studies exercise was broadly considered. Here, we will independently explore exercise modality and consider independent muscle groups, with a particular focus on functional and histological outcomes, with the intention that this more refined approach will allow us to better identify emerging patterns of exercise benefits for dystrophic muscle.

Endurance Exercise

Researchers have investigated the effects of a variety of exercise modalities in mouse and human studies. The breadth of exercise regimens, measures, durations, and disease states makes comparisons between these investigations difficult. To better elucidate the effects of low intensity exercise in dystrophic muscle, data were collected from studies using swimming, voluntary wheel running, and treadmill running

interventions (Figure 1). To visualize these data we plotted exercise modality, age of intervention initiation, duration of treatment, and effect of exercise on a single set of axes. The effect of exercise on a dependent variable was estimated from published investigations in order to calculate a percent change caused by exercise compared to sedentary dystrophic controls. In this manner, values less than 100% indicate a detrimental effect of exercise while values larger than 100% indicate a dependent variable was improved with exercise. To appropriately report and plot measurements such as fibrosis, necrosis and creatine kinase (CK) activity, in which an increase indicates a negative effect, an inverse calculation was used to appropriately place these data on the figures. Hind limb muscles were divided into two categories defined as anterior [i.e.. tibialis anterior (TA) and extensor digitorum longus (EDL)] and posterior compartments [i.e.. gastrocnemius (GAST), soleus, and plantaris]. In total, the literature provides contradictory information regarding the impact of exercise on disease severity (Figure 1). Duration, intensity and modality of exercise complicate interpretation of data supporting the use of or contraindication of exercise as an intervention for DMD patients. To better identify the effect of exercise modality on disease severity the effects of voluntary wheel running, swimming and treadmill/rota-rod exercises were considered in more depth.

Voluntary wheel running. In the investigations considered, voluntary wheel running maintained or positively affected all measures of relative tension and fatigue resistance in muscles of the forelimb and in anterior and posterior compartments of the hind limb in dystrophic mice regardless of age and duration of wheel running (Figure 2). Forelimb strength increased by over 25% after four weeks of exercise starting at 12 weeks of age (37). Fatigue resistance of the EDL *in vitro* and TA *in situ* was improved

by 45% and 48% after sixteen and eighteen weeks of exercise, respectively, starting at 4 weeks of age (92, 98). In addition, relative tension in the EDL improved while other measures of EDL function were preserved (38) and maximum torque in the plantarflexor muscles were increased with voluntary wheel running (13). Similarly, EDL fatigability decreased by 65% following forty-eight weeks of exercise started at 24-week-old mice (211). Following nine weeks of exercise 12-week old mice maintained soleus function and fatigue resistance was significantly increased (59). Relative tension and specific eccentric force of the soleus in 16-week-old mice also increased 25% following twelve weeks of exercise and tetanic force was increased 45% after sixteen weeks of exercise, while other measures of soleus and EDL function were maintained (37, 92). Following one year of voluntary wheel running EDL relative tension and soleus function, such as relative tension, fatigue resistance and half relaxation time were maintained compared to unexercised controls (59, 60, 178). While these data seem to provide compelling evidence supporting the use of exercise to maintain limb muscle health conflicting results were reported in the diaphragm (Figure 2). In three independent studies 3 to 4-week-old mice ran on a wheel for one year. In one investigation diaphragm relative tension was impaired by nearly 3-fold (178), however, a 30% increase in active tension, a 14% increase in fatigue resistance, and preservation of a variety of respiratory function and fatigue measures were reported in the other investigations (59, 60). In a shorter experiment, mice exercised for nine weeks starting at 3 weeks of age had increased diaphragm contraction time, while maintaining other measures of diaphragm function (59). The effect of voluntary wheel running on cardiac function is also unclear (Figure 2). After just four weeks of exercise, 11-week-old mice had over 25% thinning of the

left ventricle wall thickness and increased left ventricle dilation similar to dystrophin-related cardiomyopathy (47). In one investigation left ventricle ejection fraction decreased by 30% after fourteen weeks of exercise (98), but in another, after one year of exercise left ventricle ejection fraction was similar between sedentary and exercised mice while cardiac output was increased 2-fold and stroke volume increased by 80% with exercise training (178).

Integrity of the skeletal system is also compromised in DMD patients both as a function of dystrophin deficiency and common use of glucocorticoids. Kyphosis is a spinal deformity that is a hallmark of dystrophin deficiency and a negatively impacts respiratory function (114). Brereton et al. (29) indicated that after one month of voluntary wheel running kyphosis increased by 25% in 4-month-old mice. In addition to increased kyphosis, and perhaps contributing to it, fibrosis of the erector spinae increased by 40% (29). Kyphosis and injury to the erector spinae is not routinely reported in the dystrophic literature making comparisons difficult. Notably, these findings are in contrast to the bulk of data that show younger mice after a similar duration of exercise and 4-month-old mice following a longer duration of exercise have improved limb muscle function (13, 37, 38) However, given its function, the erector spinae may experience increased, damaging stress during exercise.

Swimming. Swimming interventions were beneficial for most skeletal muscles in mdx mice (Figure 3). Forelimb strength increased by 30% at 8 weeks of age following four weeks of exercise training (100). Similarly, EDL half relaxation time decreased in 20-week-old mice after fifteen weeks of swimming, indicating improved Ca^{2+} sequestration, fatigability decreased by over 20% in EDL, and EDL relative tension was

sustained (90). In addition, soleus half relaxation time was maintained and relative tension increased by 60% following fifteen weeks of swimming (90). In older animals, eight weeks of exercise begun at 44 weeks of age increased relative tension in the soleus and EDL and sustained half relaxation time suggesting improved limb muscle health with exercise in aged animals (91). Importantly, however, cardiac and respiratory muscle had increased fibrosis in exercised mdx mice compared to sedentary mdx mice after ten weeks of swimming in 19-week-old mice (Figure 3). In addition, inflammation was increased 2-fold as was the heart wall to lumen ratio (16).

The intensity of exercise in these studies and how this may affect interpretation of findings above make the impact of swimming unclear. Playing in a swimming pool is a low intensity exercise recommended by physical therapists for a variety of muscle dysfunctions including DMD. It is likely that the intensity of exercise, as a percent VO2max, in mice from these studies greatly exceeded that of DMD patients playing in a pool.

Forced running. Unlike voluntary wheel running, treadmill and rota-rod running are forced exercises that generally led to increased muscle damage and impaired function (Figure 4). Following four weeks of training 8-week-old mice had a 20-50% reduction in forelimb strength (34, 35, 39, 53, 54), increased plasma CK activity, increased fibrosis in the quadriceps and heart, and increased oxidative stress in the quadriceps and abdominal muscles (35, 88, 176). In the TA the abundance of necrotic muscle cells and inflammatory cells increased 2-fold, further supporting increased damage and decreased muscle function with treadmill training (54). Interestingly, damage and muscle regeneration were similar in TA, gastrocnemius and diaphragm muscles following four

weeks of treadmill running compared to unexercised controls. Also, diaphragm relative tension was maintained (35). Animals that began training at 8 weeks of age also had reduced forelimb strength after four weeks of training (159) and decreased force production in the gastrocnemius after twenty-four weeks (137). Twelve weeks of training starting at 12 weeks of age decreased tetanic force and increased fibrosis 2-fold in the gastrocnemius (152). Similarly, following six weeks of rota-rod training, forelimbs fatigue was similar between exercised and sedentary age-matched controls, but the gastrocnemius and quadriceps of 14-week-old mdx mice had over 2-fold more necrosis than sedentary age-matched controls (72), further supporting increased muscle damage and decreased muscle function caused by forced training. In some contrast, training for ten weeks starting at 10 weeks of age decreased soleus and gastrocnemius necrosis by over 40%, but, consistent with previous findings, dramatically increased plantaris necrosis (216). The authors suggest (216) the degree of fiber loss may be related to the increased contractile activity, though it seems likely the increased relative activity of the plantaris in combination with the fast fiber type is accountable for increased plantaris necrosis while the soleus and gastrocnemius are protected. Finally, following four weeks of treadmill training, oxidative stress was increased in quadriceps and abdominal muscles, but not the heart (176). In the same animals, fibrosis was increased in the heart and quadriceps, but the abdominal muscles were protected.

In most studies mice were forced to run for 30 min at 12 m/min (360 m/day) 2-3 times/wk, and in one investigation mice ran at 9 m/min for 60 min, 5 times/wk. By comparison, with volitional wheel running young mdx mice ran an estimated peak of 14 km/day (100 km/wk), 28-week-old mice ran nearly 3 km/day (20 km/wk), and 52-week-

old mice ran approximately 2 km/day (14 km/wk) (178). The role of distance (daily or weekly) is unclear, though data suggest that these shorter, forced bouts with treadmill running are not as efficacious as larger daily running volumes seen during wheel running. This interpretation is complicated, however, by the intermittent nature of mouse wheel running, which has typical bouts of 1-10 minutes in mdx mice (188).

Downhill running. Downhill running has been used as a method for deliberate induction of contraction-induced injury in dystrophic muscle (31, 127). Our analysis of these investigations strongly supports this conclusion (Figure 5). For example, after only three days of downhill running, there was a 40% increase in damage to the biceps brachii, triceps brachii, soleus, gastrocnemius and diaphragm in 2-month-old mice (31). Interestingly, damage was not increased in the TA or EDL (31). Following seven weeks of training, fibrosis increased 3-fold in the TA of 31-week-old mice. In addition, plasma CK activity and fibrosis of the biceps increased over 2-fold, further supporting increased damage (200). Forelimb strength also decreased by 15% in these same animals (200). Fibrosis of the diaphragm and heart following two weeks of downhill running were similar to sedentary controls (200), but after ten weeks of downhill running dystrophic lesions increased in the heart by 3-fold with a 17% increase in heart mass (142). The only improvement was the soleus in which twitch tension increased 50% after three weeks of downhill running, though half relaxation time increased (70).

Human studies

Conservative exercise protocols have been investigated in the context of both ambulatory and non-ambulatory DMD patients. Despite the advent of mechanical respiratory support, respiratory failure remains a significant cause of death in DMD

patients. Given this, inspiratory and expiratory muscle training as well as resistive training protocols have been utilized in ambulatory patients. Generally, these interventions increased respiratory endurance by 46% with training after six weeks (204) and increased respiratory pressure and markers of respiratory strength after twenty-four, thirty-six, forty and ninety-six weeks of training (84, 113, 163, 212) (Figure 6). In non-ambulatory patients, six and a half weeks of respiratory exercise increased vital capacity and airway pressure over 70% making clear that non-ambulatory patients can respond favorably to a therapeutic intervention (4).

In addition to respiratory function, range of motion and ability to complete tasks of daily living are important to the quality of life of DMD patients. To identify exercise protocols to prolong independence, non-ambulatory patients were provided jaw stretching and strengthening interventions (104, 146). Collectively, Nozaki et al (146) and Kawazoe et al. (104) discovered that masticatory performance and occlusal force and the degree of mouth opening were improved following twenty-four weeks of jaw exercises. In ambulatory patients, training by an assisted cycle or arm ergometer resulted in increased or maintained endurance and range of motion in targeted muscles (5, 102). These data suggest that stretching and exercise increased range of motion and maintain strength of skeletal muscles. However, given the concerning respiratory and cardiac data presented above more information regarding the interplay between limb muscle exercise and impact on respiratory and cardiac function is necessary.

Acute Exercise

Performance of activities of daily living in DMD patients requires consideration of acute bouts of exercise. This seems particularly urgent considering few patients are

part of regular exercise training regimens and regular play, not to mention occasional, high intensity activities, such as the violent forces experienced on inflatable playground equipment (i.e. a bouncy castle or the like), could certainly be considered an acute exercise bout. Indeed, activities like this can lead to agonizing decisions as competing parental roles are in conflict. Despite its importance, the literature does not provide fertile ground or necessary nuance for a rich discussion of acute exercise and we recognize this as an important gap in the literature. Nevertheless, summation of limited available evidence points to increased susceptibility to acute injury in dystrophic muscle.

In mdx mice, less than 30 min of swimming appeared damaging, despite being a non-weight bearing activity, as the number of damaged fibers in the TA were increased by up to 5-fold (28). Further, Evan's blue dye penetration into dystrophic muscle was dramatically elevated compared to healthy following a single 20 min swimming bout (206). Of interest, in this investigation fibers expressing a microdystrophin construct were also resistant to swimming-induced injury, while fibers from within the same section lacking microdystrophin expression had robust penetration of Evan's blue dye (206). These sections are particularly important as they clearly demonstrate increased damage in dystrophin-deficient muscle compared to dystrophin-expressing muscle when subjected to the same acute exercise bout. In addition, a single bout of treadmill running increased serum CK activity 7-fold (201) while in healthy mice only a 2 to 3-fold change might be expected following either treadmill running or even eccentric exercises (15, 110). In the quadriceps, necrosis was increased over 2-fold following 30 min of treadmill running (201), and in the EDL force was decreased 2.5-fold and membrane permeability was increased following 45 minutes of downhill running in mdx mice (209). While

direct comparison to injury in healthy muscle is rare, our expectation, based on the sensitivity of dystrophic muscle to contraction-induced injury, demonstrated elevations in serum CK activity, and increased Evan's blue dye penetration, is that this degree of damage in dystrophic muscle surpasses that anticipated in healthy muscle following performance of the same activity. To that point, and while not a single acute running bout, 3-days of downhill running increased membrane permeability in dystrophic limb muscle by 10% while in healthy muscle no permeability was noted (31). Lastly, when mdx mice ran voluntarily for twenty-four hours, damaged fibers in the gastrocnemius were increased 18% and 6-fold in the TA and quadriceps (8). This later study is of note as long-term volitional wheel running generally improved outcomes while shorter treadmill bouts exacerbated markers of injury. Collectively, these data suggest that dystrophic skeletal muscle is capable of exercise-mediated adaptations despite increased damage early in a training regimen (i.e. acute exercise) though the degree to which it may be trained and how closely the training response of dystrophic muscle follows that of healthy muscle is unclear.

Importantly, and consistent with the animal literature, acute or single bouts of exercise result in increased serum CK activity in DMD patients (154). While certainly increased serum CK activity can occur as a result of exercise in healthy patients the effect, and thus presumptive underlying muscle injury, is greater in DMD patients following similar activities. For example, eight hours after a 15 minute bout of physical therapy in the water, serum CK activity increased nearly 1,000 U/l from baseline in DMD patients compared to an increase of less than 10 U/l in healthy subjects (154). Supporting this notion of increased susceptibility to acute injury, circulating myoglobin increased

1,114.8 ng/ml from baseline in DMD patients but only 46.2 ng/ml in healthy controls eight hours post-exercise (154).

While dystrophic muscle appears capable of exercise-mediated adaptations under the right training conditions (13, 37, 38, 59, 91, 92, 211), it is associated with increased injury following acute exercise, which may suppress exercise-mediated adaptations compared to healthy. Further, despite these data seeming to make clear an acute bout of exercise is more damaging to dystrophic muscle compared to healthy muscle we cannot rule out the possibility that because DMD patients ostensibly have a lower VO2max than healthy controls, DMD patients or dystrophic muscle was operating at a higher relative workload and therefore, may be expected to have a greater degree of muscle injury. Moreover, as injury following acute exercise may be necessary for adaptation in healthy muscle, we cannot rule out the possibility that increased damage following acute exercise is necessary for a training adaptation in dystrophic muscle, though the degree to which disease and disease-related injury may alter this process, either directly or indirectly, is unknown.

Exercise mimetics

Exercise has the potential to provide a robust therapeutic effect to dystrophic muscle, however, the forces produced during exercise and its multi-systemic involvement make its use tenuous. To harness the effects of exercise without associated complications several groups have used pharmaceutical and nutraceutical approaches to mimic the effects of exercise. For example, myostatin inhibition has repeatedly resulted in increased muscle mass and function in a dystrophic muscle (25, 87), which ostensibly would translate into improved tasks of daily living. Indeed, several clinical trials are

currently making use of myostatin inhibition as a therapy for muscular dystrophy (NCT02310763, NCT02515669, NCT02907619), however the impact on cardiac function will need to be carefully monitored. In addition, induction of oxidative metabolism and the oxidative muscle phenotype has been successfully accomplished using the AMPK-activator, AICAR (121, 151), and activation of mitochondrial biogenesis pathways has been attempted via PGC-1α over-expression and gene transfer (82, 89, 181) and supplementation with resveratrol and quercetin (12, 95, 119, 179, 190). While generally further testing is needed, including long-term investigations and clinical trials, these approaches have the promise to afford DMD patients with some benefits of exercise while minimizing risk.

Conclusion

When considering exercise as a therapy for DMD patients it is essential to consider the totality of effects on patients and particularly to vital muscles. Duchenne muscular dystrophy patients typically succumb to respiratory or cardiac failure, thus exercises that protect or improve limb muscle function while impairing respiratory or cardiac function provide little benefit to the patient. In mouse studies, swimming generally improved limb muscle function, but caused histopathological damage in cardiac and respiratory muscles, suggesting that caution should be used when considering swimming as an exercise for DMD patients until the role of exercise intensity is made clearer. Similarly, voluntary wheel running provided contradictory information regarding the impact on cardiac and respiratory function, though was consistently beneficial to limb muscles. The multi-systemic nature of DMD and the impacts of exercise on these systems are also of interest for DMD patients. Increased kyphosis (29) paired with

conflicting diaphragm (59, 178) and heart function data in mice (47, 98, 178) brings to light the need to further investigate and balance the benefits of exercise while minimizing detrimental side effects. Concurrent investigation of respiratory and cardiac function as well as other systems are necessary to effectively prescribe exercise as a therapy for DMD.

Conflict of Interest and Source of Funding

The authors have no conflicts of interest. Partial support for HRS provided by Project Parent Muscular Dystrophy (PPMD), Ryan's Quest and Michael's Cause.

Figures

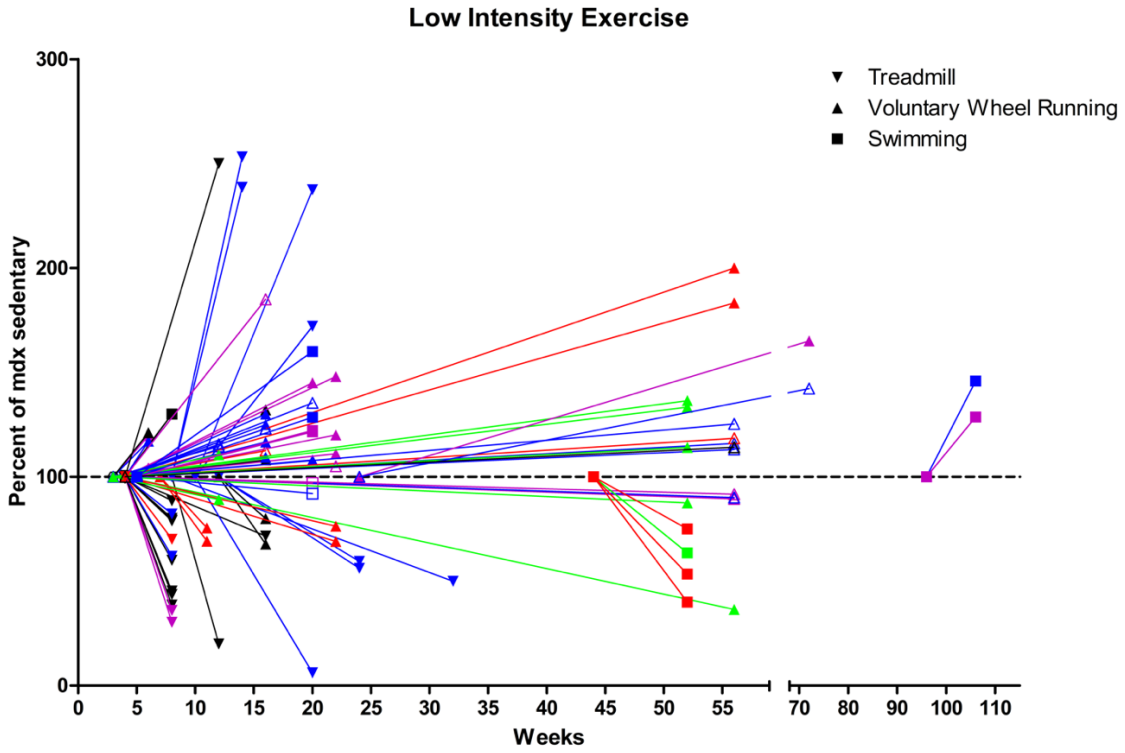

Figure 1. Effect of low intensity exercise on health outcomes in dystrophic mice. Low intensity exercise provides both beneficial and detrimental health outcomes. The breadth of initiation age, duration, and modality complicate an appreciation for the effects of exercise on disease severity. Data were obtained from the literature and the effect of exercise normalized to sedentary mdx mice. Additional statistical analyses were not performed. For any given variable age of initiation is shown at 100% (Y-axis) and the deviation from 100% and the duration of the intervention can be determined. The figure is constructed such that beneficial changes are above 100% and detrimental changes are below 100%, including those where an elevation would indicate increased pathology. Nonsignificant data were omitted from the figure but can be found in the supplementary file. Data point shapes represent activities as indicated. Colors represent muscles as follows: black = whole body, gray = forelimb, purple = anterior hind limb, blue = posterior hind limb, red = heart, and green = diaphragm

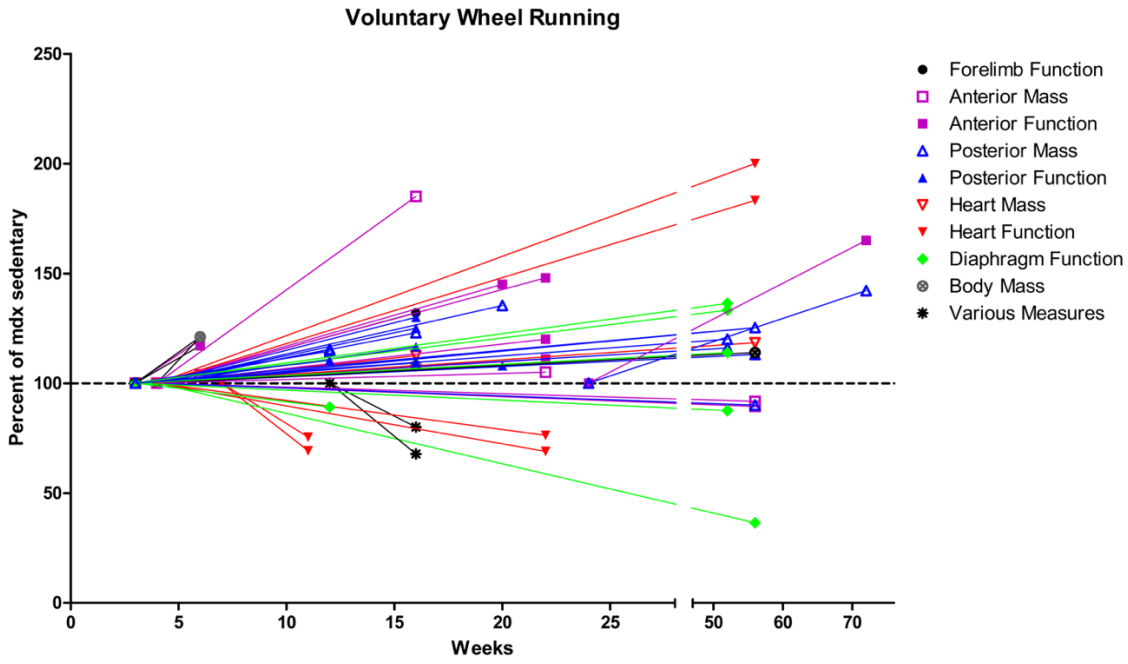

Figure 2. Effect of voluntary wheel running on health outcomes in mdx mice. All measures of hind limb muscle function were maintained or improved by voluntary wheel running. Conflicting results emerged concerning the effect of voluntary wheel running on cardiac and respiratory function. Values above 100% are measures positively affected by exercise. Nonsignificant data were omitted from the figure. Data point shapes/colors represent measures as indicated.

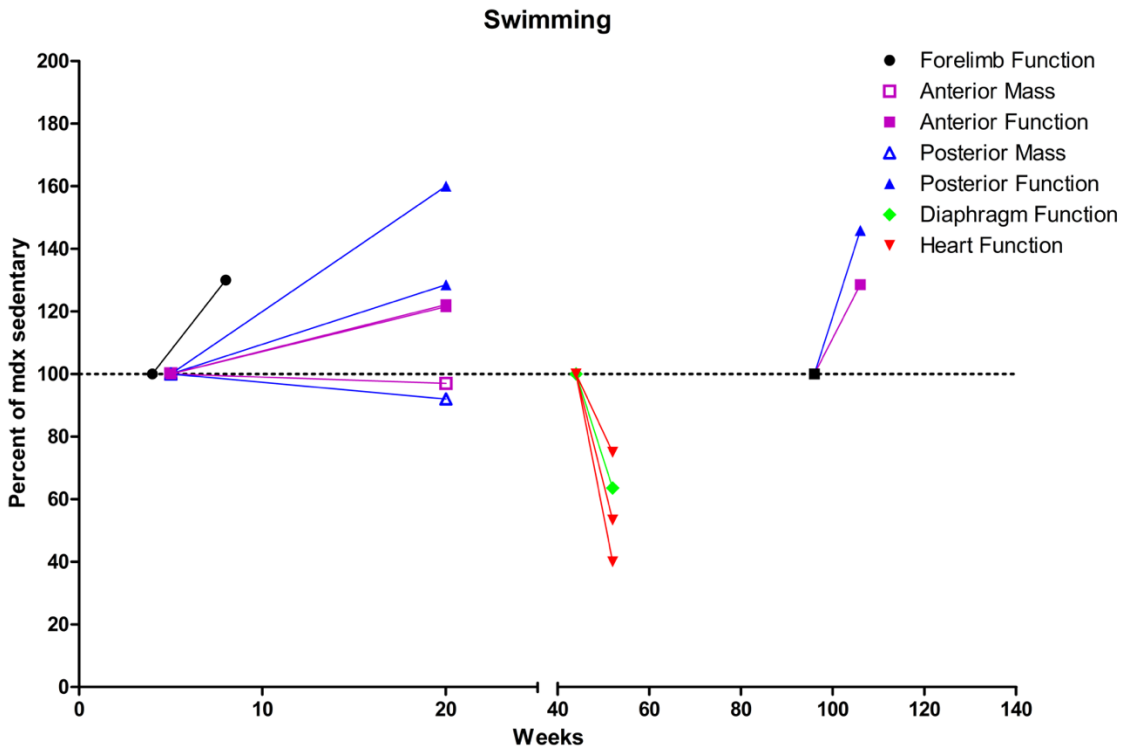

Figure 3. Effect of swimming on health outcomes in mdx mice. Exercise improved forelimb function and hindlimb muscle function but was detrimental to cardiac muscle function. Values above 100% are measures positively affected by exercise. Nonsignificant data were omitted from the figure. Data point shapes/colors represent measures as indicated.

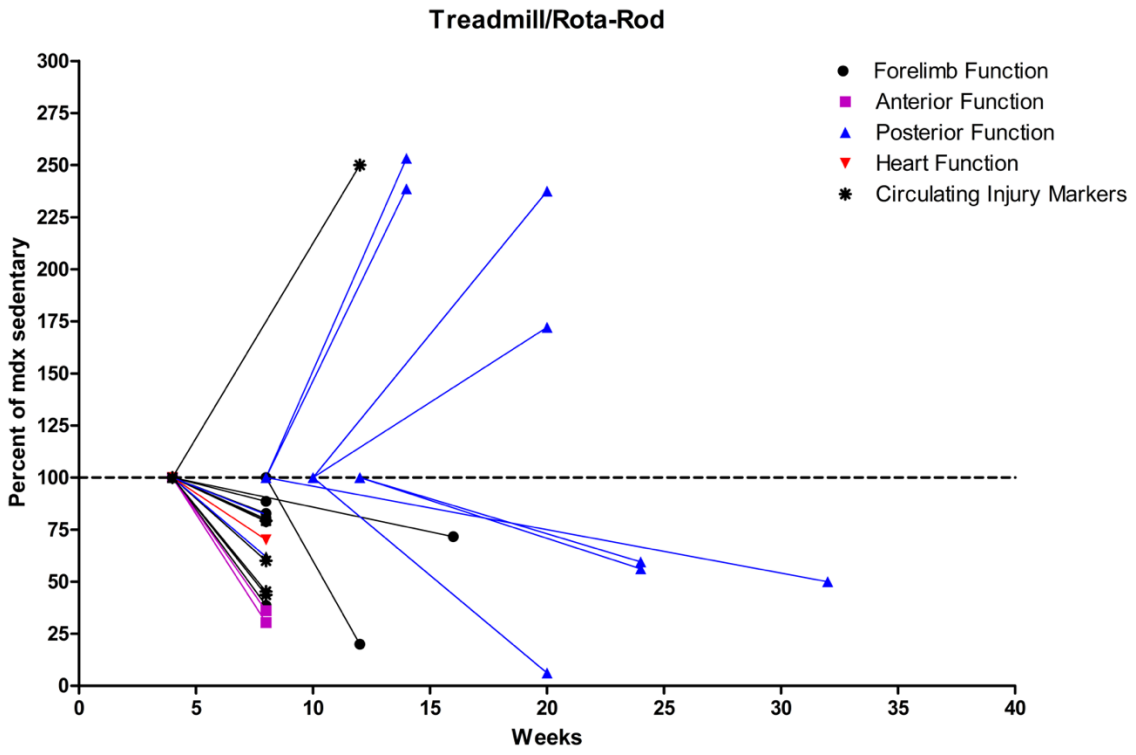

Figure 4. Effect of treadmill running/rota-rod on health outcomes in mdx mice. Forced running caused a variety of responses in dependent variables. Values above 100% are measures positively affected by exercise. Nonsignificant data were omitted from the figure. Data point shapes/colors represent measures as indicated.

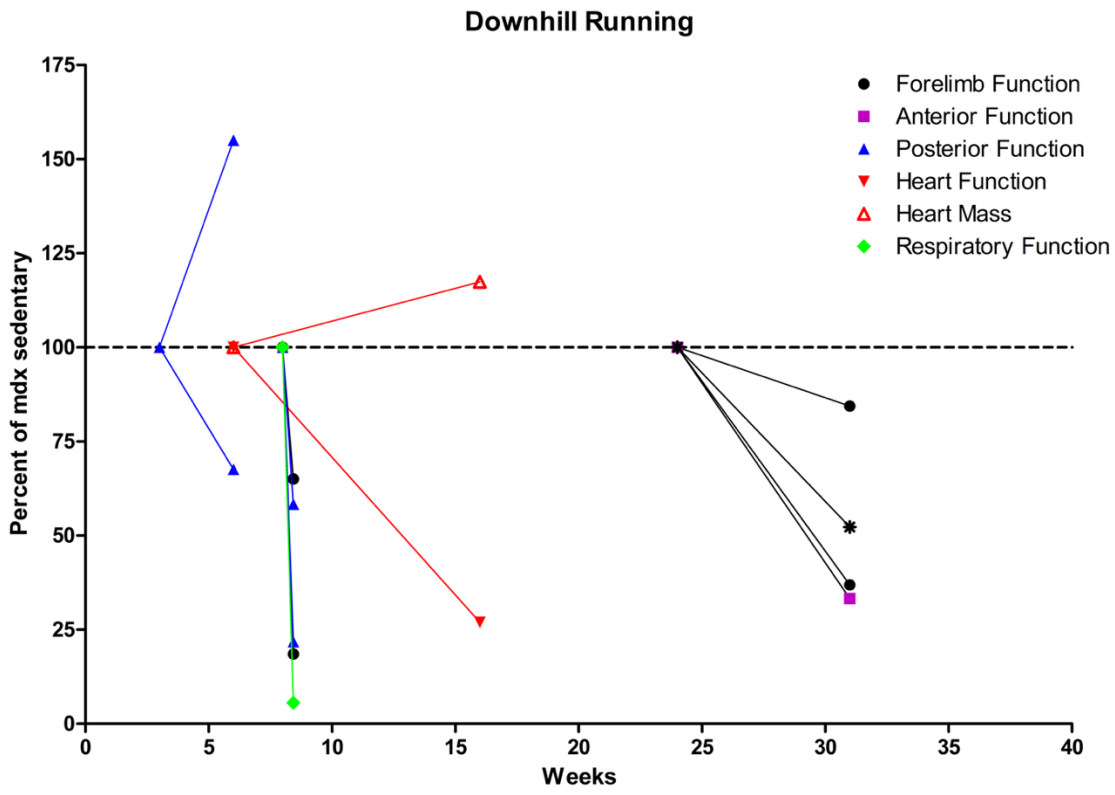

Figure 5. Effect of downhill running on health outcomes in mdx mice. Downhill running was largely detrimental hind limb (anterior and posterior compartments), forelimb, and cardiac muscles. Values above 100% are measures positively affected by exercise. Nonsignificant data were omitted from the figure. Data point shapes/colors represent measures as indicated.

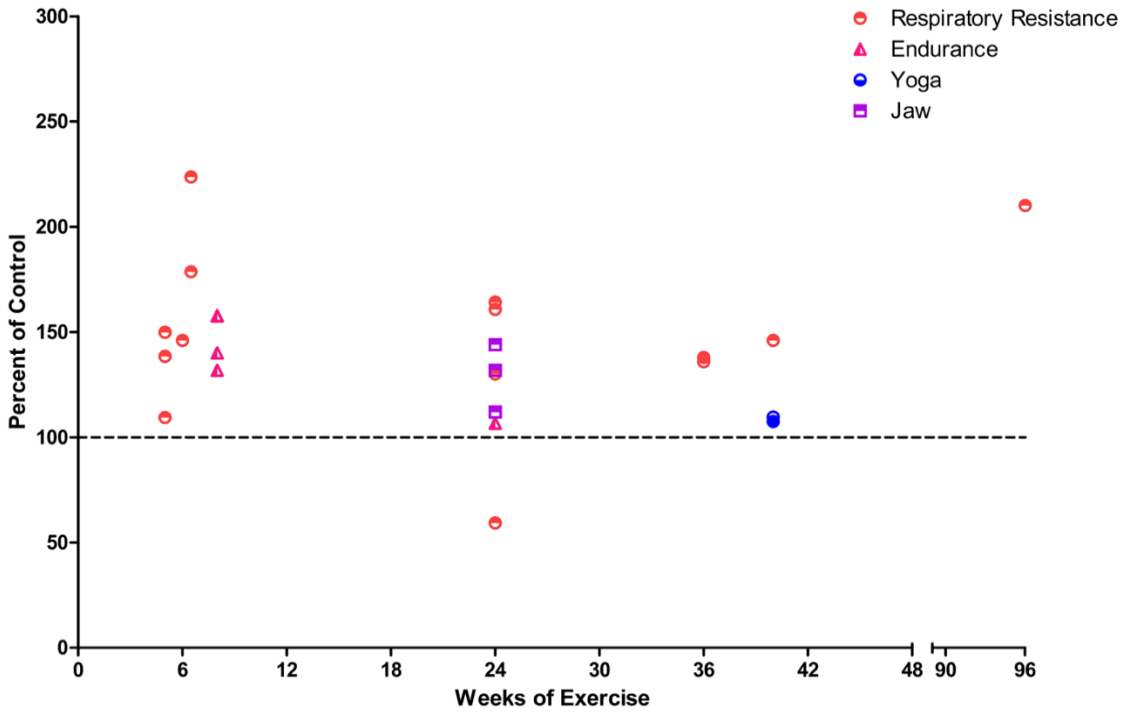

Figure 6. Effect of exercise on DMD patients. Exercises designed to improve range of motion and respiratory endurance improved health outcome measure in DMD patients. Starting ages were not provided in this figure as the range of starting ages within a study varied as did ambulatory status. Values above 100% are measures positively affected by exercise. Nonsignificant data were omitted from the figure. Data point shapes/colors represent exercises as indicated.

Exercise Mimetics, Current Therapeutics and Autophagy Relevant Therapies

Quercetin

Quercetin is a natural flavonoid with antioxidant and anti-inflammatory properties and GRAS (Generally Regarded as Safe) status (7, 27, 56). In an obesity mouse model quercetin reduced pro-inflammatory cytokines, decreased macrophage abundance and reduced muscle fiber atrophy (115). Quercetin may stimulate SIRT1 (57), a NAD+-dependent deacetylase, which interacts with metabolic regulator, PGC-1α (144). In healthy muscle, quercetin increased gene expression of Sirtuin 1 (SIRT1) and PGC-1α, and increased mitochondrial DNA content suggestive of increased mitochondrial biogenesis (51). Further, quercetin increased cytochrome c protein abundance suggestive of increased mitochondrial biogenesis (51). PGC-1α is a transcriptional coactivator that is elevated following exercise and can increase mitochondrial biogenesis and utrophin protein abundance, both of which are beneficial to dystrophic muscle (42, 118, 181). Indeed, PGC-1α overexpression has been shown to prevent/delay disease onset and rescue muscle from active decline. Hence, quercetin may decrease disease severity by decreasing oxidative stress, reducing inflammation and increasing abundance of the dystrophin-like protein, utrophin. While quercetin does appear to increase mitochondrial biogenesis the role of increased mitochondria in disease mitigation is unclear.

In support of this hypothesis, quercetin provided histological benefits to dystrophic skeletal muscle following 6 months of treatment (95). Additionally, quercetin improved respiratory function for the first 6 months of supplementation, but by 12 months respiratory

function was not preserved and markers of histological damage were similar between treated and untreated mdx mice (180).

In dystrophic hearts following 6 months of quercetin treatment, histological damage was decreased and utrophin abundance was increased (12). Additionally, cytochrome c and SOD2 content increased, which the authors suggest may be indicative of increased mitochondrial abundance (12). Following 8 months of quercetin, indices of cardiac function were improved, animal activity increased as well as increased colocalization of utrophin and DGC components by immunofluorescence (11). Additionally, markers of damage were reduced and indices of mitochondrial abundance, such as PGC-1α and electron transport complex I-V, were increased (11). Similarly, following 12 months of quercetin, mitochondrial biogenesis was elevated and indices of inflammation decreased, though quercetin did not improve cardiac function (10). These data suggest that quercetin is cardioprotective and transiently protects skeletal muscle necessitating further investigation to establish the viability of quercetin as a long-term treatment for DMD.

Nicotinamide riboside

In dystrophic muscle, NAD+ is depleted along with nicotinamide phosphor-ribosyltransferase (NAMPT), an essential enzyme in the NAD+ salvage pathway (40). Supplementation with nicotinamide riboside (NR) may increase the NAD+ pool and can protect against mitochondrial and metabolic dysfunction (71). In mdx mice, 10 weeks of NR supplementation increased stem cell function and abundance (217). After treating mdx mice with NR for 12 weeks, NAD+ bioavailability increased along with running capacity,

mitochondrial abundance, mitochondrial capacity, and dystroglycoprotein complex protein abundance (169). Furthermore, cardiac and diaphragm fibrosis, necrosis, inflammation and overall damage decreased in the diaphragm (169). Similarly, NR supplementation in a zebrafish model of DMD improved muscle structure and mobility (83). Collectively, these data strongly suggest that NR supplementation may be an effective therapeutic for DMD. Moreover, NR may restore the depleted NAD+ supply in dystrophic muscle prolonging deacetylation activity of SIRT1 (57), a deacetylase in which NAD+ is required, increasing long-term efficacy of quercetin.

Lisinopril

Lisinopril is an angiotensin converting enzyme (ACE) inhibitor that blocks the formation of angiotensin II from angiotensin I. Lisinopril was approved by the FDA to treat hypertension, but since gaining FDA approval has been used to reduce myocardial fibrosis and treat cardiomyopathy in DMD patients (155). Further, Lisinopril has been shown to increase left ventricle function (6, 205) and has been recommended for DMD patients starting as young as 10 years of age (133), prior to left ventricle ejection fraction falling to less than 55%.

While Lisinopril appears to be cardioprotective the effect of Lisinopril on dystrophic pathology in skeletal muscle is relatively unknown. Recently, Lowe et al. (123) evaluated the effect of Lisinopril on dystrophic skeletal muscle and found that Lisinopril decreased muscle damage but did not improve muscle function. Lisinopril has also been used in combination with aldosterone antagonists, spironolactone and eplerenone, and with a common glucocorticoid taken by DMD patients, prednisolone.

Spironolactone and eplerenone function as aldosterone antagonists, which disrupt the binding of aldosterone to mineralocorticoid receptors (52). Mdx/Utrn$^{+/-}$ mice treated with Lisinopril and spironolactone for 4 weeks starting at 4 weeks of age increased skeletal muscle function and decreased histological damage (160). Given that Lisinopril is beneficial to cardiac muscle, the effect of Lisinopril on skeletal muscle alone and within the context of other therapies is vital to understanding the value of Lisinopril as a therapy for DMD patients.

Glucocorticoids: Prednisone and Prednisolone

Glucocorticoids were first used to treat Duchenne muscular dystrophy in the early 1970s and are currently the standard of care for DMD patients (21, 58). In the United States, most patients receive prednisone or prednisolone (the active form of prednisone) (14), which are typically administered daily (0.75 mg/kg/d) or intermittently (10 mg/kg/weekend) (66, 81). In clinical studies prednisone and prednisolone preserved motor function and muscle strength, delayed loss of ambulation, reduced development of scoliosis and decreased rate of pulmonary function decline (81, 182). A recent examination of long-term glucocorticoid use on natural history found that the use of glucocorticoids for longer than a year delayed loss of ambulation by 2.1-4.4 years and loss of upper limb mobility by 2.8-8 years (130). In one study, treatment with prednisolone resulted in no scoliosis over 1.5-5 years compared to untreated with scoliosis (214). Though the mechanism driving therapeutic effects on dystrophic tissue are unknown, it is well known that glucocorticoids increase myoblast proliferation, stimulate regeneration, and reduce inflammation via immunosuppression (214). Despite

these benefits, prednisone and prednisolone treatments result in several side-effects, such as behavioral changes, weight gain, cushingoid appearance and cataracts (17). As a result, and despite the clear clinical benefit, dosing of steroids and age of application varies widely, and some patients remain steroid naive.

Because of these significant side effects an alternative to prednisone and prednisolone was developed. While widely available in Europe and other places globally for some time, deflazacort was approved by the FDA for use in the United States in 2017. Deflazacort is a prednisolone derivative, which has been shown to provide similar benefits (182). Deflazacort has been used routinely in Europe and has been shown to reduce growth which may delay loss of ambulation in addition to the benefits observed following prednisone and prednisolone treatment (86). Similar to prednisone and prednisolone, deflazacort has been shown to have side-effects such as weight gain, behavioral changes, cushingoid appearance and cataracts (19, 86).

Autophagy

Function of Autophagy

Autophagy is a catabolic process by which cellular components are degraded into basic units to be recycled for energy, maintenance, and rebuilding of cellular components, ie. organelles, proteins etc. Autophagy can be stimulated by a variety of stressors, such as mitochondrially generated reactive oxygen species and the accumulation of dysfunctional proteins or organelles (44), but the majority of canonical autophagy is discussed within the context of nutrient depletion. Autophagy is separated into three major types: chaperone-mediated autophagy, microautophagy and

macroautophagy. Briefly, chaperone-mediated autophagy (CMA) is a selective process by which proteins destined for degradation by CMA are identified and bound by chaperone complexes, such as heat shock-cognate protein of 70 kDa (Hsc70), or cochaperones to the KFERQ-like motif of the protein (162). Once bound, this protein is internalized by the lysosome through a translocation complex formed by lysosome-associated membrane protein 2a (Lamp2A) multimerization (49). The second type, microautophagy, occurs when cargo is taken directly into the lysosome through a mechanism of lysosomal membrane invagination (162). The third type, and the type of autophagy we will further discuss, is macroautophagy, hereafter referred to as autophagy. Autophagy is the process by which cargo, both selectively and nonselectively, are engulfed along with a portion of the cytoplasm into a developing autophagosome. The mature double-membraned autophagosome fuses with a lysosome forming an autophagolysosome (autolysosome). Upon fusion the inner membrane of the autophagosome is degraded allowing for the lysosomal enzymes to degrade the cargo.

Autophagy can be separated into four key states: initiation of phagophore formation, elongation of the phagophore, maturation of the autophagosome, and finally the fusion of the autophagosome with the lysosomes. Initiation or formation of the phagosome can be accomplished *de novo* or using previously existing membranes, such as the endoplasmic reticulum, mitochondria, lipid droplets, and golgi apparatus (9, 136). Prior to stimulation, for example in the presence of amino acids, mammalian target of rapamycin complex (mTORC1), a serine/threonine protein kinase that is known to regulate cell growth and metabolism, phosphorylates Unc-51 like autophagy activating kinase (ULK1) at Ser 757 and autophagy related protein 13 (ATG13) on Ser 258

inhibiting the kinase ability of ULK1 (105, 157). Phosphorylation of ULK and ATG13 leads to an inhibition of autophagy and inhibits the ability of ATG13 to enhance ULK1 activity and translocate the ULK1 complex to autophagy initiation sites (76, 97, 215).

Upon stimulation of autophagy, typically through increased AMP-activated protein kinase (AMPK) and/or inhibition of mammalian target of rapamycin (mTOR), the ULK1 complex and the class III phosphatidylinositol 3-kinase (PI3KC3) complex are activated to initiate phagosome nucleation. The ULK1 complex is composed of kinases, ULK1 or ULK2, and regulatory proteins, ATG13, focal adhesion kinase family-interacting protein of 200 kDa (FIP200) and ATG101, an ATG13-binding protein (162). This complex is constitutively formed, but upon amino acid depletion, ULK1 is phosphorylated at Ser555 and dephosphorylated at Ser757 along with dephosphorylation of ATG13 (76, 157). Together this activates the ULK1 complex to promote autophagosome formation. The binding of ATG13 and FIP200 to ULK1 enhances ULK1 activity and together this ULK1 complex promotes autophagosome formation and phosphorylation of Beclin-1 at Ser14 (76, 143, 167).

PI3KC3 complex, composed of PI3KC3 (VPS34), p150, ATG14L and Beclin-1, is formed to facilitate membrane formation (136, 167). The binding of Beclin-1 to PI3KC3 enhances PI3KC3 activity (75) and the phosphorylation of ATG14L by ULK further increases PI3KC3 complex activity, which promotes the synthesis of phosphatidyl-inositol-3-phosphate (PI3P), lipids known to be essential for membrane dynamics (213).

Given that role of Beclin-1 in the PI3KC3 complex and autophagosome nucleation, further research has been done to elucidate the regulation of Beclin-1.

Beclin-1 has two groups of binding proteins, some which promote and others that inhibit autophagy. Binding of autophagy Beclin-1 regulator (Ambra-1), UV radiation resistance-associated gene (UVRAG), or bax-interfering factor 1 (bif-1) to Beclin-1 induces autophagosome formation (68, 197), while binding of BCL-2 or BCL-2 homology, BCL-xL, inhibits autophagosome formation (150). Beclin-1 contains a conserved BH-3 domain allowing for it to interact with BCL-2 and BCL-xL (147). Interestingly, when nutrient-deprivation autophagy factor-1 (NAF-1) interacts with BCL-2 at the endoplasmic reticulum the interaction of NAF-1 and BCL-2 stabilize the binding of BCL-2 and Beclin-1 inhibiting autophagy (43). Conversely, the liberating of Beclin-1 from BCL-2, through the binding of p62 to BCL-2, stimulates autophagosome formation (219).

As the phagosome forms and matures, autophagy-related proteins are utilized to develop the phagophore into a mature autophagosome. Autophagosome expansion and maturation are controlled by two ubiquitin-like conjugation pathways, ATG5/ATG12/ATG16L complex and microtubule associated proteins (MAP1) light chain 3 (LC3) complex. To form the ATG12/ATG5/ATG16L complex the c-terminus of ATG12 is activated by ATG7, an E1-like enzyme (199), then transferred to ATG10, an E2-like enzyme (184). ATG12 is then conjugated to ATG5 forming ATG12/5 (135). Finally, ATG12/5 is conjugated to ATG16L completing the ATG12/ATG5/ATG16L complex, which is essential to the expansion and elongation of the autophagosome (185). Upon completion of the autophagosome, ATG12/ATG5/ATG16L complex is dissociated from the membrane (73).

In the second ubiquitin-like conjugation pathway, LC3 is lipidated to become LC3II and is then integrated into autophagosome membrane. LC3 is first cleaved at its

C-terminus by ATG4, a protease, to form LC3I, then conjugated to phosphatidylethanolamine (PE) by ATG7 and ATG3, E1 and E2-like enzymes, respectively. This lipidation converts LCI to LC3II, which is incorporated into the autophagosome membrane (101). Adaptor proteins, such as sequestosome 1 (p62), bridge LC3II to the selected cargo to be enclosed in the double-membraned autophagosome (149). Interestingly, the lipidation process has been shown to be reversible. LC3II can be liberated from the autophagosome membrane prior to fusion with the lysosome by delipidation, ie. the removal the PE group from LC3II by ATG4 (106), though delipidation by ATG4 occurs at a slower rate than the priming of LC3 for lipidation (103). Finally, autophagosomes fuse with lysosomes to degrade the cargo collected in the autophagosome.

Lysosomes are a single membrane vesicle in which v-ATPase complexes in the membrane function to maintain the highly acidic internal environment (pH 4.5-5). Lysosomes contain numerous enzymes, such as hydrolases, proteases, lipases and nucleases, to degrade cellular components, such as organelles, lipids and proteins. The resulting monomers can either diffuse or are actively transported out of lysosome to be reused (140). To prevent degradation of the lysosome membrane by resident lysosomal enzymes, membrane proteins are glycosylated such that the inner membrane is covered in glycocalyx to protect the membrane. Two proteins of interest are lysosomal associated membrane protein (LAMP) 1 and 2, which are highly glycosylated proteins known to stabilize the lysosomal membrane and make up two-thirds of the lysosomal membrane providing the glycocalyx protection of the membrane (210). Additionally, hypotheses

have been advanced that posit that LAMP proteins may also play a role in positioning of lysosomes by acting as scaffolding for motor protein complexes (161).

Lastly, interpretation of data to elucidate autophagic function must be approached delicately and have been under review and discussion within the research community. Recently, exhaustive guidelines for collecting and interpreting autophagy data have been established (108). Researchers use the ratio of lipidated LC3 (LC3II) to unlipidated LC3 (LC3I) to indicate movement, or flux, through the autophagy pathway towards degradation. Similarly, p62 has been used as an inverse correlate to autophagosome degradation as p62 is degraded along with the cargo (22). For example, a decreased ratio of LC3II/I and increased p62 have previously been used as evidence of impaired autophagy in dystrophic muscle (20, 55, 148).

To better elucidate the flux and function of the autophagy pathway, inhibitors of autophagosome-lysosome fusion and degradation have been utilized. Chloroquine is a commonly used inhibitor of autophagy, which inhibits fusion of the autophagosome (129). Bafilomycin A1, a v-ATPase inhibitor, reduces lysosome function, which may inhibit both degradation and fusion (109). By incorporating inhibitors of fusion into the experimental design, researchers can use a nuanced approach to discriminate increased autophagy resulting in increased autophagosome abundance from increased autophagosome abundance due to decreased degradation. Similarly, transgenic mice were generated to assess autophagic flux *in vivo*. Tandem fluorescent-tagged LC3 mice were generated that have an RFP-GFP-LC3 reporter in which initially both RFP and GFP are colocalized on LC3 and appear yellow, but once the autophagosome fuses with the

lysosome, the GFP is quenched and only RFP remains, thus the ratio of RFP to RFP-GFP indicates autophagic flux *in vivo* (139).

Autophagy in Duchenne muscular dystrophy

Autophagy has become a pathway of interest in Duchenne muscular dystrophy as well as a variety of other myopathies in which autophagy is abnormally regulated, such as collagen-VI-related diseases, Emery–Dreyfuss muscular dystrophy (EDMD), Danon's disease and Pompe disease (173). Impaired autophagy has also been established in Duchenne muscular dystrophy (55, 67, 148, 151, 191, 195). We and other have shown that autophagy is impaired prior to degradation of the autophagosome resulting in an accumulation of autophagosomes as indicated by increased p62 and decreased LC3II/I ratio (148, 191). Additionally, total AMPK and phosphorylated AMPK, an activator of autophagy, were decreased (120, 179) and phosphorylated mTOR/total mTOR ratio, an inhibitor of autophagy, were elevated (148) suggestive of decreased autophagic signaling in dystrophic muscle. Despite upstream signaling, autophagosome maturation and formation are increased as indicated by increased Beclin-1 and ATG12/5 in dystrophic muscle (191). Using inhibitors, Fiacco (67) further established that in aged mdx skeletal muscle autophagosome degradation was blocked as demonstrated by similar LC3II abundance when autophagosome degradation was inhibited with chloroquine. Further supporting impaired autophagy, colocalization of p62/LC3 as well as p62/LAMP1 were decreased in flexor digitorum brevis muscles isolated from mdx mice (148). Similarly, LC3II and p62 were elevated in muscle of 3- and 6-month-old golden retriever model of DMD with no change in LC3 gene expression supportive of impaired autophagy (195).

Autophagosome degradation could be impaired by several mechanistic dysfunctions. For example, impaired autophagy could be caused by an inability to fuse the autophagosome to the lysosome, decreased lysosome function and/or reduced lysosome abundance. We and other have demonstrated that LAMP1 and LAMP2 protein abundance are decreased in mdx skeletal muscle and as previously mentioned LC3/LAMP1 colocalization was decreased supporting that autophagic dysfunction could be due to insufficient lysosome abundance or impaired fusion (148, 191).

Emerging evidence also suggest that autophagy in DMD patients is impaired. Biopsies from DMD patients demonstrate decreased LC3II/I ratio and increased p62 suggestive of impaired autophagy (55). Interestingly, pAKT protein abundance, which should inhibit autophagy, was elevated despite an accumulation of p62 (55). In immortalized myoblasts from DMD patients, initiators of autophagosomes formation, PI3KC3 and ATG3, were elevated and autophagosome abundance marker, LC3II, was increased in dystrophic myoblasts (207). Upon inhibition of lysosome acidification with E64D and pepstatin, LC3II protein abundance was elevated indicating successful degradation of autophagosomes in DMD myoblasts, but LC3II accumulation was further increased in healthy controls suggesting that fusion may be slightly inhibited (207). Similarly, LC3 abundance was increased in biopsies from 2- and 8-year-old DMD patients compared to healthy controls (67). These data suggest that autophagy is activated in DMD patients but is impaired prior to autophagosome degradation. Treatments to stimulate autophagy, such as low protein diets, AICAR, an AMPK activator, and rapamycin, an mTOR inhibitor, have successfully improved autophagic signaling and reduced histological injury, suggesting that therapies to repair autophagy may be

beneficial to DMD patients (20, 55, 151). Despite success of these stimulators of autophagy, the benefits of directly improving impaired autophagosome degradation may further protect dystrophic muscle.

PGC-1α and autophagy

Peroxisome proliferator-activated receptor-gamma coactivator (PGC-1α) is a transcriptional coactivator known to drive genes involved in mitochondrial biogenesis, oxidative metabolism and maintenance of glucose, lipid and energy homeostasis, among other functions (173, 174). To regulate mitochondrial biogenesis, PGC-1α recruits histone acetyl transferases (HATs) to remodel chromatin and interacts with a variety of transcription factors to promote transcription of mitochondrial genes, such as nuclear respiratory factor 1 (NRF-1), nuclear respiratory factor 2 (NRF-2) and estrogen related receptor alpha (ERRα). Together these transcription factors upregulate expression of nuclear encoded mitochondrial proteins (NEMP) and mitochondrial transcription factor A (TFAM) resulting in mitochondrial DNA replication and transcription of mitochondrially encoded genes.

Specifically, in healthy skeletal muscle, PGC-1α overexpression increased the ratio of slow oxidative fibers to fast glycolytic fibers (118), helped maintain muscle mass and fiber volume following denervation (174), increased mitochondrial biogenesis (78, 117, 118), and increased protection against reactive oxygen specifies (ROS) (192). Similarly, when PGC-1α was overexpressed in dystrophic muscle, there was a shift toward an increased ratio of slow oxidative fibers compared to fast glycolytic fibers (181), decreased histological markers of damage (89), and increased mitochondrial

markers suggesting increased mitochondrial abundance (181). PGC-1α overexpression has also been shown to increase muscle force and fatigue resistance (94, 181). Further, PGC-1α has been shown to drive utrophin transcript and protein abundance (42, 181), a dystrophin-like protein typically localized to the neuromuscular junction that compensates for the absence of dystrophin in dystrophin-deficient skeletal muscle (202, 203). Overexpression of PGC-1α increased utrophin abundance in dystrophic muscle, further, utrophin overexpression increased abundance of dystroglycoprotein complex proteins at the sarcolemma that are mislocalized with dystrophin deficiency (203).

Importantly, PGC-1α has been shown to alter autophagy, through an elusive relationship with transcription factor EB (TFEB). TFEB is a master regulator of autophagy and lysosome biogenesis related genes. Interestingly, when TFEB was overexpressed, PGC-1α transcription abundance increased, also when PGC-1α was knocked out total TFEB protein abundance was decreased. (63). These data suggest that the relationship between TFEB and PGC-1α is unclear and it is more complex than expected. Nonetheless, these data suggest that TFEB can be manipulated through PGC-1α. Further, in an aging model, PGC-1α overexpression increased markers of autophagy (78). Similarly, in a Pompe disease model transgenic overexpression of PGC-1α increased markers of autophagy, increased lysosome abundance, and decreased autophagosome accumulation suggesting increased efficiency of autophagy (198). Collectively, these data suggest that upregulation of PGC-1α is therapeutic for dystrophic muscle and can increase autophagy and lysosome biogenesis through a TFEB-mediated mechanism.

References

1. **Adams ME, Odom GL, Kim MJ, Chamberlain JS, and Froehner SC**. Syntrophin binds directly to multiple spectrin-like repeats in dystrophin and mediates binding of nNOS to repeats 16-17. *Hum Mol Genet* 27: 2978-2985, 2018.

2. **Ahn AH, and Kunkel LM**. The structural and functional diversity of dystrophin. *Nat Genet* 3: 283-291, 1993.

3. **Alderton JM, and Steinhardt RA**. Calcium influx through calcium leak channels is responsible for the elevated levels of calcium-dependent proteolysis in dystrophic myotubes. *J Biol Chem* 275: 9452-9460, 2000.

4. **Aldrich TK, and Uhrlass RM**. Weaning from mechanical ventilation: successful use of modified inspiratory resistive training in muscular dystrophy. *Crit Care Med* 15: 247-249, 1987.

5. **Alemdaroglu I, Karaduman A, Yilmaz OT, and Topaloglu H**. Different types of upper extremity exercise training in Duchenne muscular dystrophy: effects on functional performance, strength, endurance, and ambulation. *Muscle Nerve* 51: 697-705, 2015.

6. **Allen HD, Flanigan KM, Thrush PT, Dvorchik I, Yin H, Canter C, Connolly AM, Parrish M, McDonald CM, Braunlin E, Colan SD, Day J, Darras B, and Mendell JR**. A randomized, double-blind trial of lisinopril and losartan for the treatment of cardiomyopathy in duchenne muscular dystrophy. *PLoS Curr* 5: 2013.

7. **Anhe GF, Okamoto MM, Kinote A, Sollon C, Lellis-Santos C, Anhe FF, Lima GA, Hirabara SM, Velloso LA, Bordin S, and Machado UF**. Quercetin decreases inflammatory response and increases insulin action in skeletal muscle of ob/ob mice and in L6 myotubes. *Eur J Pharmacol* 689: 285-293, 2012.

8. **Archer JD, Vargas CC, and Anderson JE**. Persistent and improved functional gain in mdx dystrophic mice after treatment with L-arginine and deflazacort. *Faseb j* 20: 738-740, 2006.

9. **Axe EL, Walker SA, Manifava M, Chandra P, Roderick HL, Habermann A, Griffiths G, and Ktistakis NT**. Autophagosome formation from membrane compartments enriched in phosphatidylinositol 3-phosphate and dynamically connected to the endoplasmic reticulum. *J Cell Biol* 182: 685-701, 2008.

10. **Ballmann C, Denney T, Beyers RJ, Quindry T, Romero M, Selsby JT, and Quindry JC**. Long term dietary quercetin enrichment as a cardioprotective countermeasure in mdx mice. *Exp Physiol* 2017.

11. **Ballmann C, Denney TS, Beyers RJ, Quindry T, Romero M, Amin R, Selsby JT, and Quindry JC**. Lifelong quercetin enrichment and cardioprotection in Mdx/Utrn+/- mice. *Am J Physiol Heart Circ Physiol* 312: H128-h140, 2017.

12. **Ballmann C, Hollinger K, Selsby JT, Amin R, and Quindry JC**. Histological and biochemical outcomes of cardiac pathology in mdx mice with dietary quercetin enrichment. *Exp Physiol* 100: 12-22, 2015.

13. **Baltgalvis KA, Call JA, Cochrane GD, Laker RC, Yan Z, and Lowe DA**. Exercise training improves plantar flexor muscle function in mdx mice. *Med Sci Sports Exerc* 44: 1671-1679, 2012.

14. **Baltgalvis KA, Call JA, Nikas JB, and Lowe DA**. The effects of prednisolone on skeletal muscle contractility in mdx mice. *Muscle Nerve* 40: 443-454, 2009.

15. **Baltusnikas J, Venckunas T, Kilikevicius A, Fokin A, and Ratkevicius A**. Efflux of Creatine Kinase from Isolated Soleus Muscle Depends on Age, Sex and Type of Exercise in Mice. In: *J Sports Sci Med*2015, p. 379-385.

16. **Barbin IC, Pereira JA, Bersan Rovere M, de Oliveira Moreira D, Marques MJ, and Santo Neto H**. Diaphragm degeneration and cardiac structure in mdx mouse: potential clinical implications for Duchenne muscular dystrophy. *J Anat* 228: 784-791, 2016.

17. **Beenakker EA, Fock JM, Van Tol MJ, Maurits NM, Koopman HM, Brouwer OF, and Van der Hoeven JH**. Intermittent prednisone therapy in Duchenne muscular dystrophy: a randomized controlled trial. *Arch Neurol* 62: 128-132, 2005.

18. **Belanto JJ, Mader TL, Eckhoff MD, Strandjord DM, Banks GB, Gardner MK, Lowe DA, and Ervasti JM**. Microtubule binding distinguishes dystrophin from utrophin. *Proc Natl Acad Sci U S A* 111: 5723-5728, 2014.

19. **Bello L, Gordish-Dressman H, Morgenroth LP, Henricson EK, Duong T, Hoffman EP, Cnaan A, and McDonald CM**. Prednisone/prednisolone and deflazacort regimens in the CINRG Duchenne Natural History Study. *Neurology* 85: 1048-1055, 2015.

20. **Bibee KP, Cheng YJ, Ching JK, Marsh JN, Li AJ, Keeling RM, Connolly AM, Golumbek PT, Myerson JW, Hu G, Chen J, Shannon WD, Lanza GM, Weihl CC, and Wickline SA**. Rapamycin nanoparticles target defective autophagy in muscular dystrophy to enhance both strength and cardiac function. *Faseb j* 28: 2047-2061, 2014.

21. **Birnkrant DJ, Bushby K, Bann CM, Apkon SD, Blackwell A, Brumbaugh D, Case LE, Clemens PR, Hadjiyannakis S, Pandya S, Street N, Tomezsko J, Wagner KR, Ward LM, and Weber DR**. Diagnosis and management of Duchenne muscular dystrophy, part 1: diagnosis, and neuromuscular, rehabilitation, endocrine, and gastrointestinal and nutritional management. *Lancet Neurol* 17: 251-267, 2018.

22. **Bjorkoy G, Lamark T, Brech A, Outzen H, Perander M, Overvatn A, Stenmark H, and Johansen T**. p62/SQSTM1 forms protein aggregates degraded by autophagy and has a protective effect on huntingtin-induced cell death. *J Cell Biol* 171: 603-614, 2005.

23. **Bladen CL, Salgado D, Monges S, Foncuberta ME, Kekou K, Kosma K, Dawkins H, Lamont L, Roy AJ, Chamova T, Guergueltcheva V, Chan S, Korngut L, Campbell C, Dai Y, Wang J, Barišić N, Brabec P, Lahdetie J, Walter MC, Schreiber-Katz O, Karcagi V, Garami M, Viswanathan V, Bayat F, Buccella F, Kimura E, Koeks Z, van den Bergen JC, Rodrigues M, Roxburgh R, Lusakowska A, Kostera-Pruszczyk A, Zimowski J, Santos R, Neagu E, Artemieva S, Rasic VM, Vojinovic D, Posada M, Bloetzer C, Jeannet PY, Joncourt F, Díaz-Manera J, Gallardo E, Karaduman AA, Topaloğlu H, El Sherif R, Stringer A, Shatillo AV, Martin AS, Peay HL, Bellgard MI, Kirschner J, Flanigan KM, Straub V, Bushby K, Verschuuren J, Aartsma-Rus A, Béroud C, and Lochmüller H**. The TREAT-NMD DMD Global Database: Analysis of More than 7,000 Duchenne Muscular Dystrophy Mutations. *Hum Mutat* 36: 395-402, 2015.

24. **Blair SN, Kohl HW, Gordon NF, and Paffenbarger RS, Jr.** How much physical activity is good for health? *Annu Rev Public Health* 13: 99-126, 1992.

25. **Bogdanovich S, Krag TO, Barton ER, Morris LD, Whittemore LA, Ahima RS, and Khurana TS**. Functional improvement of dystrophic muscle by myostatin blockade. *Nature* 420: 418-421, 2002.

26. **Boldrin L, Zammit PS, and Morgan JE**. Satellite cells from dystrophic muscle retain regenerative capacity. *Stem Cell Research* 14: 20-29, 2015.

27. **Boots AW, Drent M, de Boer VC, Bast A, and Haenen GR**. Quercetin reduces markers of oxidative stress and inflammation in sarcoidosis. *Clin Nutr* 30: 506-512, 2011.

28. **Bouchentouf M, Benabdallah BF, Mills P, and Tremblay JP**. Exercise improves the success of myoblast transplantation in mdx mice. *Neuromuscul Disord* 16: 518-529, 2006.

29. **Brereton D, Plochocki J, An D, Costas J, and Simons E**. The effects of glucocorticoid and voluntary exercise treatment on the development of thoracolumbar kyphosis in dystrophin-deficient mice. *PLoS Curr* 4: e4ffdff160de168b, 2012.

30. **Broderick MJ, and Winder SJ**. Spectrin, alpha-actinin, and dystrophin. *Adv Protein Chem* 70: 203-246, 2005.

31. **Brussee V, Tardif F, and Tremblay JP**. Muscle fibers of mdx mice are more vulnerable to exercise than those of normal mice. *Neuromuscul Disord* 7: 487-492, 1997.

32. **Buckner JL, Bowden SA, and Mahan JD**. Optimizing Bone Health in Duchenne Muscular Dystrophy. *Int J Endocrinol* 2015: 2015.

33. **Bulfield G, Siller WG, Wight PA, and Moore KJ**. X chromosome-linked muscular dystrophy (mdx) in the mouse. *Proc Natl Acad Sci U S A* 81: 1189-1192, 1984.

34. **Burdi R, Didonna MP, Pignol B, Nico B, Mangieri D, Rolland JF, Camerino C, Zallone A, Ferro P, Andreetta F, Confalonieri P, and De Luca A**. First evaluation of the potential effectiveness in muscular dystrophy of a novel chimeric compound, BN 82270, acting as calpain-inhibitor and anti-oxidant. *Neuromuscul Disord* 16: 237-248, 2006.

35. **Burdi R, Rolland JF, Fraysse B, Litvinova K, Cozzoli A, Giannuzzi V, Liantonio A, Camerino GM, Sblendorio V, Capogrosso RF, Palmieri B, Andreetta F, Confalonieri P, De Benedictis L, Montagnani M, and De Luca A**. Multiple pathological events in exercised dystrophic mdx mice are targeted by pentoxifylline: outcome of a large array of in vivo and ex vivo tests. *J Appl Physiol (1985)* 106: 1311-1324, 2009.

36. **Bushby K, Bourke J, Bullock R, Eagle M, Gibson M, and Quinby J**. The multidisciplinary management of Duchenne muscular dystrophy. *Current Paediatrics* 15: 292-300, 2005.

37. **Call JA, Mckeehen JN, Novotny SA, and Lowe DA**. Progressive resistance voluntary wheel running in the mdx mouse. *Muscle & Nerve* 42: 871-880, 2010.

38. **Call JA, Voelker KA, Wolff AV, McMillan RP, Evans NP, Hulver MW, Talmadge RJ, and Grange RW**. Endurance capacity in maturing mdx mice is markedly enhanced by combined voluntary wheel running and green tea extract. *J Appl Physiol (1985)* 105: 923-932, 2008.

39. **Camerino GM, Cannone M, Giustino A, Massari AM, Capogrosso RF, Cozzoli A, and De Luca A**. Gene expression in mdx mouse muscle in relation to age and exercise: aberrant mechanical-metabolic coupling and implications for pre-clinical studies in Duchenne muscular dystrophy. *Hum Mol Genet* 23: 5720-5732, 2014.

40. **Chalkiadaki A, Igarashi M, Nasamu AS, Knezevic J, and Guarente L**. Muscle-specific SIRT1 gain-of-function increases slow-twitch fibers and ameliorates pathophysiology in a mouse model of duchenne muscular dystrophy. *PLoS Genet* 10: e1004490, 2014.

41. **Chamberlain JS, Metzger J, Reyes M, Townsend D, and Faulkner JA**. Dystrophin-deficient mdx mice display a reduced life span and are susceptible to spontaneous rhabdomyosarcoma. *Faseb j* 21: 2195-2204, 2007.

42. **Chan MC, Rowe GC, Raghuram S, Patten IS, Farrell C, and Arany Z**. Post-natal induction of PGC-1alpha protects against severe muscle dystrophy independently of utrophin. *Skelet Muscle* 4: 2, 2014.

43. **Chang NC, Nguyen M, Germain M, and Shore GC**. Antagonism of Beclin 1-dependent autophagy by BCL-2 at the endoplasmic reticulum requires NAF-1. *Embo j* 29: 606-618, 2010.

44. **Chen Y, and Gibson SB**. Is mitochondrial generation of reactive oxygen species a trigger for autophagy? *Autophagy* 4: 246-248, 2008.

45. **Coley WD, Bogdanik L, Vila MC, Yu Q, Van Der Meulen JH, Rayavarapu S, Novak JS, Nearing M, Quinn JL, Saunders A, Dolan C, Andrews W, Lammert C, Austin A, Partridge TA, Cox GA, Lutz C, and Nagaraju K**. Effect of genetic background on the dystrophic phenotype in mdx mice. In: *Hum Mol Genet*2016, p. 130-145.

46. **Constantin B**. Dystrophin complex functions as a scaffold for signalling proteins. *Biochim Biophys Acta* 1838: 635-642, 2014.

47. **Costas JM, Nye DJ, Henley JB, and Plochocki JH**. Voluntary exercise induces structural remodeling in the hearts of dystrophin-deficient mice. *Muscle Nerve* 42: 881-885, 2010.

48. **Crosbie RH, Heighway J, Venzke DP, Lee JC, and Campbell KP**. Sarcospan, the 25-kDa transmembrane component of the dystrophin-glycoprotein complex. *J Biol Chem* 272: 31221-31224, 1997.

49. **Cuervo AM, and Wong E**. Chaperone-mediated autophagy: roles in disease and aging. *Cell Res* 24: 92-104, 2014.

50. **Davidson ZE, and Truby H**. A review of nutrition in Duchenne muscular dystrophy. *J Hum Nutr Diet* 22: 383-393, 2009.

51. **Davis JM, Murphy EA, Carmichael MD, and Davis B**. Quercetin increases brain and muscle mitochondrial biogenesis and exercise tolerance. *Am J Physiol Regul Integr Comp Physiol* 296: R1071-1077, 2009.

52. **de Gasparo M, Joss U, Ramjoue HP, Whitebread SE, Haenni H, Schenkel L, Kraehenbuehl C, Biollaz M, Grob J, Schmidlin J, and et al.** Three new epoxy-spirolactone derivatives: characterization in vivo and in vitro. *J Pharmacol Exp Ther* 240: 650-656, 1987.

53. **De Luca A, Nico B, Liantonio A, Didonna MP, Fraysse B, Pierno S, Burdi R, Mangieri D, Rolland JF, Camerino C, Zallone A, Confalonieri P, Andreetta F, Arnoldi E, Courdier-Fruh I, Magyar JP, Frigeri A, Pisoni M, Svelto M, and Conte Camerino D**. A multidisciplinary evaluation of the effectiveness of cyclosporine a in dystrophic mdx mice. *Am J Pathol* 166: 477-489, 2005.

54. **De Luca A, Pierno S, Liantonio A, Cetrone M, Camerino C, Fraysse B, Mirabella M, Servidei S, Ruegg UT, and Conte Camerino D**. Enhanced dystrophic progression in mdx mice by exercise and beneficial effects of taurine and insulin-like growth factor-1. *J Pharmacol Exp Ther* 304: 453-463, 2003.

55. **De Palma C, Morisi F, Cheli S, Pambianco S, Cappello V, Vezzoli M, Rovere-Querini P, Moggio M, Ripolone M, Francolini M, Sandri M, and Clementi E**. Autophagy as a new therapeutic target in Duchenne muscular dystrophy. *Cell Death Dis* 3: e418, 2012.

56. **Dias AS, Porawski M, Alonso M, Marroni N, Collado PS, and Gonzalez-Gallego J**. Quercetin decreases oxidative stress, NF-kappaB activation, and iNOS overexpression in liver of streptozotocin-induced diabetic rats. *J Nutr* 135: 2299-2304, 2005.

57. **Dong J, Zhang X, Zhang L, Bian HX, Xu N, Bao B, and Liu J**. Quercetin reduces obesity-associated ATM infiltration and inflammation in mice: a mechanism including AMPKalpha1/SIRT1. *J Lipid Res* 55: 363-374, 2014.

58. **Drachman DB, Toyka KV, and Myer E**. Prednisone in Duchenne muscular dystrophy. *Lancet* 2: 1409-1412, 1974.

59. **Dupont-Versteegden EE**. Exercise and clenbuterol as strategies to decrease the progression of muscular dystrophy in mdx mice. *J Appl Physiol (1985)* 80: 734-741, 1996.

60. **Dupont-Versteegden EE, McCarter RJ, and Katz MS**. Voluntary exercise decreases progression of muscular dystrophy in diaphragm of mdx mice. *J Appl Physiol* 77: 1736-1741, 1994.

61. **Eagle M, Baudouin SV, Chandler C, Giddings DR, Bullock R, and Bushby K**. Survival in Duchenne muscular dystrophy: improvements in life expectancy since 1967 and the impact of home nocturnal ventilation. *Neuromuscul Disord* 12: 926-929, 2002.

62. **Emery AE**. The muscular dystrophies. *Lancet* 359: 687-695, 2002.

63. **Erlich AT, Brownlee DM, Beyfuss K, and Hood DA**. Exercise induces TFEB expression and activity in skeletal muscle in a PGC-1alpha-dependent manner. *Am J Physiol Cell Physiol* 314: C62-c72, 2018.

64. **Ervasti JM, and Campbell KP**. A role for the dystrophin-glycoprotein complex as a transmembrane linker between laminin and actin. *J Cell Biol* 122: 809-823, 1993.

65. **Ervasti JM, and Campbell KP**. Dystrophin and the membrane skeleton. *Curr Opin Cell Biol* 5: 82-87, 1993.

66. **Escolar DM, Hache LP, Clemens PR, Cnaan A, McDonald CM, Viswanathan V, Kornberg AJ, Bertorini TE, Nevo Y, Lotze T, Pestronk A, Ryan MM, Monasterio E, Day JW, Zimmerman A, Arrieta A, Henricson E, Mayhew J, Florence J, Hu F, and Connolly AM**. Randomized, blinded trial of weekend vs daily prednisone in Duchenne muscular dystrophy. *Neurology* 77: 444-452, 2011.

67. **Fiacco E, Castagnetti F, Bianconi V, Madaro L, De Bardi M, Nazio F, D'Amico A, Bertini E, Cecconi F, Puri PL, and Latella L**. Autophagy regulates satellite cell ability to regenerate normal and dystrophic muscles. *Cell Death Differ* 23: 1839-1849, 2016.

68. **Fimia GM, Stoykova A, Romagnoli A, Giunta L, Di Bartolomeo S, Nardacci R, Corazzari M, Fuoco C, Ucar A, Schwartz P, Gruss P, Piacentini M, Chowdhury K, and Cecconi F**. Ambra1 regulates autophagy and development of the nervous system. *Nature* 447: 1121-1125, 2007.

69. **Flanigan KM, Ceco E, Lamar KM, Kaminoh Y, Dunn DM, Mendell JR, King WM, Pestronk A, Florence JM, Mathews KD, Finkel RS, Swoboda KJ, Gappmaier E, Howard MT, Day JW, McDonald C, McNally EM, and Weiss RB**. LTBP4 genotype predicts age of ambulatory loss in Duchenne muscular dystrophy. *Ann Neurol* 73: 481-488, 2013.

70. **Fowler WM, Jr., Abresch RT, Larson DB, Sharman RB, and Entrikin RK**. High-repetitive submaximal treadmill exercise training: effect on normal and dystrophic mice. *Arch Phys Med Rehabil* 71: 552-557, 1990.

71. **Frederick DW, Loro E, Liu L, Davila A, Chellappa K, Silverman IM, Quinn WJ, Gosai SJ, Tichy ED, Davis JG, Mourkioti F, Gregory BD, Dellinger RW, Redpath P, Migaud ME, Nakamaru-Ogiso E, Rabinowitz JD, Khurana TS, and Baur JA**. Loss of NAD homeostasis leads to progressive and reversible degeneration of skeletal muscle. *Cell Metab* 24: 269-282, 2016.

72. **Frinchi M, Macaluso F, Licciardi A, Perciavalle V, Coco M, Belluardo N, Morici G, and Mudo G**. Recovery of damaged skeletal muscle in mdx mice through low-intensity endurance exercise. *Int J Sports Med* 35: 19-27, 2014.

73. **Fujita N, Itoh T, Omori H, Fukuda M, Noda T, and Yoshimori T**. The Atg16L Complex Specifies the Site of LC3 Lipidation for Membrane Biogenesis in Autophagy. *Mol Biol Cell* 19: 2092-2100, 2008.

74. **Fukada S, Morikawa D, Yamamoto Y, Yoshida T, Sumie N, Yamaguchi M, Ito T, Miyagoe-Suzuki Y, Takeda S, Tsujikawa K, and Yamamoto H**. Genetic background affects properties of satellite cells and mdx phenotypes. *Am J Pathol* 176: 2414-2424, 2010.

75. **Furuya N, Yu J, Byfield M, Pattingre S, and Levine B**. The evolutionarily conserved domain of Beclin 1 is required for Vps34 binding, autophagy and tumor suppressor function. *Autophagy* 1: 46-52, 2005.

76. **Ganley IG, Lam du H, Wang J, Ding X, Chen S, and Jiang X**. ULK1.ATG13.FIP200 complex mediates mTOR signaling and is essential for autophagy. *J Biol Chem* 284: 12297-12305, 2009.

77. **Gao Q, and McNally EM**. The Dystrophin Complex: structure, function and implications for therapy. *Compr Physiol* 5: 1223-1239, 2015.

78. **Garcia S, Nissanka N, Mareco EA, Rossi S, Peralta S, Diaz F, Rotundo RL, Carvalho RF, and Moraes CT**. Overexpression of PGC-1alpha in aging muscle enhances a subset of young-like molecular patterns. *Aging Cell* 17: 2018.

79. **Gawor M, and Proszynski TJ**. The molecular cross talk of the dystrophin-glycoprotein complex. *Ann N Y Acad Sci* 1412: 62-72, 2018.

80. **Gianola S, Pecoraro V, Lambiase S, Gatti R, Banfi G, and Moja L**. Efficacy of Muscle Exercise in Patients with Muscular Dystrophy: A Systematic Review Showing a Missed Opportunity to Improve Outcomes. In: *PLoS One*2013.

81. **Gloss D, Moxley RT, 3rd, Ashwal S, and Oskoui M**. Practice guideline update summary: Corticosteroid treatment of Duchenne muscular dystrophy: Report of the Guideline Development Subcommittee of the American Academy of Neurology. *Neurology* 86: 465-472, 2016.

82. **Godin R, Daussin F, Matecki S, Li T, Petrof BJ, and Burelle Y**. Peroxisome proliferator-activated receptor γ coactivator 1-α gene transfer restores mitochondrial biomass and improves mitochondrial calcium handling in post-necrotic mdx mouse skeletal muscle. *J Physiol* 590: 5487-5502, 2012.

83. **Goody MF, Kelly MW, Reynolds CJ, Khalil A, Crawford BD, and Henry CA**. NAD+ biosynthesis ameliorates a zebrafish model of muscular dystrophy. *PLoS Biol* 10: e1001409, 2012.

84. **Gozal D, and Thiriet P**. Respiratory muscle training in neuromuscular disease: long-term effects on strength and load perception. *Med Sci Sports Exerc* 31: 1522-1527, 1999.

85. **Grange RW, and Call JA**. Recommendations to define exercise prescription for Duchenne muscular dystrophy. *Exerc Sport Sci Rev* 35: 12-17, 2007.

86. **Griggs RC, Miller JP, Greenberg CR, Fehlings DL, Pestronk A, Mendell JR, Moxley RT, 3rd, King W, Kissel JT, Cwik V, Vanasse M, Florence JM, Pandya S, Dubow JS, and Meyer JM**. Efficacy and safety of deflazacort vs prednisone and placebo for Duchenne muscular dystrophy. *Neurology* 87: 2123-2131, 2016.

87. **Haidet AM, Rizo L, Handy C, Umapathi P, Eagle A, Shilling C, Boue D, Martin PT, Sahenk Z, Mendell JR, and Kaspar BK**. Long-term enhancement of skeletal muscle mass and strength by single gene administration of myostatin inhibitors. *Proc Natl Acad Sci U S A* 105: 4318-4322, 2008.

88. **Hall JE, Kaczor JJ, Hettinga BP, Isfort RJ, and Tarnopolsky MA**. Effects of a CRF2R agonist and exercise on mdx and wildtype skeletal muscle. *Muscle Nerve* 36: 336-341, 2007.

89. **Handschin C, Kobayashi YM, Chin S, Seale P, Campbell KP, and Spiegelman BM**. PGC-1alpha regulates the neuromuscular junction program and ameliorates Duchenne muscular dystrophy. *Genes Dev* 21: 770-783, 2007.

90. **Hayes A, Lynch GS, and Williams DA**. The effects of endurance exercise on dystrophic mdx mice. I. Contractile and histochemical properties of intact muscles. *Proc Biol Sci* 253: 19-25, 1993.

91. **Hayes A, and Williams D**. Contractile function and low-intensity exercise effects of old dystrophic (mdx) mice. *Am J Physiol* 274: C1138-1144, 1998.

92. **Hayes A, and Williams DA**. Beneficial effects of voluntary wheel running on the properties of dystrophic mouse muscle. *J Appl Physiol* 80: 670-679, 1996.

93. **Hoffman EP, Brown RH, Jr., and Kunkel LM**. Dystrophin: the protein product of the Duchenne muscular dystrophy locus. *Cell* 51: 919-928, 1987.

94. **Hollinger K, Gardan-Salmon D, Santana C, Rice D, Snella E, and Selsby JT**. Rescue of dystrophic skeletal muscle by PGC-1 alpha involves restored expression of dystrophin-associated protein complex components and satellite cell signaling. *American Journal of Physiology-Regulatory Integrative and Comparative Physiology* 305: R13-R23, 2013.

95. **Hollinger K, Shanely RA, Quindry JC, and Selsby JT**. Long-term quercetin dietary enrichment decreases muscle injury in mdx mice. *Clin Nutr* 34: 515-522, 2015.

96. **Holt KH, and Campbell KP**. Assembly of the sarcoglycan complex. Insights for muscular dystrophy. *J Biol Chem* 273: 34667-34670, 1998.

97. **Hosokawa N, Hara T, Kaizuka T, Kishi C, Takamura A, Miura Y, Iemura S, Natsume T, Takehana K, Yamada N, Guan JL, Oshiro N, and Mizushima N**. Nutrient-dependent mTORC1 Association with the ULK1–Atg13–FIP200 Complex Required for Autophagy. *Mol Biol Cell* 20: 1981-1991, 2009.

98. **Hourde C, Joanne P, Medja F, Mougenot N, Jacquet A, Mouisel E, Pannerec A, Hatem S, Butler-Browne G, Agbulut O, and Ferry A**. Voluntary physical activity protects from susceptibility to skeletal muscle contraction-induced injury but worsens heart function in mdx mice. *Am J Pathol* 182: 1509-1518, 2013.

99. **Hu X, Charles JP, Akay T, Hutchinson JR, and Blemker SS**. Are mice good models for human neuromuscular disease? Comparing muscle excursions in walking between mice and humans. *Skelet Muscle* 7: 26, 2017.

100. **Hyzewicz J, Tanihata J, Kuraoka M, Ito N, Miyagoe-Suzuki Y, and Takeda S**. Low intensity training of mdx mice reduces carbonylation and increases expression levels of proteins involved in energy metabolism and muscle contraction. *Free Radic Biol Med* 82: 122-136, 2015.

101. **Ichimura Y, Kirisako T, Takao T, Satomi Y, Shimonishi Y, Ishihara N, Mizushima N, Tanida I, Kominami E, Ohsumi M, Noda T, and Ohsumi Y**. A ubiquitin-like system mediates protein lipidation. *Nature* 408: 488-492, 2000.

102. **Jansen M, van Alfen N, Geurts AC, and de Groot IJ**. Assisted bicycle training delays functional deterioration in boys with Duchenne muscular dystrophy: the randomized controlled trial "no use is disuse". *Neurorehabil Neural Repair* 27: 816-827, 2013.

103. **Kauffman KJ, Yu S, Jin J, Mugo B, Nguyen N, O'Brien A, Nag S, Lystad AH, and Melia TJ**. Delipidation of mammalian Atg8-family proteins by each of the four ATG4 proteases. *Autophagy* 14: 992-1010, 2018.

104. **Kawazoe Y, Kobayashi M, Tasaka T, and Tamamoto M**. Effects of therapeutic exercise on masticatory function in patients with progressive muscular dystrophy. *J Neurol Neurosurg Psychiatry* 45: 343-347, 1982.

105. **Kim J, Kundu M, Viollet B, and Guan KL**. AMPK and mTOR regulate autophagy through direct phosphorylation of Ulk1. *Nat Cell Biol* 13: 132-141, 2011.

106. **Kimura S, Noda T, and Yoshimori T**. Dissection of the autophagosome maturation process by a novel reporter protein, tandem fluorescent-tagged LC3. *Autophagy* 3: 452-460, 2007.

107. **King WM, Ruttencutter R, Nagaraja HN, Matkovic V, Landoll J, Hoyle C, Mendell JR, and Kissel JT**. Orthopedic outcomes of long-term daily corticosteroid treatment in Duchenne muscular dystrophy. *Neurology* 68: 1607-1613, 2007.

108. **Klionsky DJ, Abdelmohsen K, Abe A, Abedin MJ, Abeliovich H, Acevedo Arozena A, Adachi H, Adams CM, Adams PD, Adeli K, Adhihetty PJ, Adler SG, Agam G, and et al**. Guidelines for the use and interpretation of assays for monitoring autophagy (3rd edition). *Autophagy* 12: 1-222, 2016.

109. **Klionsky DJ, Elazar Z, Seglen PO, and Rubinsztein DC**. Does bafilomycin A1 block the fusion of autophagosomes with lysosomes? In: *Autophagy*. United States: 2008, p. 849-850.

110. **Kobayashi YM, Rader EP, Crawford RW, and Campbell KP**. Endpoint measures in the mdx mouse relevant for muscular dystrophy pre-clinical studies. *Neuromuscul Disord* 22: 34-42, 2012.

111. **Koenig M, and Kunkel LM**. Detailed analysis of the repeat domain of dystrophin reveals four potential hinge segments that may confer flexibility. *J Biol Chem* 265: 4560-4566, 1990.

112. **Koenig M, Monaco AP, and Kunkel LM**. The complete sequence of dystrophin predicts a rod-shaped cytoskeletal protein. *Cell* 53: 219-228, 1988.

113. **Koessler W, Wanke T, Winkler G, Nader A, Toifl K, Kurz H, and Zwick H**. 2 Years' experience with inspiratory muscle training in patients with neuromuscular disorders. *Chest* 120: 765-769, 2001.

114. **Laws N, and Hoey A**. Progression of kyphosis in mdx mice. *J Appl Physiol (1985)* 97: 1970-1977, 2004.

115. **Le NH, Kim CS, Park T, Park JH, Sung MK, Lee DG, Hong SM, Choe SY, Goto T, Kawada T, and Yu R**. Quercetin protects against obesity-induced skeletal muscle inflammation and atrophy. *Mediators Inflamm* 2014: 834294, 2014.

116. **Lefaucheur JP, Pastoret C, and Sebille A**. Phenotype of dystrophinopathy in old mdx mice. *Anat Rec* 242: 70-76, 1995.

117. **Lehman JJ, Barger PM, Kovacs A, Saffitz JE, Medeiros DM, and Kelly DP**. Peroxisome proliferator-activated receptor gamma coactivator-1 promotes cardiac mitochondrial biogenesis. *J Clin Invest* 106: 847-856, 2000.

118. **Lin J, Wu H, Tarr PT, Zhang CY, Wu Z, Boss O, Michael LF, Puigserver P, Isotani E, Olson EN, Lowell BB, Bassel-Duby R, and Spiegelman BM**. Transcriptional co-activator PGC-1 alpha drives the formation of slow-twitch muscle fibres. *Nature* 418: 797-801, 2002.

119. **Ljubicic V, Burt M, Lunde JA, and Jasmin BJ**. Resveratrol induces expression of the slow, oxidative phenotype in mdx mouse muscle together with enhanced activity of the SIRT1-PGC-1alpha axis. *Am J Physiol Cell Physiol* 307: C66-82, 2014.

120. **Ljubicic V, Khogali S, Renaud JM, and Jasmin BJ**. Chronic AMPK stimulation attenuates adaptive signaling in dystrophic skeletal muscle. *Am J Physiol Cell Physiol* 302: C110-121, 2012.

121. **Ljubicic V, Miura P, Burt M, Boudreault L, Khogali S, Lunde JA, Renaud JM, and Jasmin BJ**. Chronic AMPK activation evokes the slow, oxidative myogenic program and triggers beneficial adaptations in mdx mouse skeletal muscle. *Human molecular genetics* 20: 3478-3493, 2011.

122. **Lowe J, Kadakia FK, Zins JG, Haupt M, Peczkowski KK, Rastogi N, Floyd KT, Gomez-Sanchez EP, Gomez-Sanchez CE, Elnakish MT, Rafael-Fortney JA, and Janssen PML**. Mineralocorticoid Receptor Antagonists in Muscular Dystrophy Mice During Aging and Exercise. *J Neuromuscul Dis* 5: 295-306, 2018.

123. **Lowe J, Wodarcyk AJ, Floyd KT, Rastogi N, Schultz EJ, Swager SA, Chadwick JA, Tran T, Raman SV, Janssen PM, and Rafael-Fortney JA**. The Angiotensin Converting Enzyme Inhibitor Lisinopril Improves Muscle Histopathology but not Contractile Function in a Mouse Model of Duchenne Muscular Dystrophy. In: *J Neuromuscul Dis*2015, p. 257-268.

124. **Mah JK, Korngut L, Dykeman J, Day L, Pringsheim T, and Jette N**. A systematic review and meta-analysis on the epidemiology of Duchenne and Becker muscular dystrophy. *Neuromuscul Disord* 24: 482-491, 2014.

125. **Markert CD, Ambrosio F, Call JA, and Grange RW**. Exercise and Duchenne muscular dystrophy: toward evidence-based exercise prescription. *Muscle Nerve* 43: 464-478, 2011.

126. **Marshall JL, and Crosbie-Watson RH**. Sarcospan: a small protein with large potential for Duchenne muscular dystrophy. *Skelet Muscle* 3: 1, 2013.

127. **Mathur S, Vohra RS, Germain SA, Forbes S, Bryant ND, Vandenborne K, and Walter GA**. Changes in muscle T2 and tissue damage after downhill running in mdx mice. *Muscle Nerve* 43: 878-886, 2011.

128. **Matsumura K, Ervasti JM, Ohlendieck K, Kahl SD, and Campbell KP**. Association of dystrophin-related protein with dystrophin-associated proteins in mdx mouse muscle. *Nature* 360: 588-591, 1992.

129. **Mauthe M, Orhon I, Rocchi C, Zhou X, Luhr M, Hijlkema KJ, Coppes RP, Engedal N, Mari M, and Reggiori F**. Chloroquine inhibits autophagic flux by decreasing autophagosome-lysosome fusion. *Autophagy* 14: 1435-1455, 2018.

130. **McDonald CM, Henricson EK, Abresch RT, Duong T, Joyce NC, Hu F, Clemens PR, Hoffman EP, Cnaan A, and Gordish-Dressman H**. Long-term effects of glucocorticoids on function, quality of life, and survival in patients with Duchenne muscular dystrophy: a prospective cohort study. *Lancet* 391: 451-461, 2018.

131. **McDonald DG, Kinali M, Gallagher AC, Mercuri E, Muntoni F, Roper H, Jardine P, Jones DH, and Pike MG**. Fracture prevalence in Duchenne muscular dystrophy. *Dev Med Child Neurol* 44: 695-698, 2002.

132. **McGreevy JW, Hakim CH, McIntosh MA, and Duan D**. Animal models of Duchenne muscular dystrophy: from basic mechanisms to gene therapy. In: *Dis Model Mech*2015, p. 195-213.

133. **McNally EM, Kaltman JR, Benson DW, Canter CE, Cripe LH, Duan D, Finder JD, Hoffman EP, Judge DP, Kertesz N, Kinnett K, Kirsch R, Metzger JM, Pearson GD, Rafael-Fortney JA, Raman SV, Spurney CF, Targum SL, Wagner KR, and Markham LW**. Contemporary Cardiac Issues in Duchenne Muscular Dystrophy. *Circulation* 131: 1590-1598, 2015.

134. **Miller G, Wang EL, Nassar KL, Peter AK, and Crosbie RH**. Structural and functional analysis of the sarcoglycan-sarcospan subcomplex. *Exp Cell Res* 313: 639-651, 2007.

135. **Mizushima N, Noda T, Yoshimori T, Tanaka Y, Ishii T, George MD, Klionsky DJ, Ohsumi M, and Ohsumi Y**. A protein conjugation system essential for autophagy. *Nature* 395: 395-398, 1998.

136. **Molino D, Zemirli N, Codogno P, and Morel E**. The Journey of the Autophagosome through Mammalian Cell Organelles and Membranes. *J Mol Biol* 429: 497-514, 2017.

137. **Morales MG, Cabrera D, Cespedes C, Vio CP, Vazquez Y, Brandan E, and Cabello-Verrugio C**. Inhibition of the angiotensin-converting enzyme decreases skeletal muscle fibrosis in dystrophic mice by a diminution in the expression and activity of connective tissue growth factor (CTGF/CCN-2). *Cell Tissue Res* 353: 173-187, 2013.

138. **Morris CA, Selsby JT, Morris LD, Pendrak K, and Sweeney HL**. Bowman-Birk inhibitor attenuates dystrophic pathology in mdx mice. *J Appl Physiol* 109: 1492-1499, 2010.

139. **Moulis M, and Vindis C**. Methods for Measuring Autophagy in Mice. *Cells* 6: 2017.

140. **Mrschtik M, and Ryan KM**. Lysosomal proteins in cell death and autophagy. *Febs j* 282: 1858-1870, 2015.

141. **Nakamori M, and Takahashi MP**. The Role of Alpha-Dystrobrevin in Striated Muscle. *Int J Mol Sci* 12: 1660-1671, 2011.

142. **Nakamura A, Yoshida K, Takeda S, Dohi N, and Ikeda S**. Progression of dystrophic features and activation of mitogen-activated protein kinases and calcineurin by physical exercise, in hearts of mdx mice. *FEBS Lett* 520: 18-24, 2002.

143. **Nazarko VY, and Zhong Q**. ULK1 targets Beclin-1 in autophagy. *Nat Cell Biol* 15: 727-728, 2013.

144. **Nemoto S, Fergusson MM, and Finkel T**. SIRT1 functionally interacts with the metabolic regulator and transcriptional coactivator PGC-1{alpha}. *J Biol Chem* 280: 16456-16460, 2005.

145. **Norrbom J, Sundberg CJ, Ameln H, Kraus WE, Jansson E, and Gustafsson T**. PGC-1alpha mRNA expression is influenced by metabolic perturbation in exercising human skeletal muscle. *J Appl Physiol (1985)* 96: 189-194, 2004.

146. **Nozaki S, Kawai M, Shimoyama R, Futamura N, Matsumura T, Adachi K, and Kikuchi Y**. Range of motion exercise of temporo-mandibular joint with hot pack increases occlusal force in patients with Duchenne muscular dystrophy. *Acta Myol* 29: 392-397, 2010.

147. **Oberstein A, Jeffrey PD, and Shi Y**. Crystal structure of the Bcl-XL-Beclin 1 peptide complex: Beclin 1 is a novel BH3-only protein. *J Biol Chem* 282: 13123-13132, 2007.

148. **Pal R, Palmieri M, Loehr JA, Li S, Abo-Zahrah R, Monroe TO, Thakur PB, Sardiello M, and Rodney GG**. Src-dependent impairment of autophagy by oxidative stress in a mouse model of Duchenne muscular dystrophy. *Nat Commun* 5: 4425, 2014.

149. **Pankiv S, Clausen TH, Lamark T, Brech A, Bruun JA, Outzen H, Overvatn A, Bjorkoy G, and Johansen T**. p62/SQSTM1 binds directly to Atg8/LC3 to facilitate degradation of ubiquitinated protein aggregates by autophagy. *J Biol Chem* 282: 24131-24145, 2007.

150. **Pattingre S, Tassa A, Qu X, Garuti R, Liang XH, Mizushima N, Packer M, Schneider MD, and Levine B**. Bcl-2 antiapoptotic proteins inhibit Beclin 1-dependent autophagy. *Cell* 122: 927-939, 2005.

151. **Pauly M, Daussin F, Burelle Y, Li T, Godin R, Fauconnier J, Koechlin-Ramonatxo C, Hugon G, Lacampagne A, Coisy-Quivy M, Liang F, Hussain S, Matecki S, and Petrof BJ**. AMPK activation stimulates autophagy and ameliorates muscular dystrophy in the mdx mouse diaphragm. *Am J Pathol* 181: 583-592, 2012.

152. **Pessina P, Cabrera D, Morales MG, Riquelme CA, Gutierrez J, Serrano AL, Brandan E, and Munoz-Canoves P**. Novel and optimized strategies for inducing fibrosis in vivo: focus on Duchenne Muscular Dystrophy. *Skelet Muscle* 4: 7, 2014.

153. **Petrof BJ, Shrager JB, Stedman HH, Kelly AM, and Sweeney HL**. Dystrophin protects the sarcolemma from stresses developed during muscle contraction. *Proc Natl Acad Sci U S A* 90: 3710-3714, 1993.

154. **Poche H, Hopfenmuller W, and Hoffmann M**. Detection and identification of myoglobin in serum by immunoblotting. Effect of exercise on patients with Duchenne muscular dystrophy. *Clin Physiol Biochem* 5: 103-111, 1987.

155. **Politano L, and Nigro G**. Treatment of dystrophinopathic cardiomyopathy: review of the literature and personal results. In: *Acta Myol*2012, p. 24-30.

156. **Prins KW, Humston JL, Mehta A, Tate V, Ralston E, and Ervasti JM**. Dystrophin is a microtubule-associated protein. *J Cell Biol* 186: 363-369, 2009.

157. **Puente C, Hendrickson RC, and Jiang X**. Nutrient-regulated Phosphorylation of ATG13 Inhibits Starvation-induced Autophagy. *J Biol Chem* 291: 6026-6035, 2016.

158. **Quinlan JG, Hahn HS, Wong BL, Lorenz JN, Wenisch AS, and Levin LS**. Evolution of the mdx mouse cardiomyopathy: physiological and morphological findings. *Neuromuscul Disord* 14: 491-496, 2004.

159. **Radley-Crabb H, Terrill J, Shavlakadze T, Tonkin J, Arthur P, and Grounds M**. A single 30 min treadmill exercise session is suitable for 'proof-of concept studies' in adult mdx mice: a comparison of the early consequences of two different treadmill protocols. *Neuromuscul Disord* 22: 170-182, 2012.

160. **Rafael-Fortney JA, Chimanji NS, Schill KE, Martin CD, Murray JD, Ganguly R, Stangland JE, Tran T, Xu Y, Canan BD, Mays TA, Delfin DA, Janssen PM, and Raman SV**. Early treatment with lisinopril and spironolactone preserves cardiac and skeletal muscle in Duchenne muscular dystrophy mice. *Circulation* 124: 582-588, 2011.

161. **Rajapakshe AR, Podyma-Inoue KA, Terasawa K, Hasegawa K, Namba T, Kumei Y, Yanagishita M, and Hara-Yokoyama M**. Lysosome-associated membrane proteins (LAMPs) regulate intracellular positioning of mitochondria in MC3T3-E1 cells. *Exp Cell Res* 331: 211-222, 2015.

162. **Ravikumar B, Sarkar S, Davies JE, Futter M, Garcia-Arencibia M, Green-Thompson ZW, Jimenez-Sanchez M, Korolchuk VI, Lichtenberg M, Luo S, Massey DC, Menzies FM, Moreau K, Narayanan U, Renna M, Siddiqi FH, Underwood BR, Winslow AR, and Rubinsztein DC**. Regulation of mammalian autophagy in physiology and pathophysiology. *Physiol Rev* 90: 1383-1435, 2010.

163. **Rodrigues MR, Carvalho CR, Santaella DF, Lorenzi-Filho G, and Marie SK**. Effects of yoga breathing exercises on pulmonary function in patients with Duchenne muscular dystrophy: an exploratory analysis. *J Bras Pneumol* 40: 128-133, 2014.

164. **Rodriguez-Cruz M, Atilano-Miguel S, Barbosa-Cortes L, Bernabe-Garcia M, Almeida-Becerril T, Cardenas-Conejo A, Del Rocio Cruz-Guzman O, and Maldonado-Hernandez J**. Evidence of muscle loss delay and improvement of hyperinsulinemia and insulin resistance in Duchenne muscular dystrophy supplemented with omega-3 fatty acids: A randomized study. *Clin Nutr* 2018.

165. **Rodriguez-Cruz M, Sanchez R, Escobar RE, Cruz-Guzman Odel R, Lopez-Alarcon M, Bernabe Garcia M, Coral-Vazquez R, Matute G, and Velazquez Wong AC**. Evidence of Insulin Resistance and Other Metabolic Alterations in Boys with Duchenne or Becker Muscular Dystrophy. *Int J Endocrinol* 2015: 867273, 2015.

166. **Roig M, Roma J, Fargas A, and Munell F**. Longitudinal pathologic study of the gastrocnemius muscle group in mdx mice. *Acta Neuropathol* 107: 27-34, 2004.

167. **Russell RC, Tian Y, Yuan H, Park HW, Chang YY, Kim J, Kim H, Neufeld TP, Dillin A, and Guan KL**. ULK1 induces autophagy by phosphorylating Beclin-1 and activating VPS34 lipid kinase. *Nat Cell Biol* 15: 741-750, 2013.

168. **Rybakova IN, Amann KJ, and Ervasti JM**. A new model for the interaction of dystrophin with F-actin. *J Cell Biol* 135: 661-672, 1996.

169. **Ryu D, Zhang H, Ropelle ER, Sorrentino V, Mazala DA, Mouchiroud L, Marshall PL, Campbell MD, Ali AS, Knowels GM, Bellemin S, Iyer SR, Wang X, Gariani K, Sauve AA, Canto C, Conley KE, Walter L, Lovering RM, Chin ER, Jasmin BJ, Marcinek DJ, Menzies KJ, and Auwerx J**. NAD+ repletion improves muscle function in muscular dystrophy and counters global PARylation. *Sci Transl Med* 8: 361ra139, 2016.

170. **Sabharwal R**. The link between stress disorders and autonomic dysfunction in muscular dystrophy. *Front Physiol* 5: 2014.

171. **Sadoulet-Puccio HM, Rajala M, and Kunkel LM**. Dystrobrevin and dystrophin: An interaction through coiled-coil motifs. In: *Proc Natl Acad Sci U S A*1997, p. 12413-12418.

172. **Safdar A, Little JP, Stokl AJ, Hettinga BP, Akhtar M, and Tarnopolsky MA**. Exercise increases mitochondrial PGC-1alpha content and promotes nuclear-mitochondrial cross-talk to coordinate mitochondrial biogenesis. *J Biol Chem* 286: 10605-10617, 2011.

173. **Sandri M, Coletto L, Grumati P, and Bonaldo P**. Misregulation of autophagy and protein degradation systems in myopathies and muscular dystrophies. *J Cell Sci* 126: 5325-5333, 2013.

174. **Sandri M, Lin J, Handschin C, Yang W, Arany ZP, Lecker SH, Goldberg AL, and Spiegelman BM**. PGC-1alpha protects skeletal muscle from atrophy by suppressing FoxO3 action and atrophy-specific gene transcription. *Proc Natl Acad Sci U S A* 103: 16260-16265, 2006.

175. **Saure C, Caminiti C, Weglinski J, de Castro Perez F, and Monges S**. Energy expenditure, body composition, and prevalence of metabolic disorders in patients with Duchenne muscular dystrophy. *Diabetes Metab Syndr* 12: 81-85, 2018.

176. **Schill KE, Altenberger AR, Lowe J, Periasamy M, Villamena FA, Rafael-Fortney JA, and Devor ST**. Muscle damage, metabolism, and oxidative stress in mdx mice: Impact of aerobic running. *Muscle Nerve* 54: 110-117, 2016.

177. **Selsby JT**. Increased catalase expression improves muscle function in mdx mice. *Experimental physiology* 96: 194-202, 2011.

178. **Selsby JT, Acosta P, Sleeper MM, Barton ER, and Sweeney HL**. Long-term wheel running compromises diaphragm function but improves cardiac and plantarflexor function in the mdx mouse. *J Appl Physiol (1985)* 115: 660-666, 2013.

179. **Selsby JT, Ballmann CG, Spaulding HR, Ross JW, and Quindry JC**. Oral quercetin administration transiently protects respiratory function in dystrophin deficient mice. *J Physiol* 2016.

180. **Selsby JT, Ballmann CG, Spaulding HR, Ross JW, and Quindry JC**. Oral quercetin administration transiently protects respiratory function in dystrophin-deficient mice. *J Physiol* 594: 6037-6053, 2016.

181. **Selsby JT, Morine KJ, Pendrak K, Barton ER, and Sweeney HL**. Rescue of dystrophic skeletal muscle by PGC-1alpha involves a fast to slow fiber type shift in the mdx mouse. *PLoS One* 7: e30063, 2012.

182. **Shieh PB, McIntosh J, Jin F, Souza M, Elfring G, Narayanan S, Trifillis P, Peltz SW, McDonald CM, and Darras BT**. Deflazacort versus prednisone/prednisolone for maintaining motor function and delaying loss of ambulation: A post HOC analysis from the ACT DMD trial. *Muscle Nerve* 58: 639-645, 2018.

183. **Shimizu-Motohashi Y, Komaki H, Motohashi N, Takeda S, Yokota T, and Aoki Y**. Restoring Dystrophin Expression in Duchenne Muscular Dystrophy: Current Status of Therapeutic Approaches. *J Pers Med* 9: 2019.

184. **Shintani T, Mizushima N, Ogawa Y, Matsuura A, Noda T, and Ohsumi Y**. Apg10p, a novel protein-conjugating enzyme essential for autophagy in yeast. *Embo j* 18: 5234-5241, 1999.

185. **Shpilka T, Mizushima N, and Elazar Z**. Ubiquitin-like proteins and autophagy at a glance. *J Cell Sci* 125: 2343-2348, 2012.

186. **Sicinski P, Geng Y, Ryder-Cook AS, Barnard EA, Darlison MG, and Barnard PJ**. The molecular basis of muscular dystrophy in the mdx mouse: a point mutation. *Science* 244: 1578-1580, 1989.

187. **Skalsky AJ, and McDonald CM**. PREVENTION AND MANAGEMENT OF LIMB CONTRACTURES IN NEUROMUSCULAR DISEASES. *Phys Med Rehabil Clin N Am* 23: 675-687, 2012.

188. **Smythe GM, and White JD**. Voluntary wheel running in dystrophin-deficient (mdx) mice: Relationships between exercise parameters and exacerbation of the dystrophic phenotype. *PLoS Curr* 3: Rrn1295, 2011.

189. **Snow WM, Anderson JE, and Jakobson LS**. Neuropsychological and neurobehavioral functioning in Duchenne muscular dystrophy: a review. *Neurosci Biobehav Rev* 37: 743-752, 2013.

190. **Spaulding HR, Ballmann CG, Quindry JC, and Selsby JT**. Long-term quercetin dietary enrichment partially protects dystrophic skeletal muscle. *PloS one* 11: e0168293, 2016.

191. **Spaulding HR, Kelly EM, Quindry JC, Sheffield JB, Hudson MB, and Selsby JT**. Autophagic dysfunction and autophagosome escape in the mdx mus musculus model of Duchenne muscular dystrophy. *Acta Physiol (Oxf)* 222: 2018.

192. **St-Pierre J, Drori S, Uldry M, Silvaggi JM, Rhee J, Jager S, Handschin C, Zheng K, Lin J, Yang W, Simon DK, Bachoo R, and Spiegelman BM**. Suppression of reactive oxygen species and neurodegeneration by the PGC-1 transcriptional coactivators. *Cell* 127: 397-408, 2006.

193. **Stedman HH, Sweeney HL, Shrager JB, Maguire HC, Panettieri RA, Petrof B, Narusawa M, Leferovich JM, Sladky JT, and Kelly AM**. The mdx mouse diaphragm reproduces the degenerative changes of Duchenne muscular dystrophy. *Nature* 352: 536-539, 1991.

194. **Stone MR, O'Neill A, Catino D, and Bloch RJ**. Specific interaction of the actin-binding domain of dystrophin with intermediate filaments containing keratin 19. *Mol Biol Cell* 16: 4280-4293, 2005.

195. **Stoughton WB, Li J, Balog-Alvarez C, and Kornegay JN**. Impaired autophagy correlates with golden retriever muscular dystrophy phenotype. *Muscle Nerve* 58: 418-426, 2018.

196. **Strehle EM, and Straub V**. Recent advances in the management of Duchenne muscular dystrophy. *Arch Dis Child* 100: 1173-1177, 2015.

197. **Takahashi Y, Coppola D, Matsushita N, Cualing HD, Sun M, Sato Y, Liang C, Jung JU, Cheng JQ, Mule JJ, Pledger WJ, and Wang HG**. Bif-1 interacts with Beclin 1 through UVRAG and regulates autophagy and tumorigenesis. *Nat Cell Biol* 9: 1142-1151, 2007.

198. **Takikita S, Schreiner C, Baum R, Xie T, Ralston E, Plotz PH, and Raben N**. Fiber type conversion by PGC-1alpha activates lysosomal and autophagosomal biogenesis in both unaffected and Pompe skeletal muscle. *PLoS One* 5: e15239, 2010.

199. **Tanida I, Mizushima N, Kiyooka M, Ohsumi M, Ueno T, Ohsumi Y, and Kominami E**. Apg7p/Cvt2p: A novel protein-activating enzyme essential for autophagy. *Mol Biol Cell* 10: 1367-1379, 1999.

200. **Taniguti AP, Pertille A, Matsumura CY, Santo Neto H, and Marques MJ**. Prevention of muscle fibrosis and myonecrosis in mdx mice by suramin, a TGF-beta1 blocker. *Muscle Nerve* 43: 82-87, 2011.

201. **Terrill JR, Radley-Crabb HG, Grounds MD, and Arthur PG**. N-Acetylcysteine treatment of dystrophic mdx mice results in protein thiol modifications and inhibition of exercise induced myofibre necrosis. *Neuromuscul Disord* 22: 427-434, 2012.

202. **Tinsley J, Deconinck N, Fisher R, Kahn D, Phelps S, Gillis JM, and Davies K**. Expression of full-length utrophin prevents muscular dystrophy in mdx mice. *Nat Med* 4: 1441-1444, 1998.

203. **Tinsley JM, Potter AC, Phelps SR, Fisher R, Trickett JI, and Davies KE**. Amelioration of the dystrophic phenotype of mdx mice using a truncated utrophin transgene. *Nature* 384: 349-353, 1996.

204. **Topin N, Matecki S, Le Bris S, Rivier F, Echenne B, Prefaut C, and Ramonatxo M**. Dose-dependent effect of individualized respiratory muscle training in children with Duchenne muscular dystrophy. *Neuromuscul Disord* 12: 576-583, 2002.

205. **Viollet L, Thrush PT, Flanigan KM, Mendell JR, and Allen HD**. Effects of angiotensin-converting enzyme inhibitors and/or beta blockers on the cardiomyopathy in Duchenne muscular dystrophy. *Am J Cardiol* 110: 98-102, 2012.

206. **Wang B, Li J, and Xiao X**. Adeno-associated virus vector carrying human minidystrophin genes effectively ameliorates muscular dystrophy in mdx mouse model. *Proceedings of the National Academy of Sciences of the United States of America* 97: 13714-13719, 2000.

207. **Wattin M, Gaweda L, Muller P, Baritaud M, Scholtes C, Lozano C, Gieseler K, and Kretz-Remy C**. Modulation of Protein Quality Control and Proteasome to Autophagy Switch in Immortalized Myoblasts from Duchenne Muscular Dystrophy Patients. *Int J Mol Sci* 19: 2018.

208. **Way M, Pope B, Cross RA, Kendrick-Jones J, and Weeds AG**. Expression of the N-terminal domain of dystrophin in E. coli and demonstration of binding to F-actin. *FEBS Lett* 301: 243-245, 1992.

209. **Whitehead NP, Streamer M, Lusambili LI, Sachs F, and Allen DG**. Streptomycin reduces stretch-induced membrane permeability in muscles from mdx mice. *Neuromuscul Disord* 16: 845-854, 2006.

210. **Wilke S, Krausze J, and Bussow K**. Crystal structure of the conserved domain of the DC lysosomal associated membrane protein: implications for the lysosomal glycocalyx. *BMC Biol* 10: 62, 2012.

211. **Wineinger MA, Abresch RT, Walsh SA, and Carter GT**. Effects of aging and voluntary exercise on the function of dystrophic muscle from mdx mice. *Am J Phys Med Rehabil* 77: 20-27, 1998.

212. **Winkler G, Zifko U, Nader A, Frank W, Zwick H, Toifl K, and Wanke T**. Dose-dependent effects of inspiratory muscle training in neuromuscular disorders. *Muscle Nerve* 23: 1257-1260, 2000.

213. **Wold MS, Lim J, Lachance V, Deng Z, and Yue Z**. ULK1-mediated phosphorylation of ATG14 promotes autophagy and is impaired in Huntington's disease models. *Mol Neurodegener* 11: 2016.

214. **Yilmaz O, Karaduman A, and Topaloglu H**. Prednisolone therapy in Duchenne muscular dystrophy prolongs ambulation and prevents scoliosis. *Eur J Neurol* 11: 541-544, 2004.

215. **Zachari M, and Ganley I**. The mammalian ULK1 complex and autophagy initiation. *Essays Biochem* 61: 585-596, 2017.

216. **Zeman RJ, Peng H, Danon MJ, and Etlinger JD**. Clenbuterol reduces degeneration of exercised or aged dystrophic (mdx) muscle. *Muscle Nerve* 23: 521-528, 2000.

217. **Zhang H, Ryu D, Wu Y, Gariani K, Wang X, Luan P, D'Amico D, Ropelle ER, Lutolf MP, Aebersold R, Schoonjans K, Menzies KJ, and Auwerx J**. NAD+ repletion improves mitochondrial and stem cell function and enhances life span in mice. *Science* 2016.

218. **Zhang W, ten Hove M, Schneider JE, Stuckey DJ, Sebag-Montefiore L, Bia BL, Radda GK, Davies KE, Neubauer S, and Clarke K**. Abnormal cardiac morphology, function and energy metabolism in the dystrophic mdx mouse: an MRI and MRS study. *J Mol Cell Cardiol* 45: 754-760, 2008.

219. **Zhou L, Wang H, Ren H, Chen D, Gao F, Hu Q, Fu C, Xu R, Ying Z, and Wang G**. Bcl-2-dependent upregulation of autophagy by sequestosome 1/p62 in vitro. In: *Acta Pharmacol Sin*2013, p. 651-656.

CHAPTER 3: LONG-TERM QUERCETIN DIETARY ENRICHMENT PARTIALLY PROTECTS DYSTROPHIC SKELETAL MUSCLE

Hannah R. Spaulding[1], Christopher G. Ballmann[2], John C. Quindry[2]

and Joshua T. Selsby[1]

[1]Department of Animal Science, Iowa State University, Ames, IA
[2]School of Kinesiology, Auburn University, Auburn, AL

Modified from a manuscript published in
PLoS One. 2016; 11(12): e0168293.

Abstract

Duchenne muscular dystrophy (DMD) results from a genetic lesion in the dystrophin gene and leads to progressive muscle damage. PGC-1α pathway activation improves muscle function and decreases histopathological injury. We hypothesized that mild disease found in the limb muscles of mdx mice may be responsive to quercetin-mediated protection of dystrophic muscle via PGC-1α pathway activation. To test this hypothesis muscle function was measured in the soleus and EDL from 14 month old C57, mdx, and mdx mice treated with quercetin (mdxQ; 0.2% dietary enrichment) for 12 months. Quercetin reversed 50% of disease-related losses in specific tension and partially preserved fatigue resistance in the soleus. Specific tension and resistance to contraction-induced injury in the EDL were not protected by quercetin. Given some functional gain in the soleus it was probed with histological and biochemical approaches, however, in dystrophic muscle histopathological outcomes were not improved by quercetin and

suppressed PGC-1α pathway activation was not increased. Similar to results in the diaphragm from these mice, these data suggest that the benefits conferred to dystrophic muscle following 12 months of quercetin enrichment were underwhelming. Spontaneous activity at the end of the treatment period was greater in mdxQ compared to mdx indicating that quercetin fed mice were more active in addition to engaging in more vigorous activity. Hence, modest preservation of muscle function (specific tension) and elevated spontaneous physical activity largely in the absence of tissue damage in mdxQ suggests dietary quercetin may mediate protection.

Key Words: mdx, Duchenne muscular dystrophy, PGC-1alpha

Introduction

Duchenne muscular dystrophy (DMD) is caused by the absence of the dystrophin protein, which acts to transmit force between cytoskeleton and extracellular matrix via the dystrophin glycoprotein complex (DGC) [1, 2]. The absence of dystrophin results in cellular dysfunction including decreased calcium homeostasis, increased necrosis, and disruption of DGC along with other secondary effects producing whole muscle dysfunction. Utrophin, a dystrophin-like protein, participates in DGC formation, stability, and function in the absence of dystrophin [3, 4], hence utrophin upregulation remains an area of intense research interest [5-8]. Utrophin transcription can be driven by the exercise-sensitive PGC-1α pathway [9], however, attempts to use various exercise modalities as interventions for DMD have been met with mixed results [10-13]. Direct activation of the PGC-1α pathway using transgenic and gene transfer approaches yields consistently positive results using both prevention and rescue paradigms [14-18]. Under these conditions PGC-1α pathway activation led to increased muscle function, decreased muscle

damage, increased utrophin abundance and a physiologic and metabolic type I shift in PGC-1α over-expressing dystrophic muscle compared to control muscle [14-18].

Given the emerging success of PGC-1α pathway activation for treating dystrophic pathology we next searched for PGC-1α activators that already had FDA approval or were freely available to minimize time needed to impact patients. Quercetin, a flavonoid with antioxidant and anti-inflammatory properties [19], drives the PGC-1α pathway through SIRT1 deacetylase [20, 21] or AMPK activity [22]. We found previously that six months of dietary quercetin enrichment decreased histopathology in diaphragms [23] and hearts [24] from dystrophic mice. In a follow up experiment, we found that 12 months of quercetin dietary enrichment transiently protected dystrophic diaphragms and respiratory function though a developed quercetin insensitivity ultimately minimized therapeutic benefits [25]. Given that limb muscles from mdx mice suffer a more mild disease than diaphragms we reasoned that quercetin may continue to protect limb muscle from progressive disease and, therefore, that quercetin would have a role as a therapeutic intervention early in the disease process and would be most efficacious in the youngest DMD patients. We hypothesized that muscle function would be improved and histological injury would be decreased in dystrophic soleus and extensor digitorum longus (EDL) following 12 months of dietary quercetin enrichment compared to muscles taken from mice maintained on a control diet.

Methods

Ethical Approval and Animal Treatments

The Institutional Animal Care and Use Committee at Auburn University reviewed and approved all procedures utilized in this work. Previous work, including a detailed

study design, has been previously published [25]. Briefly, eight male C57 mice and 16 male mdx mice (Jackson Laboratories) were acclimated for one week prior to the beginning of the experiments. At 2 months of age a standard AIN93 diet (Bioserv, Flemington, NJ) was provided for C57 mice (n=8) and control mdx mice (n=8), while treated mdx mice received an AIN93 diet supplemented with 0.2% quercetin (n=8) for 12 months. Both water and food were available *ad libitum*. Throughout the study period animal food, water, bedding, general health, and environmental conditions were checked twice daily by a combination of research and vivarium staff. Over the course of this longitudinal investigation one mouse from each group was identified as severely ill (monitored criteria included: physical appearance, weight loss, and behavior). To minimize suffering animals were euthanized via CO2 inhalation followed by exsanguination consistent with our IACUC protocol. Changes in body weight throughout the study period have been previously reported as have average daily food consumption (3.9 g/day) and resultant daily quercetin exposure (204 mg/kg/day) [25]. At 14 months of age, activity was measured using an ethological approach. Soleus and EDL *in vitro* muscle function were assessed at the Physiological Assessment Core of the Wellstone Muscular Dystrophy Cooperative Center at the University of Pennsylvania. Prior to *in vitro* function all animals were assigned new numbers to establish blinded data collection and further preserve blinded conditions upon distribution of tissues for subsequent analyses. Sample numbers and animal groups were revealed prior to biochemical analysis for properly controlled experiments. Due to the length of this study several animals did not reach 14 months of age or tissues were unusable for some measures, thus number/group is identified for all measurements in the figure legends.

Animal Activity

At 14 months of age, activity was recorded for 10 consecutive minutes in conscious mice and were averaged over two observation periods for occurrences of sitting, grooming, eating/drinking, socializing, standing, walking, wall pacing, running, and jumping. This technique represents a species-specific ethogram (repertoire of discrete animal activities) using the "0-1 recording" method, which has been applied across many species. When an observed mouse performed a particular activity (sitting, walking, etc.) it was recorded as 1. Activity counts were performed on two occasions by two investigators and activity recordings were performed every 15 seconds for 10 minutes and collectively equaled 40 activity time periods. Twenty total minutes of activity were recorded for the two sessions and final counts were averaged from scores generated by the two blinded observers. Activity counts were performed at a common time at the end of the photo light and photo dark cycles [26].

Tissue Collection and Muscle Function

After 12 months of treatment, mice were sedated to a surgical level of anesthesia using a ketamine/xylazine cocktail at the Physiological Assessment Core of the Wellstone Muscular Dystrophy Cooperative Center at the University of Pennsylvania (now housed at the University of Florida). Upon sedation, soleus and EDL muscles were removed from each animal and used for measures of muscle function. *In vitro* muscle function was measured using standard techniques as has been done previously [27-29]. Briefly, the tetanic force was determined in the EDL and soleus using stimulation of 120 Hz and 100 Hz, respectively. To determine fatigue resistance the soleus was stimulated for 10 minutes with one contraction/sec (100 Hz for 330 msec with 200 μsec pulse). To determine

resistance to contraction-induced injury the EDL was given a series of five lengthening contractions (500 msec at 80 hz followed by 10% beyond Lo for 20 msec). To determine fatigue resistance and resistance to contraction induced injury data are expressed relative to peak force produced during the first contraction. Specific tension and cross sectional area were calculated using standard equations [30]. As there were changes in soleus muscle function suggestive of a therapeutic effect tissues were examined with histological and biochemical approaches. Following the fatigue test the soleus was frozen in melting isopentane and used for histological measures while the contralateral soleus was snap frozen upon removal and used for biochemical measures.

Histological Analyses

Muscle injury and fibrosis were measured as recently described [25]. Briefly, 10 μm sections were cut and stained with either hematoxylin and eosin (H&E) or Masson's Trichrome (KTMTR, American MasterTech, Lodi, CA). H&E and trichrome stained slides were imaged with an inverted DMI3000 B microscope and QICAM MicroPublisher 5.0 (MP5.0-RTV-CLR-10, QIMAGING) camera using QCapture software. Trained, blinded technicians took 3-5 images at 10x magnification for each soleus section. Overlapping images allowed for reconstruction of the entire muscle cross section using the Photoshop merge option (Adobe). H&E sections were then analyzed by these technicians using Open Lab (Improvision) to quantify 1) total number of muscle cells, 2) central nucleation, 3) extracellular nuclei, 4) necrotic area, and 5) total contractile area (area of the section comprised of muscle fibers). Trichrome staining was used to quantify areas of fibrosis.

Immunohistochemistry was utilized to confirm fibrosis findings and measure fiber area distribution. To measure fibrosis and fiber area distribution anti-fibronectin (Sigma,

St. Louis, MO) and anti-laminin (1:100, Thermo Scientific, Waltham, MA) primary antibodies were applied to the samples at 4°C overnight, respectively. At room temperature, sections were exposed to donkey anti-rabbit rhodamine secondary antibody (1:200, Millipore, Billerica, MA) for 1 hour. 3-5 non-overlapping images were taken with a QICAM 12-bit Mono Fast 1394 Cooled (QIC-F-M-12-C, QIMAGING) camera at 10x magnification attached to the Leica microscope under blinded conditions.

qPCR

Measurement of transcript abundance was performed in the soleus employing Fluidigm technology as we have done previously [25]. Our complete list of primer pairs has also been previously published. Briefly, mRNA was isolated using TriZol (ThermoScientific) and reverse transcribed to cDNA using QuantiTect Reverse Transcriptase Kit (Qiagen) as described by the manufacture, but random hexamers (IDT PreMade Primers) were substituted for the RT Primer Mix (Qiagen). cDNA was further prepared as suggested by Fluidigm then loaded onto a 96x96 Fluidigm chip.

Western Blot

Measurement of relative protein abundance was performed as previously described. Briefly, 200 µl of whole muscle buffer (10mM Sodium Phosphate buffer, pH 7.0, 2% SDS) was added to powdered soleus tissue and homogenized. Once homogenized, samples were spun at 20,000 RCF for 15 minutes and supernatant containing the protein was collected for western blotting. Protein concentration was measured using Pierce BCA Protein Assay Kit (ThermoScientific, 23225) and diluted with 2x Laemmli buffer. Once diluted, samples were heated for 5 minutes at 95°C. Thirty micrograms of protein were separate by mass using 4-20% gradient gels (Lonza). Separation was run at 60 volts for 20 minutes followed

by 120 volts for 60 minutes, then transferred for 60 minutes at 100 volts onto a nitrocellulose membrane. Membranes were probed for the following antibodies overnight at 4°C then incubated for 1 hour with anti-rabbit secondary: phosphorylated (p-) AMPKα (thr172) (P 1:500, S 1:2000, Cell Signaling), SIRT1 (P 1:500, S 1:2000, Millipore), Histone 3 Lysine 9 Acetylation (H3K9ac) (P 1:1000, S 1:5000 in 0% milk, Cell Signaling), ERRα (P 1:1000, S 1:2000), TFAM (P 1:375 in 1% milk, S 1:1000 in 0% milk), Cytochrome C (P 1:1000, S 1:2000), SDHA (P 1:500, S 1:2000), VDAC (P 1:300, S 1:2000).

Statistics

All data were assessed using one-way ANOVA with a Newman-Keuls post-hoc test to assess significance of $p<0.05$. Unless otherwise noted, data are shown as mean ± SEM.

Results

To determine the extent to which quercetin decreased dystrophic injury mdx mice were treated with a 0.2% quercetin enriched diet or maintained on a control diet from 2-14 months of age. We have previously reported detailed food consumption and growth data [25]. In brief, animal growth was largely similar between groups though the mdxQ group was statistically smaller than the mdx group at the conclusion of the investigation (C57 – 44.07 ± 2.13 g, mdx – 56.57 ± 2.30 g, mdxQ – 38.07 ± 2.35 g). In the soleus, dystrophin-deficiency caused a 40% increase in absolute muscle mass regardless of treatment (Table 1). Relative muscle mass was nearly doubled in mdx compared to C57 and mdxQ was 11% greater ($p<0.05$) than mdx (Table 1). In the EDL, absolute mass was 30 and 13% greater in mdx compared to C57 and mdxQ, respectively, and mdxQ was 20% greater than C57 (Table 1). Relative EDL mass in dystrophic mice was increased by 60% compared to C57 (Table 1).

***In vitro* function**

Tetanic force was similar between groups in the soleus. Specific tension, however, was decreased by 40% in mdx compared to C57. Importantly, dietary quercetin enrichment attenuated approximately 50% of this loss (Fig 1). Following a fatigue protocol, the percent of initial force produced by the mdx soleus was decreased by 50% compared to C57. The addition of quercetin appeared to attenuate this loss but this numerical difference was not statistically significant from the other treatments (Fig 1C).

Consistent with the soleus muscle, tetanic tension in the EDL was similar between groups (Table 1). Specific tension was decreased by 36% in mdx and mdxQ groups compared to C57 (Figure 1B). In addition, dietary quercetin failed to provide protection from eccentric injury in the EDL as the percent decline was similar in mdx and mdxQ and considerably less than C57 for each contraction (Fig 1E).

Animal activity was assessed by counts of sedentary and active behaviors during 15 second sampling windows averaged over two 10 minute observation periods. For the sitting/standing metrics, mdx mice were 35% more stationary than C57 and mdxQ was less stationary than both C57 and mdx mice by 65% and 74%, respectively (Fig 2A). Total activity followed a similar pattern such that mdx were 47% less active than C57 whereas mdxQ were 2-fold more active than C57 (Fig 2B).

Histopathology

Given that improved specific tension and fatigue resistance in the soleus provided some limited optimism for a successful intervention histological and biochemical studies were pursued. The quantity of extracellular nuclei was increased by 4-fold and the percent of cells with a centralized nucleus was increased by 15-fold in dystrophic muscle compared

to healthy muscle and both measures were resistant to quercetin (Fig 3A-F). Consistent with disease-related injury the total contractile area was decreased 20% in mdx and mdxQ mice compared to C57 due to an accumulation of non-contractile material in the whole muscle cross-section (Fig 3G). Fibrotic tissue in the soleus of mdx mice measured via trichrome staining was 3.6-fold higher while mdxQ mice were 4-fold higher than C57. In addition, trichrome staining revealed that fibrosis in mdxQ increased by 12.5% compared to mdx (Fig 4A-D). To verify these changes we also assessed relative fibronectin abundance using an immunohistochemical approach. We found that fibronectin was 9.0-fold higher in both mdx and mdxQ compared to C57 and importantly, that mdx and mdxQ were similar between groups (Fig 5A-D).

Lastly, we also measured fiber area distribution (Fig 6A-D). We found that at 14 months of age mean fiber area was similar between groups, however, the variance coefficient was 40% higher in dystrophic muscle compared to healthy muscle (Fig 6E-F). Further, we found that dystrophic muscle had a greater frequency of smaller diameter fibers and a smaller frequency of larger diameter fibers compared to healthy muscle (Fig 6G). While dystrophic muscle tended to have a greater frequency of very large fibers (>3000 μm) this observation was not statistically significant from C57 (Fig 6D).

Biochemistry

We also assessed the impact of dystrophin deficiency on alterations in transcript expression and the degree to which these were corrected by dietary quercetin enrichment (Table 2). Our findings largely suggest that following 12 months of quercetin treatment transcript expression was similar between mdx and mdxQ, however, numerous differences between dystrophic and healthy muscle were noted. Specifically, metabolic

transcripts were significantly decreased in mdx mice compared to C57 as were transcripts related to mitochondrial biogenesis, redox balance, and cellular stability.

Lastly, we evaluated the pathway driven by quercetin (Fig 7). SIRT1 promotes PGC-1α pathway activity [31-33], thus protein abundance of SIRT1 was measured and was 20% higher in dystrophic muscle regardless of treatment compared to healthy muscle. In contrast, SIRT1 activity was lower in dystrophic muscle as histone 3 lysine 9 acetylation (H3K9ac) was 80% higher in dystrophic muscle compared to control. Due to the deacetylase activity of active SIRT1 increased H3K9ac is indicative of decreased SIRT1 activity. Downstream pathway components and end products of the PGC-1α pathway were similar between all groups. Due to the potential function of quercetin as an AMPK activator [32, 34, 35], pAMPK T172 was measured to assess AMPK activity. We found that AMPK activity was lower by more than 40% in dystrophic muscle compared to control, and independent of feeding treatment.

Discussion

Duchenne muscular dystrophy is a muscle wasting disease that leads to progressive deterioration of muscle function and muscle health. Muscle atrophy and increased muscle injury negatively impact motor function and eventually lead to death from cardiac or respiratory failure. Protection of muscle from secondary effects of dystrophin deficiency such as inflammation, metabolic dysfunction and free radical injury while simultaneously driving utrophin expression and mitochondrial biogenesis may slow disease progression and prolong muscle function. Up regulation of PGC-1α in dystrophic muscle is well recognized to maintain muscle function, decrease histological damage and increase utrophin protein abundance and localization [14-18]. Currently needed is a pragmatic

strategy to translate this mechanistic understanding into clinical practice. As such, quercetin is a promising therapeutic supplement that exhibits both antioxidant and anti-inflammatory properties and also drives mitochondrial biogenesis and utrophin upregulation through PGC-1α activation. Supporting a rationale for clinical applicability, quercetin is commonly sold as an over-the-counter supplement and is readily available to the DMD community. Experimental evidence to support this postulate is derived from an initial investigation where we found that a 6 month dietary intervention with quercetin decreased histological injury in the dystrophic diaphragm [23] and heart [24]. In a subsequent 12-month study the beneficial effects following six months of treatment were recapitulated [25]. These effects appeared to be transient, however, in that control diaphragms from dystrophic mice were functionally, histologically, and biochemically indistinguishable from quercetin-treated diaphragms by the end of the study period. We hypothesized that advanced disease progression in the diaphragm may limit the therapeutic potential of quercetin and that the milder phenotype found in dystrophic limb muscles would be a more amenable intracellular environment to support the therapeutic effects of quercetin.

Similar to our previous findings in diaphragms [25] from the same animals used herein, most outcomes examined at the end of the treatment period were not responsive to the quercetin intervention. Of note, dietary quercetin consumption was associated with prevention of approximately 50% of the disease-related losses in specific tension and fatigue resistance in the soleus. Improved specific tension in the soleus is surprising considering histological parameters were not improved by dietary quercetin enrichment. Hence, muscle function was improved in quercetin-treated mdx mice compared to control

mice despite similar degrees of muscle damage/unit cross sectional area. We encourage future studies intended to improve clarity regarding the broad therapeutic effects of this strategy.

While these functional benefits are cause for limited enthusiasm our biochemical and histological findings require caution. On the whole, transcript expression was similar between treated and untreated mdx mice and cellular functions probed in this investigation were largely suppressed compared to C57. Published studies indicate that quercetin drives the PGC-1α pathway through the deacetylase activity of SIRT1 [32, 36, 37] such that SIRT1 deacetylates PGC-1α and ultimately leads to mitochondrial biogenesis, increased utrophin abundance, a shift toward more oxidative fiber types, and decreased disease severity [14-18]. We previously noted quercetin insensitivity in diaphragm tissues marked by increased SIRT1 protein abundance coupled with impaired SIRT1 function [25]. In this investigation a similar mechanism is apparent despite continued quercetin supplementation. We proposed previously that decreased ATP content found in dystrophic muscle may be part of that mechanism by limiting the potential of quercetin to increase SIRT1 activity via a blunted ATP/cAMP/pSIRT1 pathway. Alternatively, we speculate that the lower abundance of NAD+ in dystrophic muscle [38], a cofactor of SIRT1 activation [39], may also limit the capacity of quercetin to drive SIRT1 activity. Intriguingly, in a short-term investigation, supplementation with nicotinamide riboside to augment the muscle NAD+ pool was sufficient to increase regeneration following cardiotoxin injection in dystrophic muscle [40]. Hence, we propose that the combination of quercetin, to increase SIRT1 activity, and nicotinamide riboside, to increase muscle NAD+ content in order to sustain increased SIRT1 activity, may provide long term

therapeutic relief and greater impact than either approach applied independently and may overcome limitations in SIRT1 activation caused by age and/or disease severity.

Given the largely unremarkable histological and biochemical findings in this investigation, one of the most notable findings in the current study was the quercetin-mediated elevations in spontaneous activity in caged mice. It is unclear if quercetin directly impacts behavior such that it serves to stimulate activity via mechanisms beyond the scope of this investigation [41] or below our detection threshold, or if quercetin supports improved function such that it permits increased spontaneous activity. Nevertheless, that there was increased spontaneous physical activity provides an alternative interpretation of data contained herein. Increased physical activity may hasten the decline of dystrophic muscle [42-44]; hence, improved specific tension in the face of increased activity supports the potential therapeutic role of quercetin. This effect seems particularly profound in the diaphragm as increased spontaneous physical activity led to significantly impaired diaphragmatic function in animals of similar age [11]. Hence, that respiratory and diaphragmatic function and histopathology were not further impaired compared to untreated mdx mice in our previous investigation [25] may also be suggestive of a therapeutic success. These histopathological results were largely recapitulated in limb muscle in this investigation, aside from the potential of increased fibrosis detected via trichrome staining but not fibronectin immunohistochemistry. Given this integrated understanding from an established model of DMD, the current findings may be all the more important in the eventual translation of findings to clinical populations.

Comprehensive reports comparing dystrophic and healthy muscle from old animals, as performed currently, are rarely reported in the existing literature [45]. Absolute

and relative muscle mass was increased in dystrophic muscle compared to age-matched C57 mice suggestive of pseudohypertrophy. Further, tetanic force was similar between groups but specific tension was greatly impaired in both the soleus and EDL at the end of the treatment periods indicating a compromised muscle quality in mdx mice. Consistent with previous .reports, in dystrophic mice the soleus had compromised resistance to fatigue [43] and the EDL was more susceptible to contraction-induced injury compared to control [2]. Histologically, the dystrophic soleus had damage consistent with dystrophinopathy including increased centralized nuclei, necrotic area, immune cell infiltration, and fibrosis [46, 47]. Fiber area distribution was also consistent with dystrophin deficiency with a large proportion of small diameter fibers and much higher variability in fiber size resulting in similar mean fiber area compared to control [48]. Our biochemical evaluation found decreased transcript expression related to mitochondrial biogenesis, mitochondrial content, resistance to oxidative stress, and cellular stability.

In total, the results of this investigation are in agreement with our previous report of age-dependent quercetin insensitivity leading to underwhelming therapeutic effects by the conclusion of the study period. Specifically, quercetin insensitivity is made clear by a failure to increase SIRT1 activity and may be due to decreased ATP and/or NAD+ content in dystrophic muscle. Future investigations should combine quercetin with an agent to increase the NAD+ pool in order to maximize therapeutic benefits. Furthermore, this study underscores the importance of long-term investigations as therapeutics applied to the DMD community would be expected to be employed for years. Only after 8 months of treatment was the transient therapeutic nature of quercetin apparent in respiratory function [25]. Given the histological and biochemical data from the soleus improved function will likely

be lost with advancing age. Data interpretation is complicated by our finding of increased spontaneous activity in quercetin-treated mice without widespread activity-induced tissue damage in the limb muscles. This latter finding highlights a novel experimental facet of this investigation and may hold implications for clinical translation.

References

1. Ervasti, J.M., et al., *Alpha-dystroglycan deficiency correlates with elevated serum creatine kinase and decreased muscle contraction tension in golden retriever muscular dystrophy.* FEBS Lett, 1994. **350**(2-3): p. 173-6.

2. Petrof, B.J., et al., *Dystrophin protects the sarcolemma from stresses developed during muscle contraction.* Proc Natl Acad Sci U S A, 1993. **90**(8): p. 3710-4.

3. Tinsley, J.M., et al., *Amelioration of the dystrophic phenotype of mdx mice using a truncated utrophin transgene.* Nature, 1996. **384**(6607): p. 349-53.

4. Tinsley, J., et al., *Expression of full-length utrophin prevents muscular dystrophy in mdx mice.* Nat Med, 1998. **4**(12): p. 1441-4.

5. Wakefield, P.M., et al., *Prevention of the dystrophic phenotype in dystrophin/utrophin-deficient muscle following adenovirus-mediated transfer of a utrophin minigene.* Gene Ther, 2000. **7**(3): p. 201-4.

6. Cerletti, M., et al., *Dystrophic phenotype of canine X-linked muscular dystrophy is mitigated by adenovirus-mediated utrophin gene transfer.* Gene Ther, 2003. **10**(9): p. 750-7.

7. Peladeau, C., et al., *Combinatorial therapeutic activation with heparin and AICAR stimulates additive effects on utrophin A expression in dystrophic muscles.* Hum Mol Genet, 2016. **25**(1): p. 24-43.

8. Gordon, B.S., D.C. Delgado Diaz, and M.C. Kostek, *Resveratrol decreases inflammation and increases utrophin gene expression in the mdx mouse model of Duchenne muscular dystrophy.* Clin Nutr, 2013. **32**(1): p. 104-11.

9. Angus, L.M., et al., *Calcineurin-NFAT signaling, together with GABP and peroxisome PGC-1{alpha}, drives utrophin gene expression at the neuromuscular junction.* Am J Physiol Cell Physiol, 2005. **289**(4): p. C908-17.

10. Hyzewicz, J., U.T. Ruegg, and S.i. Takeda, *Comparison of Experimental Protocols of Physical Exercise for mdx Mice and Duchenne Muscular Dystrophy Patients.* Journal of Neuromuscular Diseases, 2015. **2**(4): p. 325-342.

11. Selsby, J.T., et al., *Long-term wheel running compromises diaphragm function but improves cardiac and plantarflexor function in the mdx mouse.* J Appl Physiol (1985), 2013. **115**(5): p. 660-6.

12. Hourde, C., et al., *Voluntary physical activity protects from susceptibility to skeletal muscle contraction-induced injury but worsens heart function in mdx mice.* Am J Pathol, 2013. **182**(5): p. 1509-18.

13. Barbin, I.C., et al., *Diaphragm degeneration and cardiac structure in mdx mouse: potential clinical implications for Duchenne muscular dystrophy.* J Anat, 2016. **228**(5): p. 784-91.

14. Selsby, J.T., et al., *Rescue of dystrophic skeletal muscle by PGC-1alpha involves a fast to slow fiber type shift in the mdx mouse.* PLoS One, 2012. **7**(1): p. e30063.

15. Godin, R., et al., *Peroxisome proliferator-activated receptor γ coactivator 1-α gene transfer restores mitochondrial biomass and improves mitochondrial calcium handling in post-necrotic mdx mouse skeletal muscle.* J Physiol, 2012. **590**(Pt 21): p. 5487-502.

16. Hollinger, K., et al., *Rescue of dystrophic skeletal muscle by PGC-1 alpha involves restored expression of dystrophin-associated protein complex components and satellite cell signaling.* American Journal of Physiology-Regulatory Integrative and Comparative Physiology, 2013. **305**(1): p. R13-R23.

17. Hollinger, K. and J.T. Selsby, *PGC-1alpha gene transfer improves muscle function in dystrophic muscle following prolonged disease progress.* Exp Physiol, 2015. **100**(10): p. 1145-58.

18. Handschin, C., et al., *PGC-1alpha regulates the neuromuscular junction program and ameliorates Duchenne muscular dystrophy.* Genes Dev, 2007. **21**(7): p. 770-83.

19. Boots, A.W., et al., *Quercetin reduces markers of oxidative stress and inflammation in sarcoidosis.* Clin Nutr, 2011. **30**(4): p. 506-12.

20. Nemoto, S., M.M. Fergusson, and T. Finkel, *SIRT1 Functionally Interacts with the Metabolic Regulator and Transcriptional Coactivator PGC-1α.* 2005.

21. Guedes-Dias, P. and J.M. Oliveira, *Lysine deacetylases and mitochondrial dynamics in neurodegeneration.* Biochim Biophys Acta, 2013. **1832**(8): p. 1345-59.

22. Jager, S., et al., *AMP-activated protein kinase (AMPK) action in skeletal muscle via direct phosphorylation of PGC-1alpha.* Proc Natl Acad Sci U S A, 2007. **104**(29): p. 12017-22.

23. Hollinger, K., et al., *Long-term quercetin dietary enrichment decreases muscle injury in mdx mice.* Clin Nutr, 2015. **34**(3): p. 515-22.

24. Ballmann, C., et al., *Histological and biochemical outcomes of cardiac pathology in mdx mice with dietary quercetin enrichment.* Exp Physiol, 2015. **100**(1): p. 12-22.

25. Selsby, J.T., et al., *Oral quercetin administration transiently protects respiratory function in dystrophin deficient mice.* J Physiol, 2016.

26. Martin, P. and P. Bateson, *Measuring Behaviour*. 2007, Cambridge, UK: Cambridge University Press,.

27. Selsby, J., et al., *Leupeptin-based inhibitors do not improve the mdx phenotype.* Am J Physiol Regul Integr Comp Physiol, 2010. **299**(5): p. R1192-201.

28. Selsby, J.T., *Increased catalase expression improves muscle function in mdx mice.* Exp Physiol, 2011. **96**(2): p. 194-202.

29. Selsby, J., et al., *Rescue of dystrophic skeletal muscle by PGC-1a involves a fast to slow fiber type shift in the mdx mouse.* PLoS One, 2012. **7**(1): p. e30063.

30. Brooks, S.V. and J.A. Faulkner, *Contractile properties of skeletal muscles from young, adult and aged mice.* J Physiol, 1988. **404**: p. 71-82.

31. Davis, J.M., et al., *Quercetin increases brain and muscle mitochondrial biogenesis and exercise tolerance.* Am J Physiol Regul Integr Comp Physiol, 2009. **296**(4): p. R1071-7.

32. Dong, J., et al., *Quercetin reduces obesity-associated ATM infiltration and inflammation in mice: a mechanism including AMPKalpha1/SIRT1.* J Lipid Res, 2014. **55**(3): p. 363-74.

33. Zhao, L.R., et al., *Quercetin protects against high glucose-induced damage in bone marrow-derived endothelial progenitor cells.* Int J Mol Med, 2014. **34**(4): p. 1025-31.

34. Ahn, J., et al., *The anti-obesity effect of quercetin is mediated by the AMPK and MAPK signaling pathways.* Biochem Biophys Res Commun, 2008. **373**(4): p. 545-9.

35. Suchankova, G., et al., *Concurrent regulation of AMP-activated protein kinase and SIRT1 in mammalian cells.* Biochem Biophys Res Commun, 2009. **378**(4): p. 836-41.

36. Howitz, K.T., et al., *Small molecule activators of sirtuins extend Saccharomyces cerevisiae lifespan.* Nature, 2003. **425**(6954): p. 191-196.

37. Gerhart-Hines, Z., et al., *Metabolic control of muscle mitochondrial function and fatty acid oxidation through SIRT1/PGC-1alpha.* Embo J, 2007. **26**(7): p. 1913-23.

38. Chalkiadaki, A., et al., *Muscle-specific SIRT1 gain-of-function increases slow-twitch fibers and ameliorates pathophysiology in a mouse model of duchenne muscular dystrophy.* PLoS Genet, 2014. **10**(7): p. e1004490.

39. Imai, S., et al., *Transcriptional silencing and longevity protein Sir2 is an NAD-dependent histone deacetylase.* Nature, 2000. **403**(6771): p. 795-800.

40. Zhang, H., et al., *NAD+ repletion improves mitochondrial and stem cell function and enhances life span in mice.* Science, 2016.

41. Alexander, S.P., *Flavonoids as antagonists at A1 adenosine receptors.* Phytother Res, 2006. **20**(11): p. 1009-12.

42. Camerino, G.M., et al., *Gene expression in mdx mouse muscle in relation to age and exercise: aberrant mechanical-metabolic coupling and implications for pre-clinical studies in Duchenne muscular dystrophy.* Hum Mol Genet, 2014. **23**(21): p. 5720-32.

43. Wineinger, M.A., et al., *Effects of aging and voluntary exercise on the function of dystrophic muscle from mdx mice.* Am J Phys Med Rehabil, 1998. **77**(1): p. 20-7.

44. Bueno Junior, C.R., et al., *Combined effect of AMPK/PPAR agonists and exercise training in mdx mice functional performance.* PLoS One, 2012. **7**(9): p. e45699.

45. Lynch, G.S., et al., *Force and power output of fast and slow skeletal muscles from mdx mice 6-28 months old.* J Physiol, 2001. **535**(Pt 2): p. 591-600.

46. Pastoret, C. and A. Sebille, *mdx mice show progressive weakness and muscle deterioration with age.* J Neurol Sci, 1995. **129**(2): p. 97-105.

47. Stedman, H.H., et al., *The mdx mouse diaphragm reproduces the degenerative changes of Duchenne muscular dystrophy.* Nature, 1991. **352**(6335): p. 536-9.

48. Anderson, J.E., B.H. Bressler, and W.K. Ovalle, *Functional regeneration in the hindlimb skeletal muscle of the mdx mouse.* J Muscle Res Cell Motil, 1988. **9**(6): p. 499-515.

Figures and Tables

Table 1. Soleus and EDL muscle weights and function. Rel – relative * indicates significantly different from C57; # indicates significantly different from mdx. C57 (n=6-7) mdx (n=6) mdxQ (n=5-6).

	Soleus			EDL		
	C57	**mdx**	**mdxQ**	**C57**	**Mdx**	**mdxQ**
Mass (mg)	11.39 ± 0.17	17.61 ± 0.54*	15.96 ± 1.08*	12.73 ± 0.31	18.65 ± 0.67*	16.30 ± 0.76*#
Rel Mass (mg/g)	0.25 ± 0.01	0.45 ± 0.01*	0.49 ± 0.02*#	0.28 ± 0.01	0.47 ± 0.01*	0.47 ± 0.03*
Tetanic Force (mN)	224.7 ± 8.1	209.6 ± 21.5	252.9 ± 8.8	506.8 ± 13.7	461.1 ± 33.4	451.2 ± 13.0

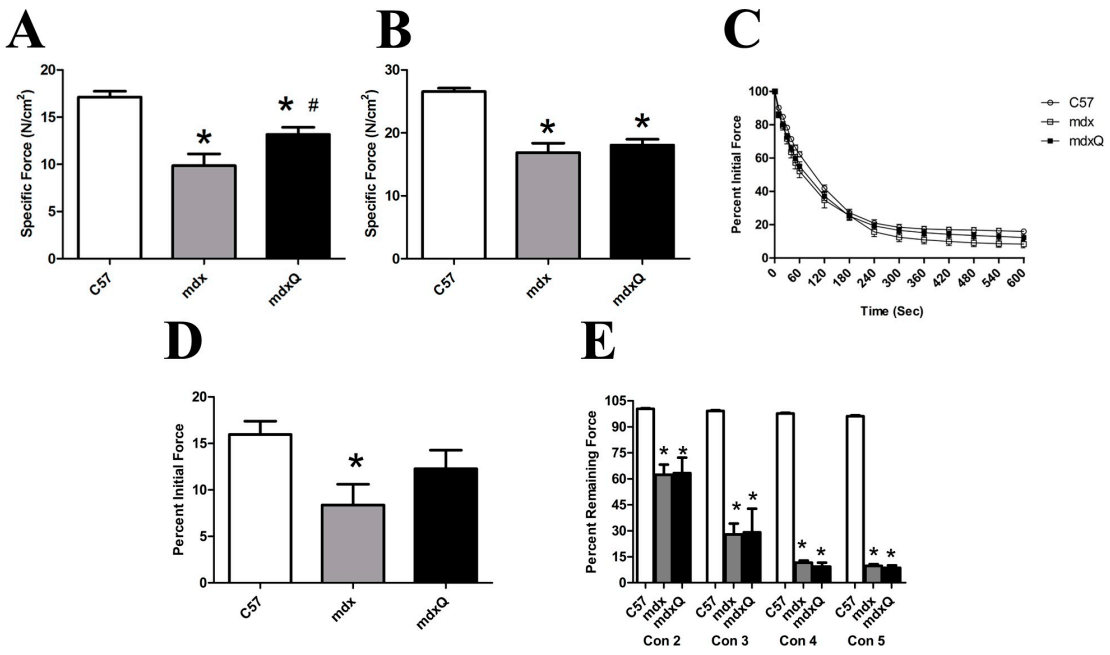

Figure 1. Soleus and EDL muscle function at 14 months of age. A) Specific tension measured in the soleus and B) in the EDL. C) The soleus was then subjected to a fatigue test where it was stimulated once per second for 10 minutes. Force was normalized to force produced in the first contraction. D) The relative force produced in the final contraction is shown. Relative force produced in the final contraction was significantly less in mdx than C57. E) The EDL was subjected to a series of five eccentric contractions and peak force normalized to peak force generated in the first contraction. * indicates significantly different from C57; # indicates significantly different from mdx. C57 (n=7) mdx (n=6) mdxQ (n=6).

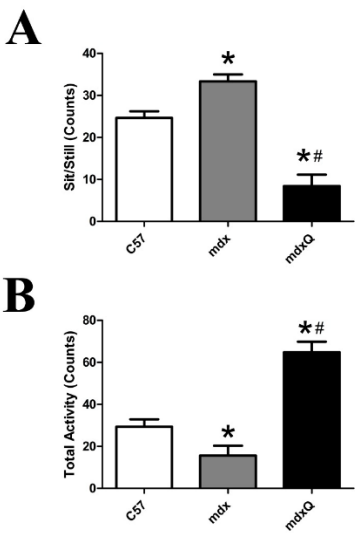

Figure 2. Animal activity was increased by dietary quercetin enrichment. At the conclusion of the investigation animal behavior was quantified using an ethological approach where a 10 minute observation period was divided into 15 second blocks. A) The number of time blocks spent sitting or exhibiting sedentary behavior was quantified. B) We also quantified the number of active behaviors. * indicates significantly different from C57; # indicates significantly different from mdx. C57 (n=7) mdx (n=7) mdxQ (n=6).

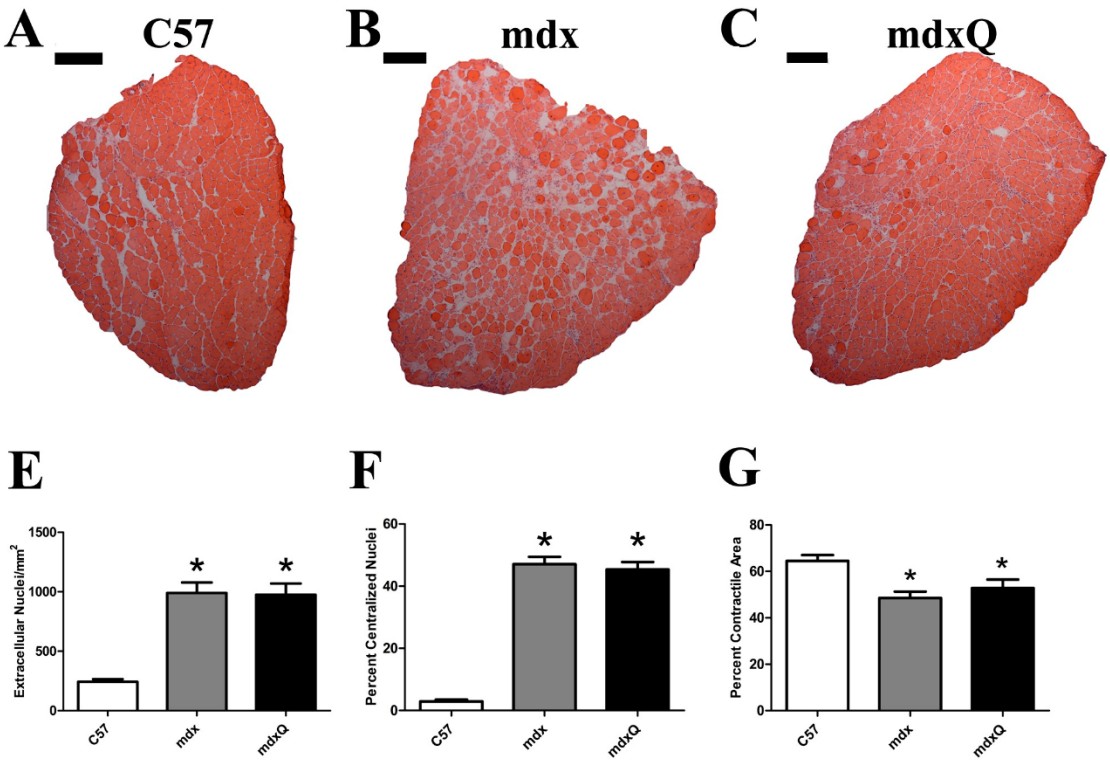

Figure 3. Dystrophin deficiency causes histological injury that is not corrected by quercetin. A-C) Representative images from H&E-stained, reconstructed soleus muscle cross sections. D) Extra cellular nuclei, E) centralized nuclei, and F) total contractile area were calculated. * indicates significantly different from C57. Width of black bar represents 250 microns. C57 (n=7) mdx (n=6) mdxQ (n=6).

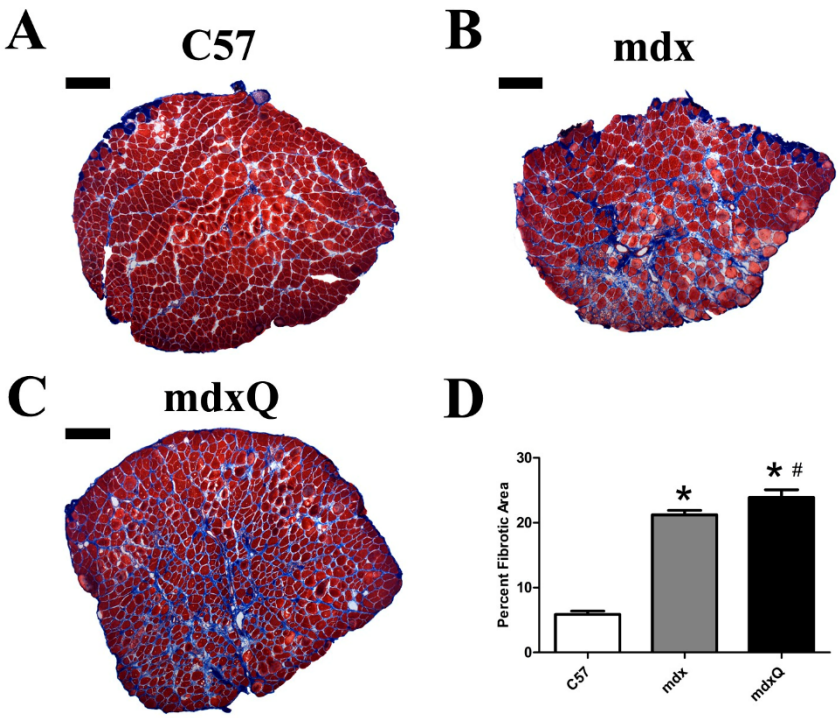

Figure 4. Dystrophin deficiency increased muscle fibrosis. A-C) Representative images from trichrome-stained, reconstructed soleus cross sections. D) Total fibrotic area was calculated by quantifying the blue staining material in the entire muscle cross section. * indicates significantly different from C57. Width of black bar represents 250 microns. C57 (n=7) mdx (n=6) mdxQ (n=6).

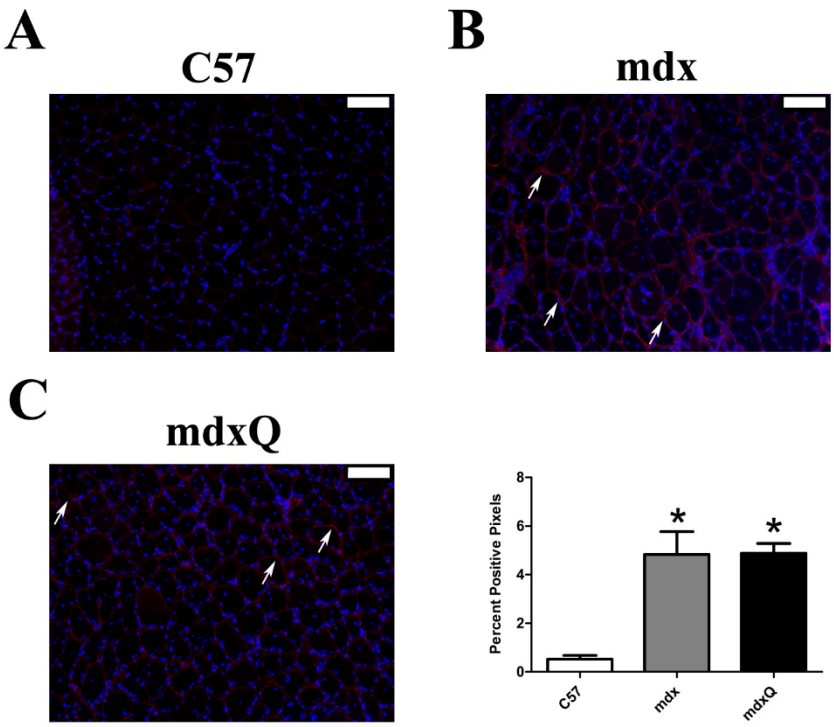

Figure 5. Dystrophin deficiency increased fibronectin in soleus muscles compared to healthy muscles. A-C) Representative 10x immunohistochemical images for fibronectin (red) and DAPI (blue). All images have been uniformly brightened to make the fibronectin signal easier to see. D) The percent positive pixels were quantified. * indicates significantly different from C57. Width of white bar represents 100 microns. C57 (n=7) mdx (n=6) mdxQ (n=6).

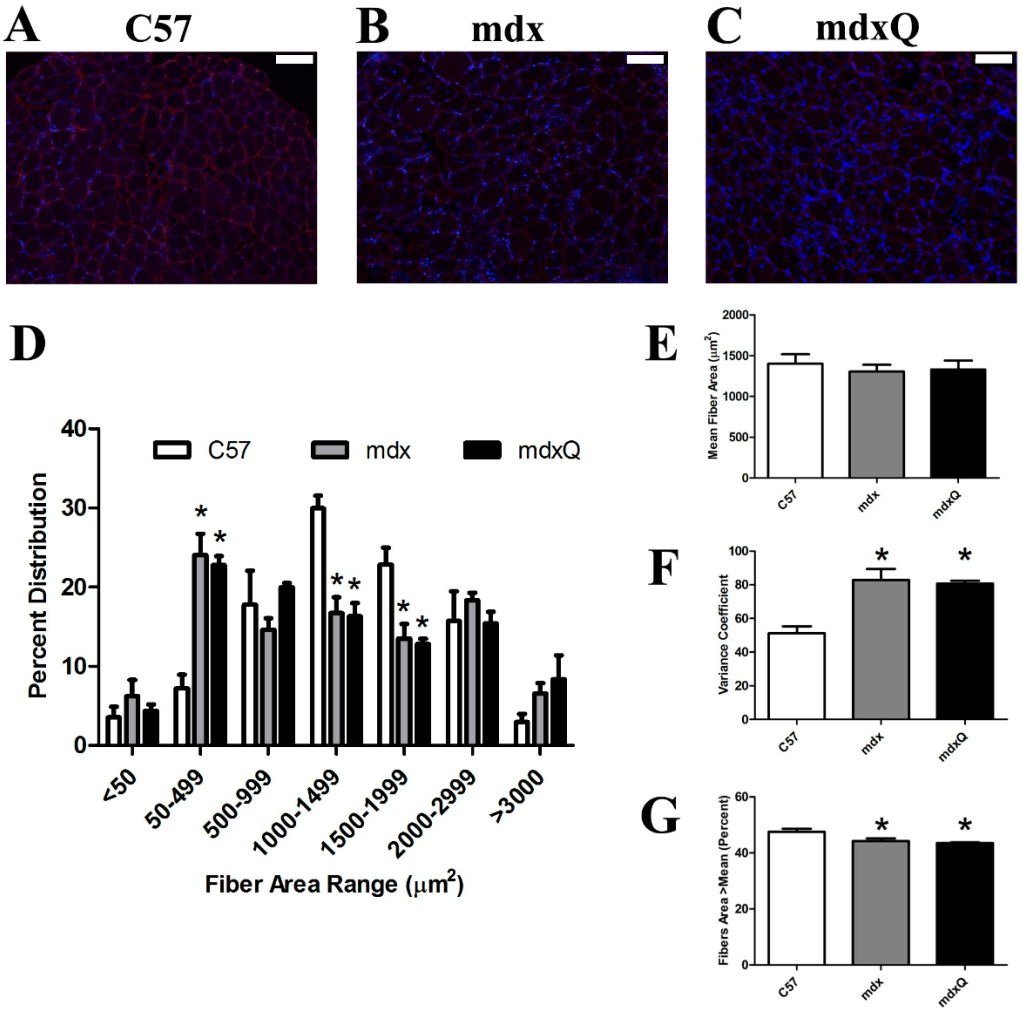

Figure 6. Fiber area distribution is altered by dystrophin deficiency in soleus muscle. A-C) Representative 10x images from an immunohistological experiment where laminin (red) was detected. DAPI is shown in blue. D) Fiber area distribution was measured and quantified in bins. E) Mean fiber area and F) the variance coefficient were calculated. G) We also determined the percent of fibers greater than the mean cross-sectional area as another indicator of fiber area variability. * indicates significantly different from C57. Width of white bar represents 100 microns. C57 (n=7) mdx (n=6) mdxQ (n=6).

Table 2. Transcript expression in the soleus. Data are shown as fold change relative to C57. * indicates significantly different from C57; # indicates significantly different from mdx. C57 (n=7) mdx (n=6) mdxQ (n=6).

	C57	**Mdx**	**mdxQ**
	Average ± SEM	**Average ± SEM**	**Average ± SEM**
Mitochondrial Biogenesis (PGC-1α Pathway Genes)			
Sirt1	1.00 ± 0.25	2.02 ± 0.45	1.94 ± 0.54
Ppargc1a (Pgc-1α)	1.00 ± 0.11	-1.67 ± 0.09*	-1.72 ± 0.09*
Esrra (Errα)	1.00 ± 0.18	-3.47 ± 0.11*	-2.65 ± 0.06*
Nrf1	1.00 ± 0.23	-1.93. ± 0.11	-1.24 ± 0.28
Nrip1	1.00 ± 0.18	-1.45 ± 0.20	-1.46 ± 0.21
Tfam	1.00 ± 0.48	-1.34 ± 0.16	-2.07 ± 0.11
Metabolic Genes			
Fnip1	1.00 ± 0.25	-1.84 ± 0.06	-2.08 ± 0.04
Mtor	1.00 ± 0.27	-2.48 ± 0.12*	-2.57 ± 0.10*
Prkaa1	1.00 ± 0.16	-1.05 ± 0.14	-1.72 ± 0.12
Gapdh	1.00 ± 0.20	-3.48 ± 0.04*	-2.97 ± 0.04*
Pfkm	1.00 ± 0.16	-2.38 ± 0.04*	-2.38 ± 0.06*
Pparg	1.00 ± 0.19	-1.32 ± 0.27	-1.18 ± 0.40
Cs	1.00 ± 0.16	-3.64 ± 0.05*	-3.60 ± 0.04*
Mdh1	1.00 ± 0.15	-1.94 ± 0.07*	-2.27 ± 0.08*
Atp1a2	1.00 ± 0.07	-1.76 ± 0.10*	-2.09 ± 0.06*
Cybb	1.00 ± 0.30	-1.35 ± 0.03	2.77 ± 1.35
Cycs	1.00 ± 0.27	1.11 ± 0.29	-2.45 ± 0.11
Mb	1.00 ± 0.17	-4.35 ± 0.03*	-4.61 ± 0.04*
Mt-atp6	1.00 ± 0.07	-2.14 ± 0.05*	-2.38 ± 0.06*
Mt-co1	1.00 ± 0.17	-2.78 ± 0.04*	-3.18 ± 0.05*
Mt-co2	1.00 ± 0.14	-2.15 ± 0.07*	-2.50 ± 0.06*

	C57	Mdx	mdxQ
	Average ± SEM	**Average ± SEM**	**Average ± SEM**
Mt-cyb	1.00 ± 0.09	-2.35 ± 0.04*	-2.59 ± 0.06*
Mt-nd1	1.00 ± 0.06	-2.32 ± 0.04*	-2.66 ± 0.06*
Mt-nd4	1.00 ± 0.21	-2.32 ± 0.05*	-2.85 ± 0.06*
Uqcrc1	1.00 ± 0.17	-2.01 ± 0.09*	-2.59 ± 0.05*
Tfb1m	1.00 ± 0.66	-1.49 ± 0.26	-2.95 ± 0.06
Tfb2m	1.00 ± 0.13	-2.50 ± 0.09*	-1.70 ± 0.16
Ucp3	1.00 ± 0.21	-3.50 ± 0.11*	-4.50 ± 0.04*
Ak1	1.00 ± 0.35	-2.68 ± 0.12	-2.18 ± 0.27
Akt1	1.00 ± 0.56	-4.43 ± 0.07	-2.97 ± 0.11
Ckm	1.00 ± 0.15	-1.87 ± 0.08	-1.92 ± 0.10
Inflammation/antioxidant Genes			
Nfκb1	1.00 ± 0.24	-1.35 ± 0.31	-1.10 ± 0.40
Il1b	1.00 ± 0.28	-1.23 ± 0.21	-2.55 ± 0.02
Tlr4	1.00 ± 0.61	-2.18 ± 0.19	-3.56 ± 0.06
Traf2	1.00 ± 0.16	-1.02 ± 0.40	1.23 ± 0.32
Cat	1.00 ± 0.51	-5.53 ± 0.03*	-4.96 ± 0.06*
Gpx1	1.00 ± 0.47	-2.27 ± 0.17	-3.64 ± 0.07
Gpx4	1.00 ± 0.31	-2.29 ± 0.09*	-2.69 ± 0.05*
Gsr	1.00 ± 0.29	2.02 ± 0.93	-1.25 ± 0.17
Nfe2l2	1.00 ± 0.15	-1.98 ± 0.13*	-2.11 ± 0.13*
Prdx2	1.00 ± 0.25	-2.96 ± 0.06*	-4.00 ± 0.04*
Sod1	1.00 ± 0.40	-2.36 ± 0.10	-3.37 ± 0.05*
Sod2	1.00 ± 0.25	-2.64 ± 0.05*	-2.88 ± 0.06*
Apoptosis Genes			
Apaf1	1.00 ± 0.27	-1.03 ± 0.07	1.68 ± 0.68

	C57	Mdx	mdxQ
	Average ± SEM	**Average ± SEM**	**Average ± SEM**
Bax	1.00 ± 0.37	1.12 ± 0.22	1.16 ± 0.28
Bcl2	1.00 ± 0.13	-1.59 ± 0.18	-1.63 ± 0.22
Bnip2	1.00 ± 0.17	-2.45 ± 0.08*	-1.29 ± 0.12*#
Casp3	1.00 ± 0.44	-1.29 ± 0.33	-2.10 ± 0.18
Trp53	1.00 ± 0.33	-2.97 ± 0.14	-1.19 ± 0.47
Xiap	1.00 ± 0.27	-2.05 ± 0.12	-1.92 ± 0.12
Muscle Repair and Protein Turnover Genes			
Fbl	1.00 ± 0.35	-1.48 ± 0.21	-1.15 ± 0.26
Gata2	1.00 ± 0.60	-2.16 ± 0.19	-3.78 ± 0.12
Hspa1a	1.00 ± 0.87	-1.88 ± 0.03	-2.47 ± 0.02
Hspa5	1.00 ± 0.36	-2.60 ± 0.07*	-1.97 ± 0.11
Hspb1	1.00 ± 0.21	-1.33 ± 0.18	-1.99 ± 0.11*
Mef2c	1.00 ± 0.17	-1.96 ± 0.09*	-2.68 ± 0.03*
Mstn	1.00 ± 0.26	-1.35 ± 0.19	-1.20 ± 0.21
Myf5	1.00 ± 0.38	-3.32 ± 0.08	-1.39 ± 0.38
Myocd	1.00 ± 0.26	-1.77 ± 0.33	-1.13 ± 0.71
Myod1	1.00 ± 0.67	-1.33 ± 0.53	-2.48 ± 0.15
Myof	1.00 ± 0.58	-2.06 ± 0.19	-2.39 ± 0.15
Myog	1.00 ± 0.59	-2.24 ± 0.17	-4.87 ± 0.07
Poldip2	1.00 ± 0.16	-1.24 ± 0.17	-2.11 ± 0.03*
Tgfb1	1.00 ± 0.10	1.45 ± 0.47	2.10 ± 1.00
Structural and Sarcomeric Genes			
Dag1	1.00 ± 0.10	-1.53 ± 0.13*	-2.27 ± 0.07*
Dtna	1.00 ± 0.16	-1.43 ± 0.08	-1.40 ± 0.12
Dysf	1.00 ± 0.16	-1.40 ± 0.15	-1.58 ± 0.10

	C57	Mdx	mdxQ
	Average ± SEM	**Average ± SEM**	**Average ± SEM**
Myh1	1.00 ± 0.39	-1.22 ± 0.15	-1.78 ± 0.05
Myh2	1.00 ± 0.17	-3.24 ± 0.04*	-3.29 ± 0.06*
Myh7	1.00 ± 0.17	-2.56 ± 0.05*	-2.92 ± 0.09*
Sgca	1.00 ± 0.17	-2.74 ± 0.05*	-3.49 ± 0.06*
Utrn 3’	1.00 ± 0.24	-1.15 ± 0.15	-1.32 ± 0.22
Utrn 5’	1.00 ± 0.15	-1.54 ± 0.14	-1.17 ± 0.32

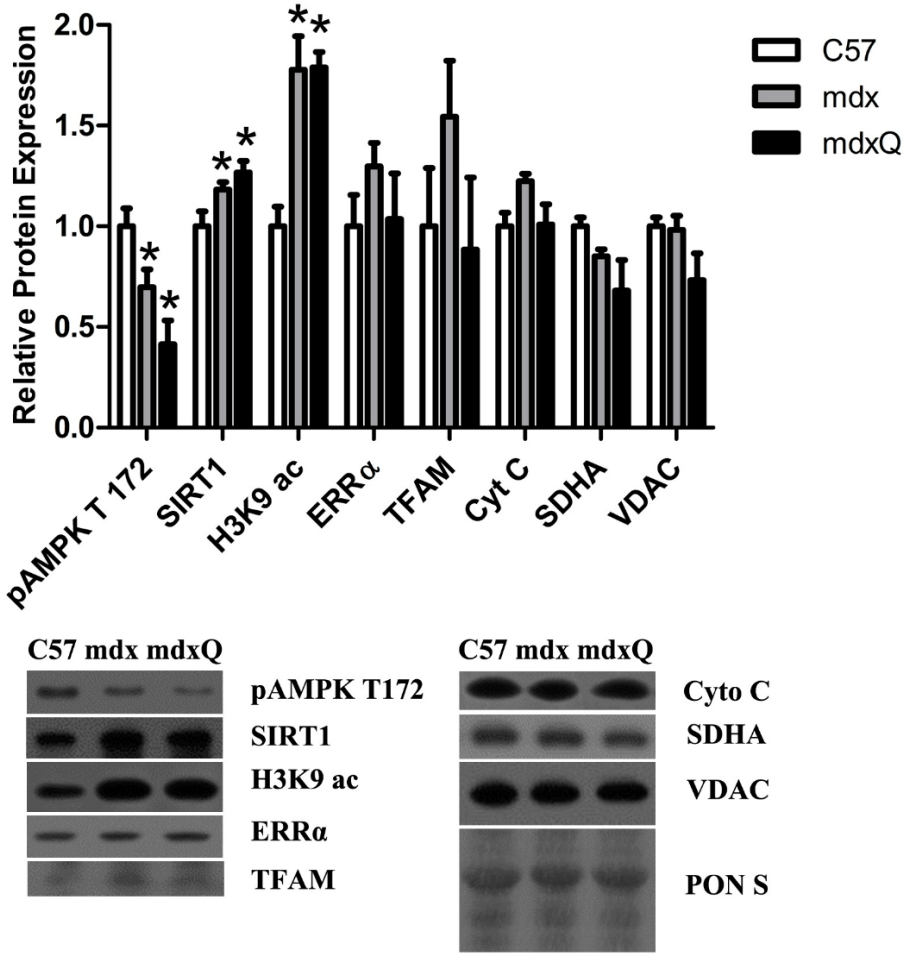

Fig 7. Relative protein abundance was altered by dystrophin deficiency. A) Protein abundance of PGC-1α pathway components was largely depressed by dystrophin deficiency independent of intervention compared to muscle from C57 mice. B)

Representative blots were included and Ponceau S stain was included to demonstrate equal loading. * indicates significantly different from C57. C57 (n=5) mdx (n=6) mdxQ (n=5).

CHAPTER 4: NUTRACEUTICAL AND PHARMACEUTICAL COCKTAILS DID NOT IMPROVE MUSCLE FUNCTION OR REDUCE HISTOLOGICAL DAMAGE IN D2-MDX MICE

HR Spaulding[1], T Quindry[2], K Hammer[1], JC Quindry[2] and JT Selsby[1]

[1]Department of Animal Science, Iowa State University, Ames, IA

[2]Department of Health and Human Performance, University of Montana, Missoula, MT 59812, USA

A manuscript in review at

Journal of Applied Physiology

Abstract

Progressive muscle injury and weakness are hallmarks of Duchenne muscular dystrophy, which is caused by the absence of functional dystrophin protein. We showed previously that quercetin (Q) partially protected dystrophic limb muscles from disease-related injury. As quercetin activates PGC-1α through Sirtuin 1, an NAD+-dependent deacetylase, the depleted NAD+ in dystrophic skeletal muscle may limit quercetin efficacy, hence, supplementation with the NAD+ donor, nicotinamide riboside (NR), may facilitate quercetin efficacy. Lisinopril (Lis) also protects skeletal muscle and improves cardiac function in dystrophin deficient mice, therefore it was included in this study to evaluate the effects of lisinopril with quercetin and NR. Our purpose was to determine the extent to which Q, NR, and Lis alone and in combination decreased dystrophic injury. We hypothesized that Q, NR or Lis alone would improve muscle function and decrease histological injury and when used in combination would have additive or synergistic

effects. To address this hypothesis muscle function of 11-month-old DBA (healthy), D2-mdx (dystrophin-deficient), and D2-mdx mice following treatment with Q, NR, or Lis independently or in combination for 7 months was assessed. To mimic typical pharmacology of DMD patients an additional group was treated with prednisolone (Pred) in combination with Q, NR and Lis. At 11 months of age, dystrophin deficiency decreased specific tension and tetanic force in both the soleus and extensor digitorum longus muscles and was not corrected by any treatment. Dystrophic muscle was more sensitive to contraction induced injury, which was partially offset in the QNRLisPred group, while fatigue was similar between all groups. Histological damaged was increased in D2-mdx mice compared to DBA and not improved with treatments. These data suggest that treatment with Q, NR, Lis and Pred in combination failed to adequately maintain dystrophic limb muscle function or decrease histological damage.

Keywords: DMD, prednisolone, glucocorticoid, ACE inhibitor, quercetin

New and Noteworthy

Despite a compelling rationale and previous evidence to the contrary in short-term investigations, quercetin, nicotinamide riboside, or Lisinopril, alone or in combination, failed to restore muscle function or decrease histological injury in dystrophic limb muscle from D2-mdx mice following long-term administration. Importantly, we also found that in the D2-mdx model, an emerging and relatively understudied model of DMD, dystrophin deficiency caused profound muscle dysfunction and histopathology in skeletal muscle.

Introduction

Duchenne muscular dystrophy (DMD) is a progressive muscle wasting disease caused by a mutation in the dystrophin gene resulting in dystrophin protein deficiency. By the age of twelve children with DMD are usually wheelchair bound and will typically succumb to the disease in their 3rd decade of life due to respiratory or cardiac failure (12). In addition to muscle fragility, dystrophin deficiency results in a host of cellular dysfunctions including, but not limited to, impaired autophagy, calcium mishandling, oxidative stress, and mitochondrial dysfunction (4, 19, 28). Collectively, this structural injury and cellular dysfunction results in histopathologic changes including immune cell infiltration, fibrosis, increased necrotic area, increased fatty infiltration, and a reduction in contractile tissue (5, 16).

Transgenic or vector-mediated overexpression of PGC-1α reduced histological damage and preserved muscle function in dystrophic skeletal muscle (8, 15, 16, 26). We have pursued the capacity of quercetin, a natural flavonoid with anti-oxidant and anti-inflammatory properties (1, 6, 10), to attenuate disease severity as it drives PGC-1α activity through Sirtuin 1 (SIRT1), an NAD+-dependent deacetylase (11, 21). We discovered previously that six months of oral quercetin delivery decreased histopathological injury in dystrophic diaphragms and hearts of mdx mice (3, 17), however, long-term administration of quercetin transiently maintained respiratory function and modestly protected limb muscles, while in corresponding hearts indices of inflammation were reduced and markers of mitochondrial biogenesis were increased (2, 25, 27).

As quercetin relies on SIRT1 activity to drive signaling, we proposed that limited NAD+ in dystrophic muscle (7) may hinder the efficacy of quercetin (27) and that supplementation with nicotinamide riboside (NR), an NAD+ precursor, would maintain quercetin-mediated elevations in SIRT1 activity, PGC-1α activity, and muscle function. Indeed, it was recently demonstrated that muscle function was improved following 12 weeks of NR supplementation (24). Independent of quercetin, early intervention with angiotensin-converting enzyme (ACE) inhibitor, Lisinopril (Lis), improved histological injury (20) and in combination with aldosterone receptor antagonist, spironolactone, improved function and reduced histological damage of dystrophic cardiac and skeletal muscle (18, 22). The goal of this investigation was to determine the extent to which NR and/or Lis would augment therapeutic effects of quercetin on disease severity in dystrophic limb muscles. We hypothesized that the oral administration of quercetin in combination with NR and/or Lis would improve muscle function and decrease histological injury in dystrophic muscle compared to untreated dystrophic muscle. We utilized an emerging model of DMD, the D2-mdx mouse (D2.B10-Dmd^{mdx}/J), which was produced by crossing the traditional BL10-mdx mouse onto the DBA background such that dystrophin deficiency is caused by the identical nonsense mutation in exon 23 of the dystrophin gene. The DBA background has 12-amino acid deletion in the latent TGF-β-binding protein gene 4 (Ltbp4), a gene which when mutated may accelerate loss of ambulation in DMD patients (9, 13). Additionally, the DBA background has a mutation to the Anxa6 gene leading to the truncation of annexin A6 protein, which is involved in satellite cell self-renewal and membrane repair (29). This DBA background provides a

more severe phenotype resulting in increased fibrosis, increased muscle damage, and decreased regenerative capacity in the D2-mdx mouse (9, 14, 23).

Methods

Animal Treatments. All animal procedures were approved by the Institutional Animal Care and Use Committees at University of Montana (047-16JQHHP-072616) and the University of Florida (201508822). Ten male DBA2/J (DBA; control) mice and 80 male D2.B10-Dmd^{mdx}/J (D2-mdx; dystrophin deficient) mice were obtained from Jackson Laboratory (Bar Harbor, ME). Following an acclimation period of at least one week, 4 month old mice were assigned to nine groups (n=10/group): DBA, untreated D2-mdx, and D2-mdx treated with quercetin (Q, 0.2% by diet, 275 mg/kg/d), nicotinamide riboside (NR, 0.04% by diet, 55 mg/kg/d), Q and NR (QNR), Lisinopril (Lis, 33 mg/L in water, 9.15 ng/kg/d), Q and Lis (QLis), QNRLis, or QNRLis + prednisolone (QNRLisPred, 10 mg/L by water, 2.77 mg/kg/d). The QNRLisPred group was included to test the most complete cocktail (QNRLis) in the context of common pharmacology used to treated DMD patients. Treatments were initiated at 4 months of age to demonstrate the efficacy of these treatments using a rescue paradigm, which more closely replicates the onset of treatment for DMD patients. All animals were given access to food and water *ad libitum* regardless of treatment. Caregivers and technicians were blinded to animal treatment and treatment groups were assigned numbers to ensure blinded conditions throughout data collection. Following 7 months of treatment soleus and extensor digitorum longus (EDL) were collected.

Muscle function. *In vitro* muscle function was assessed in the soleus and EDL at the University of Florida Myology Institute Physiological Assessment Core as previously

described (27, 30). Briefly, soleus and EDL muscles were removed following surgical sedation with ketamine and xylazine and placed in a bath of oxygenated Ringers solution (120mM NaCl, 4.7mM KCl, 2.5mM $CaCl_2$, 1.2mM KH_2PO_4, 1.2mM $MgSO_4$, 25mM HEPES and 5.5mM Glucose). Isometric tetanic force was measured at 120 Hz and 100 Hz for EDL and soleus, respectively. To determine fatigue resistance, the soleus was stimulated with 1 contraction/sec at 100Hz for 330 msec with 200 μsec pulses for 10 min. Fatigue resistance was reported as percentage of remaining initial force. Finally, to assess resistance to contraction-induced injury, five lengthening contractions of 500 msec duration at 80 Hz followed by a final 10% stretch beyond Lo for 200 msec were applied to EDL muscles. Resistance to contraction-induce injury was reported as percent of initial force production.

Histology. Muscle damage and fibrotic area were assessed using hematoxylin & eosin (H&E) and Masson's Trichrome (KTMTRPT, American MasterTech, Lodi, CA) staining as previously described (25, 27). Soleus and EDL muscles were coated in OCT and frozen for histology in liquid nitrogen-chilled isopentane. Briefly, 10 μm sections were stained with H&E or Masson's Trichrome, and imaged at 10x and 40x magnification by a blinded, trained technician on an inverted Lecia DMI3000 B microscope and QICAM MicroPublisher 5.0 (MP5.0-RTV-CLR-10, QIMAGING) camera with QCapture software (Surrey, BC, Canada). Contractile area was quantified using the H&E images by alternatively density slicing for the hypercontracted cells and necrotic areas, then subtracting that sum from the total area using Open Lab Software (Improvision). The density slice function uses prescribed pixel parameters to select the dark red hypercontracted cells and the light pink necrotic areas. Similarly, fibrotic area

was quantified by using the density slice function of the Open Lab Software to quantify the blue area of the trichrome images, which was divided by the total area to identify the percent of the total area that was fibrotic.

Fiber area distribution was assessed using immunohistochemistry (IHC). Sections were incubated with anti-laminin (anti-rabbit, ThermoScientific, RB-082-A) using our standard IHC protocol as previously described (28). Briefly, after washing (phosphate buffered saline (PBS)) and blocking (5% goat serum, 5% bovine serum albumin, 1% DMSO in 2X PBS) slides were incubated in primary antibody (laminin, 1:100 in blocking solution) overnight at 4°C, then washed and incubated in secondary antibody (anti-rabbit AlexaFluor 488, 1:500, Cell Signaling 4412S) for 1 h at room temperature. Slide covers were mounted with SlowFade™ Gold Antifade Mountant with DAPI (S36938, ThermoFisher) and sealed with nail polish. Slides were imaged at 10x magnification on the same inverted microscope. For each sample, two independent images were taken and quantified (100-400 fibers/image). Fiber areas were objectively measured using OpenLab Software.

Statistics. To determine significant sources of variation in single time point measures, such as muscle masses, tetanic force, specific force, fiber area distribution, contractile area, and fibrotic area, one-way ANOVAs were performed using GraphPad Prism with a Newman-Keuls post hoc test. Data from soleus fatigue experiments were analyzed utilizing a repeated measure model in which a spatial power variance structure was used. EDL contraction induced injury data were analyzed using a repeated measures model that implemented an autoregressive variance structure. A mixed model method was used to determine significant sources of variation (Proc Mixed, SAS V9.0, SAS Inst.

Inc., Cary, NC) that included fixed effects for treatment, time, and treatment×time interaction with pre-treatment value (20 min baseline measurement at 4 months of age) as a linear covariate. When fixed effects were significant sources of variation, the PDIFF statement of SAS was used at the fixed effect level of LS means to separate pairwise differences.

Results

Animal characteristics. Mouse body mass was decreased by 13-38% in untreated and treated D2-mdx mice compared to healthy (DBA) mice ($p<0.05$). In addition, the QNRLisPred group was decreased 38% and 28% compared to DBA and D2-mdx ($p<0.05$), respectively, and was significantly decreased compared to the remaining treatment groups except Q and QNRLis. Additionally, body mass of Q-treated mice decreased 17% compared to D2-mdx untreated ($p<0.05$). Soleus, extensor digitorum longus (EDL), gastrocnemii and tibialis anterior (TA) muscles were weighed. EDL, gastrocnemius and TA masses were decreased 29-47%, 58-71% and 42-56%, respectively, in untreated and treated D2-mdx mice compared to muscles from DBA mice ($p<0.05$). Interestingly, the soleus was similar between all groups with the exception of D2-mdx mice treated with QNRLisPred, which was decreased approximately 13% compared to all groups ($p<0.05$). Similarly, the EDL and gastrocnemius muscles from QNRLisPred were significantly decreased 18-29% compared to treated and untreated D2-mdx ($p<0.05$). Lastly, EDLs from Q-treated D2-mdx mice were 7-11% greater than untreated D2-mdx and NR-treated D2-mdx ($p<0.05$). When tissues masses were normalized to body mass, gastrocnemius and TA masses were decreased by 45-53% and 22-35%, respectively, in all D2-mdx groups compared to DBA ($p<0.05$). Similarly, D2-

mdx EDL relative mass was decreased by 26% compared to DBA ($p<0.05$), and treatment with Q or QNRLis increased muscle mass by 23-29% compared to EDLs from untreated D2-mdx mice ($p<0.05$). Additionally, Q-treated D2-mdx EDL relative mass was increased 10-16% compared to NR, QNR, Lis and QLis ($p<0.05$),. Lastly, soleus relative mass was increased by 16-32% in treated and untreated D2-mdx mice compared to DBA ($p<0.05$) and were similar to each other.

In vitro muscle function. Muscle function was assessed in the soleus and EDL following 7 months of treatment (Figures 1 and 2). Soleus tetanic force and specific tension were decreased by 25% in D2-mdx compared to DBA ($p<0.05$) with no effect of treatments (Figure 1A). Following 10 sec of a fatigue protocol, force production was similar between groups, however, following 120 sec QNRLisPred produced 25% greater force than DBA ($p<0.05$) mice while DBA and D2-mdx were similar. Additionally, QNRLisPred produced 32% more force than D2-mdx and DBA following 300 sec of fatigue protocol that was maintained through 600 sec of 1 contraction/sec fatigue protocol ($p<0.05$; Figure 1C).

In the EDL, tetanic and specific tension were significantly decreased by 50% and 20%, respectively, in D2-mdx groups compared to DBA (Figure 2A&B; $p<0.05$). Additionally, EDL tetanic tension was further decreased by 25% in QNRLisPred treated mice compared to remaining D2-mdx groups ($p<0.05$). Resistance to contraction-induced injury was assessed by measuring peak force during five eccentric contractions, in which the muscles were stretched 10% past Lo. Following contractions 3, 4 and 5, D2-mdx produced 18%, 27% and 36% less force compared to DBA ($p<0.05$), respectively. Following contraction 4, Q, NR, QNR and Lis produced 17-19% less force than DBA

($p<0.05$). Similarly, after contraction 5, Q, NR, Lis, QLis and QNRLis-treated groups produced 20-29% less for than DBA ($p<0.05$). QNRLisPred-treated mice produced 32% more force during the 5th contraction than D2-mdx and was statistically similar to DBA, suggesting protection from contraction induced injury (Figure 2B).

Histology. Given that muscle function was largely similar between untreated and treated D2-mdx mice, we performed histopathological examination on groups that showed therapeutic promise (numerical changes suggestive of therapeutic potential) (Figure 3). Hence, we assessed histological muscle damage in the DBA, D2-mdx, QLis, QNRLis, and QNRLisPred groups. Soleus contractile area decreased from 95% in DBA mice to approximately 65-73% in D2-mdx, QNRLis, and QNRLisPred ($p<0.05$). Surprisingly, contractile area was only 41% in QLis. In the EDL, contractile area was decreased by 41-64% in D2-mdx groups compared to DBA mice (Figure 3; $p<0.05$). Treatment with QNRLis further decreased contractile area compared to QLis and QNRLisPred.

Given the above findings, secondary analyses were performed on the soleus in order to gain further insights. Fibrotic area increased from less than 5% in DBA to 11-18% in D2-mdx groups ($p<0.05$). Treatments did not significantly decrease fibrotic area compared to D2-mdx, but treatment with QNRLisPred significantly increased fibrotic area compared to QLis, (Figure 4; $p<0.05$).

Distribution of fiber cross-sectional area was shifted toward an overabundance of smaller fibers and a corresponding underrepresentation of larger fibers in D2-mdx groups compared to DBA (Figure 5A). The mean fiber area was similar between DBA, D2-mdx and QLis, but was decreased by 32% in QNRLis and QNRLisPred compared to DBA

(Figure 5B; $p<0.05$). Median fiber cross-sectional area was decreased by 20-45% in all D2-mdx groups compared to DBA (Figure 5B; $p<0.05$). Additionally, the variance coefficient was at least doubled in all D2-mdx groups compared to DBA and increased 19% in QNRLis compared to D2-mdx and QLis (Figure 5B; $p<0.05$).

Discussion

DMD is caused by a mutation in the dystrophin gene resulting in the absence of functional dystrophin protein and a complicated sequela due to DMD. Researchers and clinicians continue to pursue a variety of strategies intended to counter these cellular dysfunctions and slow or prevent disease progression. While transformative therapies are currently in various phases of FDA approval to treat tomorrow's patients, pragmatic solutions are urgently needed to treat today's patients. In this study, our purpose was to determine the extent to which treatment of D2-mdx mice with quercetin, nicotinamide riboside (NR), and/or Lisinopril (Lis) improved muscle function and decreased disease-related muscle damage. Counter to our hypotheses, we failed to demonstrate that treatment with quercetin, NR, or Lisinopril independently or in combination meaningfully improved muscle function or decreased histopathological injury. Only a cocktail containing Pred (QNRLisPred) provided some protection to fatigue and contraction induced injury but did not decrease histological.

Consistent with our earlier work using long-term quercetin treatment of mdx mice, a relatively less severe rodent model of DMD (27), application of quercetin over 7 months to D2-mdx mice did not correspond to improved limb muscle function. Previously, we demonstrated that quercetin improved soleus specific force, but did not potentiate other parameters of muscle function. We then surmised that the transient

nature of quercetin-mediated protection (27) may be due to depleted NAD+ and successfully treated with NR (27). Early support for this rationale was established by prior observations that NAD+ depletion in mdx mice was corrected following 12 weeks of NR supplementation (24). This promising outcome was accompanied by an improved exercise capacity despite elevated energetic stress due to decreased mitochondrial oxidative phosphorylation rate and increased mitochondrial ATP production load (24). Despite dosing differences in this investigation, it is likely that the advanced disease progression in the present investigation (older mice, more severe model) and/or the long-term use of NR limited its efficacy. Given that 1) the D2-mdx model more accurately recapitulates injury in humans than the mdx mouse model and 2) long-term treatment should be expected with DMD patients, the applicability of NR to DMD seems tenuous based on the current findings.

In the present investigation, Lisinopril did not improve measures of muscle function nor decrease histological damage. Similarly, short-term treatment with Lisinopril did not improve muscle function in an mdx/Utrn$^{+/-}$ model, though Lisinopril decreased histological injury (20). When used in combination with spironolactone, an aldosterone receptor antagonist, Lisinopril increased EDL and diaphragm function and decreased histological injury in the quadriceps when treatment was started at 4 weeks but not at 8 weeks in mdx/Utrn$^{+/-}$ mice (22). Interestingly, in the mdx model, treatment with Lisinopril and spironolactone did not improve muscle function nor decrease histological damage (18). While differences in animal model, duration of study, dose (33 mg/L or 66 mg/L) and use of drug in combination likely account for some differences between these investigations, collectively they provide underwhelming support for continued use of

Lisinopril, alone, as a skeletal muscle therapy for DMD. Notably, the combination of Lisinopril and metoprolol (β-blocker) mitigate some aspects of disease severity in cardiac muscle in a clinical population (31).

Within the context of preclinical murine experiments to date, DMD has been most commonly modeled by the C57BL/10-mdx (mdx) mouse. While this mouse model has been useful for studies related to disease mechanism, its mild phenotype may contribute to translational limitations of therapeutic findings to human populations. In this study we used an emerging model of DMD, the DBA/2J-mdx (D2-mdx) mouse, which has a relatively severe, progressive pathology and early-onset cardiac dysfunction (9). Consistent with our data from 48-week-old D2-mdx mice, EDL tetanic force and specific force were decreased at 7, 28 and 52 weeks (9). Moreover, similar to our current findings in soleus, increased fibrosis was previously reported in tibialis anterior, gastrocnemius, and quadriceps in 6- and 8-month-old D2-mdx mice compared to control (14). Interestingly, fat accumulation was significantly increased at 6 months in the gastrocnemius and at 6 and 8 months in the quadriceps (14), but in this investigation fatty infiltration was not visually apparent in the 11-month-old soleus or EDL. Ostensibly, increased fatty infiltration decreased contractile cross-sectional area is this prior work (14), and support functional observations in the current investigation. Moreover, as in this investigation, Coley et al. (9) discovered that the distribution of fiber area was shifted toward a greater frequency of small fibers. These data in combination with current findings, when paired with decreased muscle mass and findings from H&E and trichrome analyses, support a reduction in fiber size as well as functional cross section area of the whole muscle, which translate to dramatic reductions in muscle function.

In summary, and counter to our study hypotheses, quercetin, nicotinamide riboside, and Lisinopril (alone and in combination), were not associated with resistance to dystrophic disease progression in limb muscle. Treatment with QNRLisPred provided partial improvements in muscle function but did not mitigate other indices of disease progression. Collectively, these data indicate that quercetin and these quercetin-based cocktails have limited value in the treatment of dystrophin-deficient limb muscles and alternative approaches should be considered.

Acknowledgements

Project Parent Muscular Dystrophy (01297), Ryan's Quest, and Michael's Cause supported this work. University of Florida Myology Institute Physiological Assessment Core collected the muscle function data (U54 AR052646).

References

1. **Anhe GF, Okamoto MM, Kinote A, Sollon C, Lellis-Santos C, Anhe FF, Lima GA, Hirabara SM, Velloso LA, Bordin S, and Machado UF**. Quercetin decreases inflammatory response and increases insulin action in skeletal muscle of ob/ob mice and in L6 myotubes. *Eur J Pharmacol* 689: 285-293, 2012.

2. **Ballmann C, Denney T, Beyers RJ, Quindry T, Romero M, Selsby JT, and Quindry JC**. Long term dietary quercetin enrichment as a cardioprotective countermeasure in mdx mice. *Exp Physiol* 2017.

3. **Ballmann C, Hollinger K, Selsby JT, Amin R, and Quindry JC**. Histological and biochemical outcomes of cardiac pathology in mdx mice with dietary quercetin enrichment. *Exp Physiol* 100: 12-22, 2015.

4. **Bellinger AM, Reiken S, Carlson C, Mongillo M, Liu X, Rothman L, Matecki S, Lacampagne A, and Marks AR**. Hypernitrosylated ryanodine receptor calcium release channels are leaky in dystrophic muscle. *Nat Med* 15: 325-330, 2009.

5. **Blake DJ, Weir A, Newey SE, and Davies KE**. Function and genetics of dystrophin and dystrophin-related proteins in muscle. *Physiol Rev* 82: 291-329, 2002.

6. **Boots AW, Drent M, de Boer VC, Bast A, and Haenen GR**. Quercetin reduces markers of oxidative stress and inflammation in sarcoidosis. *Clin Nutr* 30: 506-512, 2011.

7. **Chalkiadaki A, Igarashi M, Nasamu AS, Knezevic J, and Guarente L**. Muscle-specific SIRT1 gain-of-function increases slow-twitch fibers and ameliorates pathophysiology in a mouse model of duchenne muscular dystrophy. *PLoS Genet* 10: e1004490, 2014.

8. **Chan MC, Rowe GC, Raghuram S, Patten IS, Farrell C, and Arany Z**. Post-natal induction of PGC-1alpha protects against severe muscle dystrophy independently of utrophin. *Skelet Muscle* 4: 2, 2014.

9. **Coley WD, Bogdanik L, Vila MC, Yu Q, Van Der Meulen JH, Rayavarapu S, Novak JS, Nearing M, Quinn JL, Saunders A, Dolan C, Andrews W, Lammert C, Austin A, Partridge TA, Cox GA, Lutz C, and Nagaraju K**. Effect of genetic background on the dystrophic phenotype in mdx mice. In: *Hum Mol Genet*2016, p. 130-145.

10. **Dias AS, Porawski M, Alonso M, Marroni N, Collado PS, and Gonzalez-Gallego J**. Quercetin decreases oxidative stress, NF-kappaB activation, and iNOS overexpression in liver of streptozotocin-induced diabetic rats. *J Nutr* 135: 2299-2304, 2005.

11. **Dong J, Zhang X, Zhang L, Bian HX, Xu N, Bao B, and Liu J**. Quercetin reduces obesity-associated ATM infiltration and inflammation in mice: a mechanism including AMPKalpha1/SIRT1. *J Lipid Res* 55: 363-374, 2014.

12. **Eagle M, Baudouin SV, Chandler C, Giddings DR, Bullock R, and Bushby K**. Survival in Duchenne muscular dystrophy: improvements in life expectancy since 1967 and the impact of home nocturnal ventilation. *Neuromuscul Disord* 12: 926-929, 2002.

13. **Flanigan KM, Ceco E, Lamar KM, Kaminoh Y, Dunn DM, Mendell JR, King WM, Pestronk A, Florence JM, Mathews KD, Finkel RS, Swoboda KJ, Gappmaier E, Howard MT, Day JW, McDonald C, McNally EM, and Weiss RB**. LTBP4 genotype predicts age of ambulatory loss in Duchenne muscular dystrophy. *Ann Neurol* 73: 481-488, 2013.

14. **Fukada S, Morikawa D, Yamamoto Y, Yoshida T, Sumie N, Yamaguchi M, Ito T, Miyagoe-Suzuki Y, Takeda S, Tsujikawa K, and Yamamoto H**. Genetic background affects properties of satellite cells and mdx phenotypes. *Am J Pathol* 176: 2414-2424, 2010.

15. **Handschin C, Kobayashi YM, Chin S, Seale P, Campbell KP, and Spiegelman BM**. PGC-1alpha regulates the neuromuscular junction program and ameliorates Duchenne muscular dystrophy. *Genes Dev* 21: 770-783, 2007.

16. **Hollinger K, Gardan-Salmon D, Santana C, Rice D, Snella E, and Selsby JT**. Rescue of dystrophic skeletal muscle by PGC-1 alpha involves restored expression of dystrophin-associated protein complex components and satellite cell signaling. *American Journal of Physiology-Regulatory Integrative and Comparative Physiology* 305: R13-R23, 2013.

17. **Hollinger K, Shanely RA, Quindry JC, and Selsby JT**. Long-term quercetin dietary enrichment decreases muscle injury in mdx mice. *Clin Nutr* 34: 515-522, 2015.

18. **Janssen PM, Murray JD, Schill KE, Rastogi N, Schultz EJ, Tran T, Raman SV, and Rafael-Fortney JA**. Prednisolone attenuates improvement of cardiac and skeletal contractile function and histopathology by lisinopril and spironolactone in the mdx mouse model of Duchenne muscular dystrophy. *PLoS One* 9: e88360, 2014.

19. **Kuznetsov AV, Winkler K, Wiedemann FR, von Bossanyi P, Dietzmann K, and Kunz WS**. Impaired mitochondrial oxidative phosphorylation in skeletal muscle of the dystrophin-deficient mdx mouse. *Mol Cell Biochem* 183: 87-96, 1998.

20. **Lowe J, Wodarcyk AJ, Floyd KT, Rastogi N, Schultz EJ, Swager SA, Chadwick JA, Tran T, Raman SV, Janssen PM, and Rafael-Fortney JA**. The Angiotensin Converting Enzyme Inhibitor Lisinopril Improves Muscle Histopathology but not Contractile Function in a Mouse Model of Duchenne Muscular Dystrophy. In: *J Neuromuscul Dis*2015, p. 257-268.

21. **Nemoto S, Fergusson MM, and Finkel T**. SIRT1 functionally interacts with the metabolic regulator and transcriptional coactivator PGC-1{alpha}. *J Biol Chem* 280: 16456-16460, 2005.

22. **Rafael-Fortney JA, Chimanji NS, Schill KE, Martin CD, Murray JD, Ganguly R, Stangland JE, Tran T, Xu Y, Canan BD, Mays TA, Delfin DA, Janssen PM, and Raman SV**. Early treatment with lisinopril and spironolactone preserves cardiac and skeletal muscle in Duchenne muscular dystrophy mice. *Circulation* 124: 582-588, 2011.

23. **Rodrigues M, Echigoya Y, Maruyama R, Lim KRQ, Fukada S, and Yokota T**. Impaired regenerative capacity and lower revertant fibre expansion in dystrophin-deficient mdx muscles on DBA/2 background. *Sci Rep* 6: 2016.

24. **Ryu D, Zhang H, Ropelle ER, Sorrentino V, Mazala DA, Mouchiroud L, Marshall PL, Campbell MD, Ali AS, Knowels GM, Bellemin S, Iyer SR, Wang X, Gariani K, Sauve AA, Canto C, Conley KE, Walter L, Lovering RM, Chin ER, Jasmin BJ, Marcinek DJ, Menzies KJ, and Auwerx J**. NAD+ repletion improves muscle function in muscular dystrophy and counters global PARylation. *Sci Transl Med* 8: 361ra139, 2016.

25. **Selsby JT, Ballmann CG, Spaulding HR, Ross JW, and Quindry JC**. Oral quercetin administration transiently protects respiratory function in dystrophin-deficient mice. *J Physiol* 594: 6037-6053, 2016.

26. **Selsby JT, Morine KJ, Pendrak K, Barton ER, and Sweeney HL**. Rescue of dystrophic skeletal muscle by PGC-1alpha involves a fast to slow fiber type shift in the mdx mouse. *PLoS One* 7: e30063, 2012.

27. **Spaulding HR, Ballmann CG, Quindry JC, and Selsby JT**. Long-Term Quercetin Dietary Enrichment Partially Protects Dystrophic Skeletal Muscle. *PLoS One* 11: e0168293, 2016.

28. **Spaulding HR, Kelly EM, Quindry JC, Sheffield JB, Hudson MB, and Selsby JT**. Autophagic dysfunction and autophagosome escape in the mdx mus musculus model of Duchenne muscular dystrophy. *Acta Physiol (Oxf)* 222: 2018.

29. **Swaggart KA, Demonbreun AR, Vo AH, Swanson KE, Kim EY, Fahrenbach JP, Holley-Cuthrell J, Eskin A, Chen Z, Squire K, Heydemann A, Palmer AA, Nelson SF, and McNally EM**. Annexin A6 modifies muscular dystrophy by mediating sarcolemmal repair. *Proc Natl Acad Sci U S A* 111: 6004-6009, 2014.

30. **Vassilakos G, Lei H, Yang Y, Puglise J, Matheny M, Durzynska J, Ozery M, Bennett K, Spradlin R, Bonanno H, Park S, Ahima RS, and Barton ER**. Deletion of muscle IGF-I transiently impairs growth and progressively disrupts glucose homeostasis in male mice. *Faseb j* 33: 181-194, 2019.

31. **Viollet L, Thrush PT, Flanigan KM, Mendell JR, and Allen HD**. Effects of angiotensin-converting enzyme inhibitors and/or beta blockers on the cardiomyopathy in Duchenne muscular dystrophy. *Am J Cardiol* 110: 98-102, 2012.

Figures and Tables

Table 1. Animal and muscle masses. Body mass was decreased in dystrophic (D2-mdx) compared to healthy (DBA) mice, and treatment with QNRLisPred further decreased body mass. Absolute muscle masses were reduced in dystrophic mice compared to healthy, except the soleus was similar between groups. Treatment with QNRLisPred further decreased absolute muscle masses. Similarly, relative muscle masses were decreased in dystrophic mice, regardless of tissue or treatment, DBA (n=10), D2-mdx (n=8), Q (n=9), NR (n=8), QNR (n=8), Lis (n=7), QLis (n=10), QNRLis (n=8), and QNRLisPred (n=9). Values are reported as mean ± SEM.

	DBA	*D2-mdx*	*Q*	*NR*	*QNR*	*Lis*	*QLis*	*QNRLis*	*QNRLisPred*
Body Mass (g)	39.53 ± 1.81	34.36 ± 1.13*	28.36 ± 1.25*#	29.63 ± 1.14*†	31.18 ± 1.49*†	32.28 ± 1.71*†	31.38 ± 0.76*†	28.92 ± 0.84*	24.57 ± 0.98*#
Soleus (mg)	7.5 ± 0.2	7.6 ± 0.2	7.1 ± 0.3†	6.9 ± 0.3†	7.1 ± 0.2†	7.2 ± 0.2†	7.5 ± 0.2†	6.9 ± 0.2†	6.0 ± 0.2*#
Rel Soleus (mg/g)	0.19 ± 0.01	0.22 ± 0.01*	0.25 ± 0.01*	0.24 ± 0.01*	0.23 ± 0.01*	0.23 ± 0.01*	0.24 ± 0.01*	0.24 ± 0.01*	0.25 ± 0.01*
EDL (mg)	8.9 ± 0.1	5.9 ± 0.1*	6.3 ± 0.2*#†	5.7 ± 0.2*†‡	5.9 ± 0.1*†	6.0 ± 0.2*†	5.9 ± 0.1*†	5.9 ± 0.2*†	4.7 ± 0.1*#
Rel EDL (mg/g)	0.23 ± 0.01	0.17 ± 0.00*	0.22 ± 0.01#†	0.19 ± 0.01*‡	0.19 ± 0.01*‡	0.19 ± 0.01*‡	0.20 ± 0.00*‡	0.21 ± 0.01#	0.20 ± 0.01*
Gast (mg)	123.30 ± 2.2	51.30 ± 1.6*	49.43 ± 2.14*†	47.93 ± 1.49*†	46.99 ± 1.36*†	48.26 ± 1.12*†	48.85 ± 1.58*†	46.03 ± 2.03*†	36.29 ± 1.09*#
Rel Gast (mg/g)	3.17 ± 0.09	1.50 ± 0.05*	1.74 ± 0.06*	1.63 ± 0.06*	1.52 ± 0.06*	1.52 ± 0.07*	1.56 ± 0.05*	1.60 ± 0.08*	1.49 ± 0.05*
TA (mg)	50.00 ± 3.5	28.40 ± 0.9*	28.24 ± 0.73*	25.83 ± 0.75*	26.73 ± 0.86*	27.33 ± 0.82*	28.87 ± 0.74*†	28.03 ± 0.71*	22.01 ± 0.95*
Rel TA (mg/g)	1.28 ± 0.08	0.83 ± 0.03*	1.00 ± 0.03*	0.88 ± 0.04*	0.87 ± 0.03*	0.85 ± 0.03*	0.92 ± 0.02*	0.97 ± 0.03*	0.91 ± 0.05*

Masses and relative (rel) masses are represented as mean ± SEM. EDL – extensor digitorum longus; Gast – gastrocnemius; TA – tibialis anterior. *Indicates significantly different from DBA, # indicates significantly different from D2-mdx, ‡ - significantly different from Q and † = significantly different from QNRLisPred, $P<0.05$.

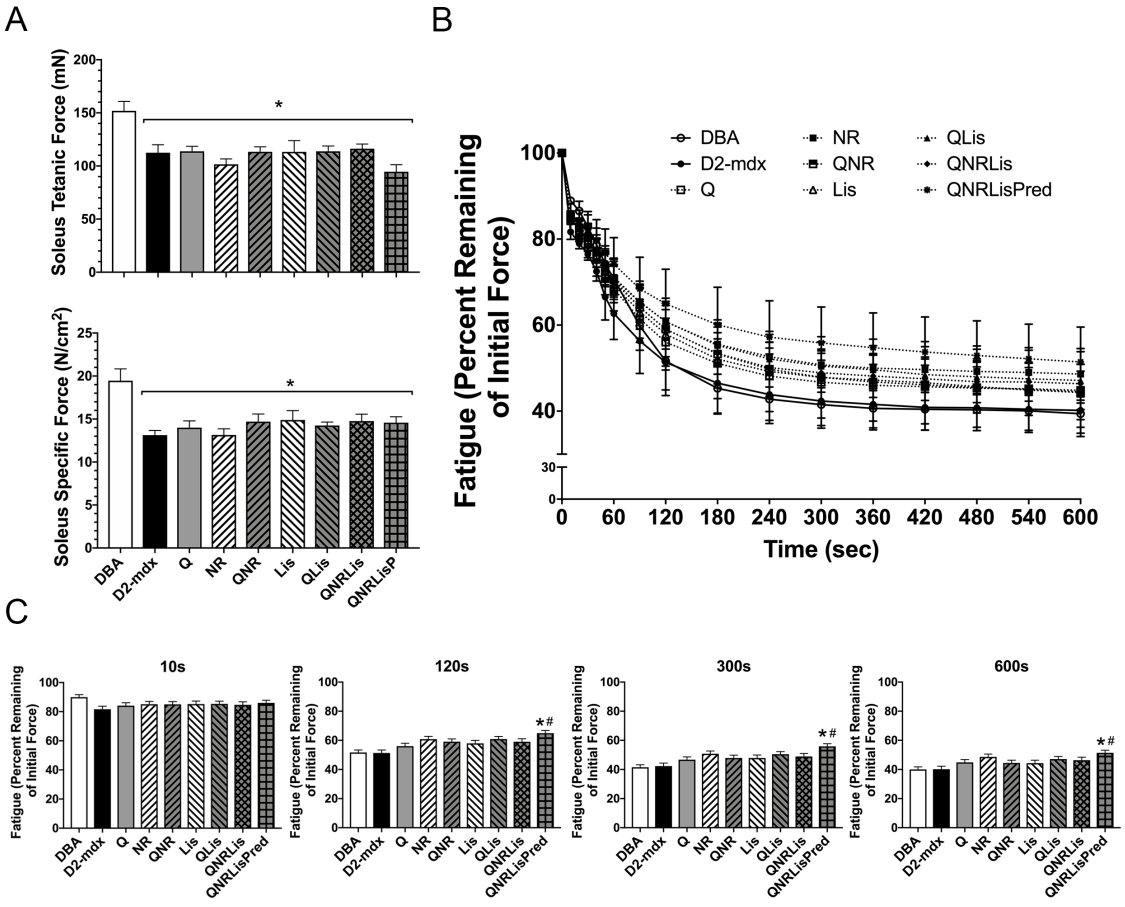

Figure 1. Soleus muscle function. A) Tetanic force and specific force were decreased in D2-mdx mice, regardless of treatment, compared to DBA. B) Resistance to fatigue was measured over 10 min. C) Despite similar fatigue resistance between DBA and D2-mdx at these time points, QNRLisPred increased fatigue resistance at 120, 300 and 600 seconds compared to D2-mdx. DBA (n=10), D2-mdx (n=7-8), Q (n=8), NR (n=8), QNR (n=8), Lis (n=7), QLis (n=9-10), QNRLis (n=7), and QNRLisPred (n=9). Statistical significance was established at $p<0.05$, * = significantly different from DBA, # = significantly different from D2-mdx.

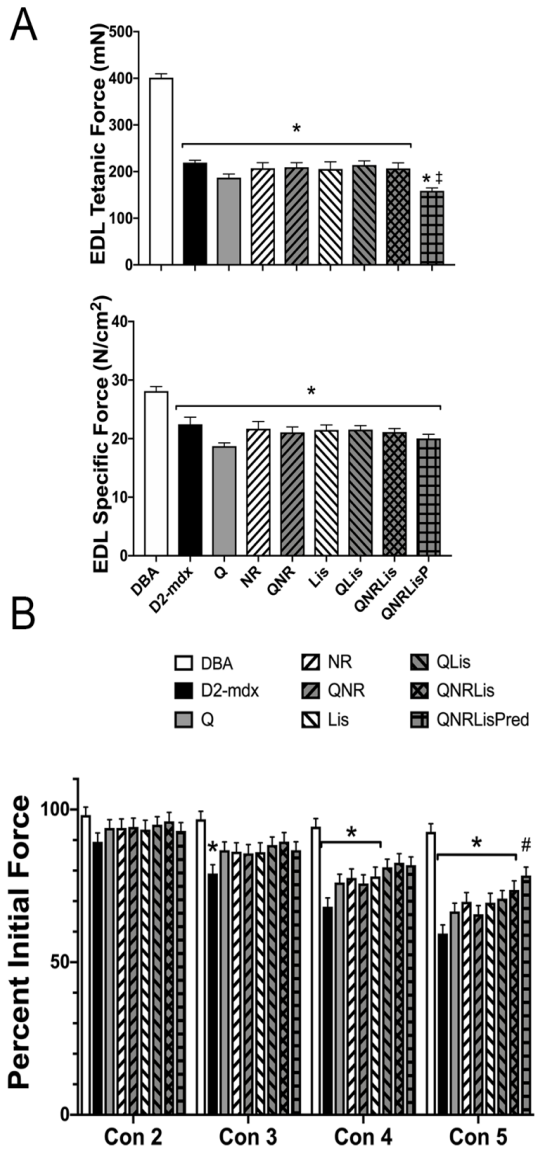

Figure 2. Extensor digitorum longus muscle function. A) Tetanic force and specific force were decreased in D2-mdx mice, regardless of treatment, compared to DBA. QNRLisPred further decreased tetanic force compared to all groups, but specific tension similar to D2-mdx groups. B) Resistance to contraction induce injury was decreased in D2-mdx mice. Treatment with QNRLisPred improved resistance to contraction induced injury following the 5th contraction. DBA (n=9), D2-mdx (n=7-8), Q (n=8-9), NR (n=8), QNR (n=8), Lis (n=7), QLis (n=9-10), QNRLis (n=7-8), and QNRLisPred (n=9). Statistical significance was established at $p<0.05$, * = significantly different from DBA, # = significantly different from D2-mdx.

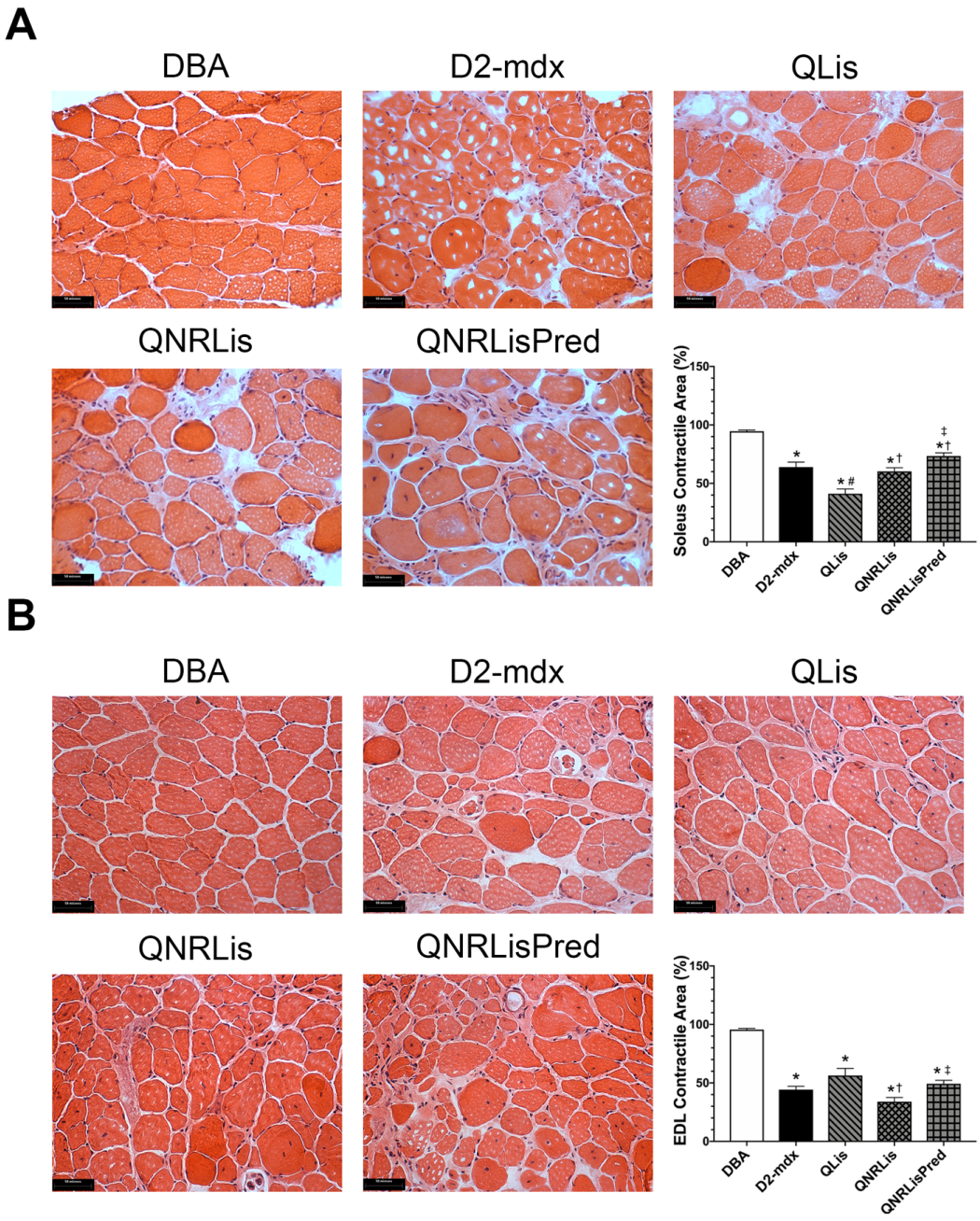

Figure 3. H&E staining of soleus and EDL. A) Representative H&E images (40X) of soleus muscle and quantification of contractile area. B) Representative H&E images (40X) of EDL and quantification of contractile area. Contractile area was significantly decreased in D2-mdx mice, which was not corrected by these treatments. DBA (n=8-9), D2-mdx (n=8), QLis (n=10), QNRLis (n=7-9), and QNRLisPred (n=8). Statistical significance was established at $p<0.05$, * = significantly different from DBA, # = significantly different from D2-mdx, † = significantly different from QLis, ‡ = significantly different from QNRLis.

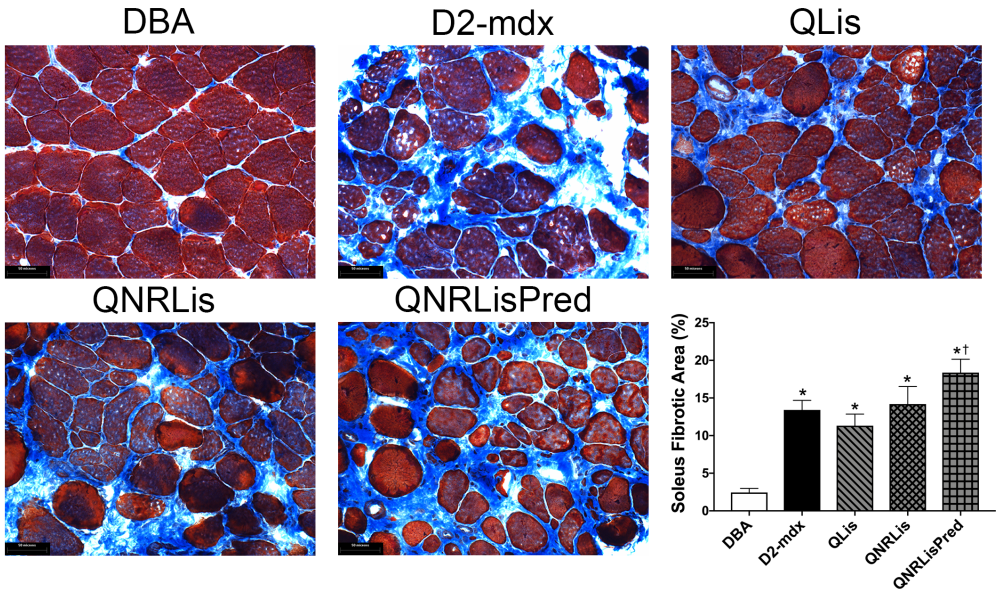

Figure 4. Trichrome staining of the soleus. Representative trichrome images (40X) of soleus muscle and quantification of fibrotic area. Fibrotic area was increased in dystrophic muscle. DBA (n=9), D2-mdx (n=8), QLis (n=10), QNRLis (n=8), and QNRLisPred (n=8). Statistical significance was established at $p<0.05$, * = significantly different from DBA, † = significantly different from QLis.

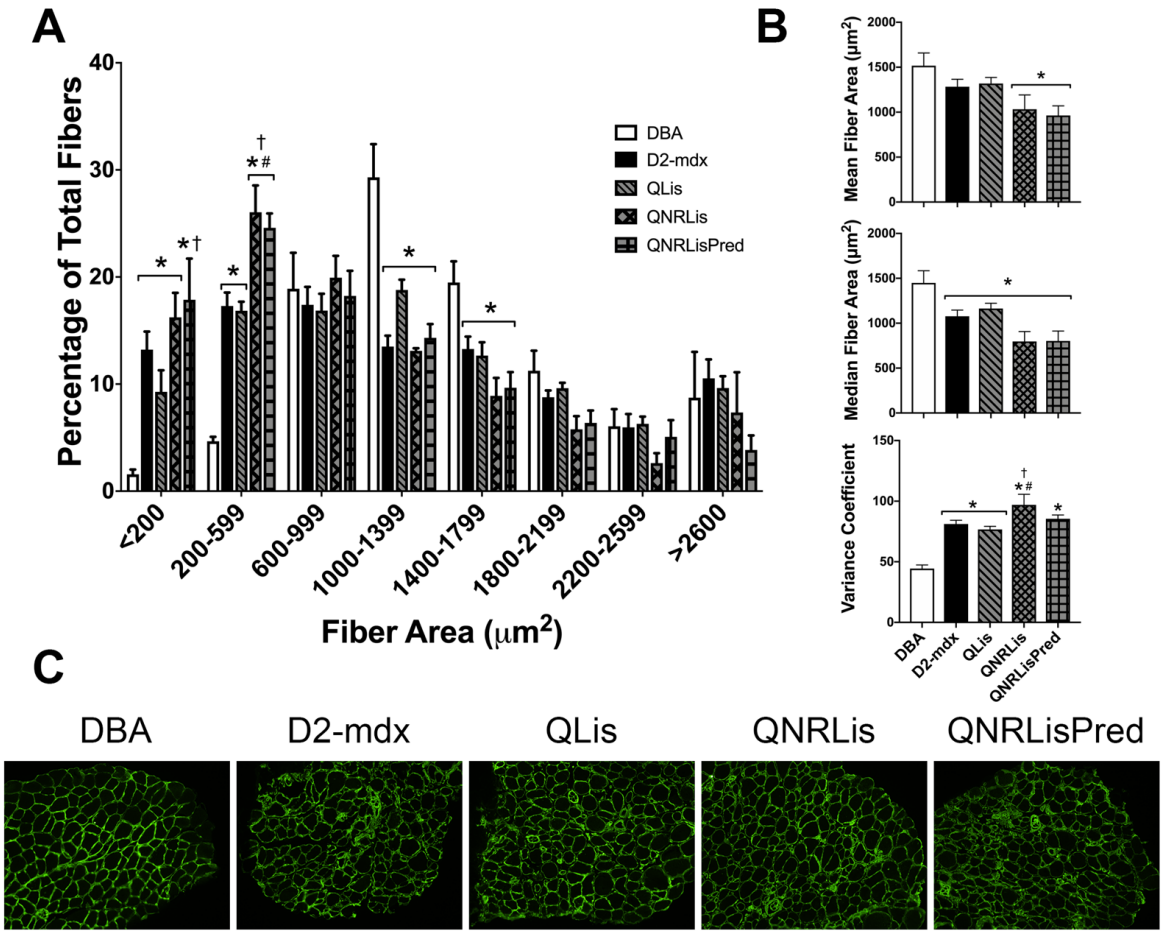

Figure 5. Fiber area distribution of the soleus. A) Dystrophic fiber area distribution was shifted towards an abundance of small fibers. B) Mean fiber area was similar between health and dystrophic muscle, but median was decreased in all D2-mdx groups. Additionally, the variance coefficient was elevated in dystrophic muscle, regardless of treatment. C) Representative IHC images (10X) of laminin in soleus muscle. DBA (n=8), D2-mdx (n=7), QLis (n=7), QNRLis (n=4), and QNRLisPred (n=5). Groups were compared within each fiber area bin using a one-way ANOVA. Significance was established at $p<0.05$, * = significantly different from DBA, # = significantly different from D2-mdx, † = significantly different from QLis.

CHAPTER 5: NUTRACEUTICAL AND PHARMACEUTICAL COCKTAILS DID NOT PRESERVE DIAPHRAGM MUSCLE FUNCTION OR REDUCE MUSCLE DAMAGE IN D2-MDX MICE

Hannah R. Spaulding[1], Tiffany Quindry[2], John C. Quindry[2] and Joshua T. Selsby[1]

[1]Department of Animal Science, Iowa State University, Ames, IA 50011

[2]Health and Human Performance, University of Montana, Missoula, MT 59812

Abstract

Duchenne muscular dystrophy (DMD) is characterized by the absence of dystrophin protein and causes muscle weakness and muscle injury culminating in respiratory failure and cardiomyopathy. Quercetin has been shown to transiently improve respiratory function but failed to maintain long-term therapeutic benefits in mdx mice. In this study we combined quercetin with nicotinamide riboside, Lisinopril and prednisolone to assess the efficacy of quercetin-based cocktails. Nicotinamide riboside (NR) alone has been shown to improve dystrophic muscle function, and when combined with quercetin may replenish the NAD+ pool depleted in dystrophic muscle that is necessary to main the SIRT1 activity, an NAD+-dependent deacetylase, and prolong benefits of quercetin. Additionally, Lisinopril, an ACE-inhibitor, has been shown to prevent injury in both dystrophic hearts and skeletal muscle. We hypothesized that quercetin, NR and Lisinopril independently would improve respiratory function and decrease diaphragm injury, and when administered in combination would have additive effects. To address this

hypothesis, *in vivo* respiratory function, *in vitro* diaphragm function, and histological injury were assessed in DBA (healthy), D2-mdx (dystrophic) and D2-mdx mice treated with combinations of quercetin, NR and Lisinopril from 4-11 months of age. Lastly, we included prednisolone in the most complete cocktail to mimic the pharmacology of many DMD patients. Contrary to our expectations, treatments largely failed to improve respiratory and diaphragmatic function, or histological injury. Manifestations of disease were apparent as respiratory and diaphragm function were decreased and histological injury was increased in dystrophic mice compared to healthy mice in this emerging DMD mouse model. Together these data suggest that quercetin, NR and Lisinopril independently and in combination did not prevent diaphragm injury nor preserve respiratory function.

Keywords: DMD, prednisolone, glucocorticoid, ACE inhibitor, quercetin

Introduction

Duchenne muscular dystrophy (DMD) is caused by a mutation to the dystrophin gene resulting in the absence of functional dystrophin protein. Dystrophin is a structural protein and anchor of the dystroglycoprotein complex that protects the sarcolemma during muscle contraction (26). Patients experience progressive muscle wasting that causes muscle weakness, wheelchair confinement and ultimately respiratory or cardiac failure (14). The absence of dystrophin is accompanied by a multitude of cellular dysfunctions including increased oxidative stress, calcium mishandling, chronic inflammation and impaired autophagy (5, 22, 34). Development of therapeutics to restore dystrophin protein to dystrophic muscles are ongoing (32), but immediate interventions are needed in order to protect and preserve muscle function. We and others are pursuing

pharmaceutical and nutraceutical interventions to treat the secondary dysfunctions of DMD with the goal of using these agents to preserve muscle function, improve quality of life, and prolong life expectancy, e.g. Hollinger et al. (19), Lowe et al (23), Ryu et al. (29).

Given these cellular dysfunctions, exercise-mediated adaptations would appear to offset many pathological hallmarks of disease, however, when considered in aggregate, the effects of exercise on DMD are equivocal (35). Activation of the transcriptional co-activator PGC-1α may be a means by which to acquire exercise-mediated protection without the risk of contraction induced injury. Indeed, vector-mediated and transgenic overexpression of PGC-1α in dystrophic muscle reduced muscle damage and preserved muscle function (10, 16-18, 31). Given the success of PGC-1α overexpression, we began to investigate the effect of quercetin, a natural flavonoid that stimulates PGC-1α activity, on disease severity in dystrophic muscle (2-4, 19, 30, 33). Quercetin serves to increase PGC-1α activity through SIRT1, an NAD+-dependent deacetylase (13, 25). Quercetin also functions as an anti-oxidant and anti-inflammatory, which may assist in protecting dystrophic muscle from damage (1, 6, 12).

In studies in which quercetin was administered for 6 months, quercetin decreased histological injury in dystrophic diaphragms and hearts (4, 19), however, following 12 months of treatment, skeletal muscle function and histological damage were similar in quercetin-treated and untreated muscle (30, 33). We also found that quercetin improved respiratory function for the first 4-6 months of treatment, but by the conclusion of the study (14 months of age) respiratory function was similar between treated and untreated dystrophic mice (30). As NAD+ plays a role in SIRT1 function, and in dystrophic

skeletal muscle NAD+ abundance is decreased (8, 29), NAD+ depletion may limit quercetin-mediated PGC-1α activation. We hypothesized that treatment of dystrophic mice with quercetin in combination with the NAD+ donor, nicotinamide riboside (NR), would enhance the efficacy of quercetin, particularly during long-term treatment (33). Indeed, 10-12 weeks of NR supplementation improved dystrophic muscle function and enhanced satellite cell and mitochondrial function (29, 36).

In this study, our objective was to determine the extent to which quercetin-based cocktails protect respiratory function, diaphragm function, and decrease histological damage in the diaphragm of dystrophin-deficient mice. We hypothesized that quercetin in combination with NR would prolong quercetin-mediated improvements in *in vivo* respiratory function and increase *in vitro* diaphragm function while reducing histological damage in 11-month-old dystrophic mice. Additionally, DMD disease pathology includes cardiomyopathy, therefore cardioprotective drugs may be used alongside skeletal muscle-targeted therapies. Lisinopril, a cardioprotective drug, has been shown to protect the dystrophic myocardium and skeletal muscle (21, 28). Therefore, in this study, we evaluated the effect of Lisinopril, a cardioprotective drug, on respiratory function, diaphragm function and muscle damage both alone and in combination with quercetin-based cocktails. Lastly, prednisolone was combined with the most complete quercetin-based cocktail to understand the effect of these agents within the context of the current pharmacological standard of care, glucocorticoids.

Methods

Animal Treatments. Animal protocols were approved by the Institutional Animal Care and Use Committees at University of Montana (047-16JQHHP-072616) and the

University of Florida (201508822). Male DBA2/J (DBA; control) mice and D2.B10-Dmd^{mdx}/J (D2-mdx; dystrophin-deficient) mice were obtained from Jackson Laboratory (Bar Harbor, ME). Mice were acclimated for at least one week, then at 4 months of age mice were separated into treatment groups (n=10/group): DBA, untreated D2-mdx, and D2-mdx treated with quercetin (Q, 0.2% by diet, 275 mg/kg/d), nicotinamide riboside (NR, 55 mg/kg/d by diet), Q and NR (QNR), Lisinopril (Lis, 33 mg/L in water), Q and Lis (QLis), QNRLis, or QNRLis with prednisolone (QNRLisPred, 10 mg/L by water). Mice weighed approximately 26 g throughout the investigation, ate approximately 3.6 g/day, and drank approximately 7.2 ml/day. Given the use of glucocorticoids in the treatment of DMD patients, a QNRLisPred group was included to assess the QNRLis cocktail within a common pharmacological context. All animals had *ad libitum* access to food and water. Prior to the start of the treatments, groups were assigned numbers to preserve blinded conditions throughout data collection.

Respiratory function. *In vivo* respiratory function was assessed using whole body plethysmograph as previously reported (27, 30). Briefly, beginning at 4 months of age, *in vivo* respiratory function was measured every 2 months until 10 months of age using a four-chamber whole body unrestrained plethysmography system (Buxco, now Data Sciences International, St. Paul, MN, USA), which has been shown to effectively identify differences between healthy and dystrophic mice (20, 30). As previously described, mice were allowed a 20 min acclimation period, then data were collected over 8 minutes (27).

Muscle function. *In vitro* muscle function of the diaphragm was assessed at the University of Florida Myology Institute Physiological Assessment Core as previously described (24, 31). Briefly, costal diaphragms were removed following sedation with

ketamine and xylazine and then separated into two hemi-diaphragms: one for *in vitro* function measures and the other for histology. The hemi-diaphragm for histology was coated in OCT, rolled to create a tube, then frozen in liquid nitrogen-chilled isopentane. Specific tension and resistance to fatigue were measured in the second hemi-diaphragm. The hemi-diaphragm strip was placed in oxygenated Ringer's solution (NaCl, 4.7mM KCl, 2.5mM $CaCl_2$, 1.2mM KH_2PO_4, 1.2mM $MgSO_4$, 25mM HEPES and 5.5mM glucose), then attached at one end to a force transducer and the other end to an anchor. Muscles were simulated at 100 Hz for 500ms to established optimum length (L_o) during tetanic contractions. To measure tetanic force, tetanic contractions were performed once every 10 minutes for 30 minutes. Specific force and cross-sectional area were calculated using standard equations (7). Data were collected with an Aurora dual mode lever system (Ontario, Canada) using DMC software (version 3.2). Fatigue resistance was measured at 1 contraction/sec at 100 Hz for 330 msec with 200 μsec pulses for 10 min. Fatigue resistance was reported as percentage of remaining initial force.

Histology. Hematoxylin & eosin (H&E) and Masson's Trichrome (KTMTRPT, American MasterTech, Lodi, CA) staining were used to assess muscle damage and fibrosis as previously described (30, 33). Ten-micron sections were stained with H&E or Masson's Trichrome, and 3-5 sections/muscle were imaged at 40x magnification on an inverted Lecia DMI3000 B microscope and QICAM MicroPublisher 5.0 (MP5.0-RTV-CLR-10, QIMAGING) camera with QCapture software (Surrey, BC, Canada) by a blinded, trained technician. H&E-stained muscle sections were used to quantify contractile area using the Open Lab Software (Improvision) density slice function, which identifies regions based on prescribed pixel parameters. Areas of necrosis, connective

tissue, and hypercontracted cells were quantified using the density slice function were subtracted from the total area to calculate area of healthy contractile tissue. The healthy tissue area was expressed relative to the total image cross sectional area. Similarly, the density slice function was used to selectively identify the fibrotic area (blue area) in trichrome images. Fibrotic area was divided by the total area to determine the percent of fibrosis in each muscle section.

Statistics. To analyze single time point measurements such as specific force, necrotic area and fibrotic area ANOVAs were preformed using GraphPad Prism with a Newman-Keuls post-hoc test. *In vivo* respiratory function data were analyzed using a repeated measures model that assumes the variance-covariance structure was auto-regressive. Fatigue resistance data were analyzed using repeated measures where the model incorporated a spatial power variance-covariance structure. In both respiratory function and fatigue resistance the repeated effect was time relative to age of the animal. Using mixed model methods (Proc Mixed, SAS V9.0, SAS Inst. Inc., Cary, NC) where the model included group, time, and group×time interaction as fixed effects and pre-treatment value (20min baseline measurement at 4 months of age) was used as a linear covariate. The experimental unit was individual mouse (n=7-10 per group) and model fixed effects were considered significant when their $p \leq 0.05$. When model fixed effects were significant sources of variation, the fixed effect level of LS means were separated using the PDIFF statement of SAS to determine pairwise differences.

Results

To determine the extent to which quercetin, nicotinamide riboside, Lisinopril and prednisolone protect respiratory function, diaphragm function and muscle damage, D2-

mdx mice were treated with a 0.2% quercetin enriched diet, a 55 mg/kg per day nicotinamide riboside enriched diet, 33 mg/L Lisinopril enriched water, and 10 mg/L prednisolone enriched water. Body mass was decreased 13-38% in all D2-mdx mice compared to DBA (please refer to Chapter 3). Additionally, the QNRLisPred group was further decreased by over 25% compared to untreated D2-mdx and DBA mice. Similarly, absolute and relative EDL, gastrocnemius and TA masses were decreased in D2-mdx groups compared to DBA. Consistent with body weight, gastrocnemius and EDL absolute muscle masses in the QNRLisPred group were further decreased compared to DBA and untreated D2-mdx. Interestingly, soleus mass was similar between all groups, though it was decreased with QNRLisPred treatment.

In vivo respiratory function. Respiratory function was assessed using whole body plethysmography in alternating months starting at 4 months (mo) of age through the conclusion of the study. For clarity, all statistically significant differences are discussed below, but only comparisons that were significantly different from DBA or D2-mdx mice were noted in Figure 1. Peak inspiratory flow (PIF) was similar between healthy (DBA) and diseased (D2-mdx) mice at each time point, regardless of treatment. At 6 mo of age, PIF of D2-mdx mice treated with QLis was increased 16% compared to DBA ($p<0.05$). Additionally, QLis was increased as a main effect of treatment compared to DBA (Figure 1A; $p<0.05$). Peak expiratory flow (PEF) was similar between all groups, but PEF was decreased in QNRLisPred-treated mice compared to QLis and QNRLis as a main effect of treatment (Figure 1B; $p<0.05$). Similarly, tidal volume was decreased in QNRLisPred as a main effect of treatment compared to all groups but was specifically decreased by approximately 15% compared to QLis at 6 mo and 8 mo ($p<0.05$), 10% compared to

QNR at 6 mo ($p<0.05$), and 9% compared to Q at 8 mo ($p<0.05$). Additionally, QLis tidal volume increased 12% compared to DBA at 6 mo. QNRLisPred tidal volume was decreased 16% compared to DBA at 10 mo ($p<0.05$) and 13% compared to untreated D2-mdx at 8 mo ($p<0.05$) and 10 mo (Figure 1C; $p=0.076$).

Frequency of breaths was elevated 12-14% in QNRLisPred compared to DBA and untreated D2-mdx at 8 mo ($p<0.05$) and 10 mo of age ($p<0.05$). Similarly, breath frequency of mice treated with Lis was decreased 12-14% to DBA and D2-mdx at 8 mo and QLis and QNRLis frequency of breaths were increased 10-16% at 10 mo of age compared to DBA ($p<0.05$) and 13-18% compared to untreated D2-mdx ($p<0.05$). Additionally, QNRLisPred was increased 12-19% at 6 mo compared to Q, Lis, and QLis, 11-30% at 8 mo compared to NR, Lis and QLis, and 16% compared to Lis at 10 mo. Lis breath frequency was decreased 14-16% compared to Q, NR and QNR at 8 mo, while QLis increased 14% at 10 mo compared to Lis alone. Lastly, Lis was decreased as a main effect of treatment compared to DBA, D2-mdx, Q, NR, and QNR, while QNRLisPred was increased as a main effect of treatment compared to all other groups, except for QNRLis. QLis and QNRLis frequency of breaths were increased as a main effect of time compared to Lis alone (Figure 1D). Minute ventilation was similar between all groups regardless of treatment (Figure 1E). Collectively these data suggest that respiratory function was similar between DBA and D2-mdx. When treatments were compared to either DBA or D2-mdx, occasional comparisons deviated from DBA or D2-mdx, but as a whole these quercetin-based cocktails did not improve respiratory function.

In vitro diaphragm function. Specific force and fatigue resistance were assessed in diaphragms. Specific force decreased 48-65% in all D2-mdx groups compared to DBA

($p<0.05$; Figure 2A). NR-treated D2-mdx diaphragm specific force was further decreased by 25% compared to Q and QNRLisPred ($p<0.05$). QNR, Lis, QLis and QNRLis specific force was decreased 20-32% relative to QNRLisPred ($p<0.05$). Fatigue resistance was similar between all groups regardless of treatment at 10s, 120s, 300s and 600s during the fatigue protocol (Figure 2B&C).

Histology. Given that *in vivo* and *in vitro* function data were largely similar between treatment groups, we narrowed our investigation to evaluate histological injury in treatment groups with the most therapeutic potential (Figure 3). We quantified diaphragm contractile area and fibrotic area in DBA, D2-mdx, QNR, QLis, QNRLis, QNRLisPred groups (Figures 3 and Figure 4). Contractile area was decreased over 10% in all D2-mdx groups compared to DBA ($p<0.05$). Contractile area was further decreased by 7% in QNRLis compared to QLis ($p<0.05$) (Figure 3). Fibrotic area was increased 5-12 fold in all D2-mdx groups compared to DBA ($p<0.05$; Figure 4). QNR was further increased 1.5-2 fold compared to untreated D2-mdx, QLis and QNRLisPred ($p<0.05$). Additionally, QNRLis fibrotic area was increased 2-fold compared to QLis ($p<0.05$).

Discussion

Duchenne muscular dystrophy is caused by the absence of functional dystrophin protein due to a mutation to the dystrophin gene. Dystrophin deficiency results in progressive muscle wasting culminating in respiratory or cardiac failure (14). While some researchers are developing approaches to restore dystrophin protein (32), we and others are working to identify pharmaceutical and nutraceutical interventions with potential for immediate application to mitigate disease pathology. In these experiments we investigated the extent to which quercetin-based cocktails preserved respiratory and

diaphragm function and prevented histological damage in the D2-mdx mouse model of DMD. Specifically, we treated dystrophic mice with quercetin, nicotinamide riboside, or Lisinopril alone and in various combinations including one complete combination with prednisolone. We hypothesized that *in vivo* respiratory function and *in vitro* diaphragm function would be reduced and histological damage would be increased in D2-mdx mice compared to DBA and that treatment with quercetin-based cocktails would mitigate these disease-related changes. We found that dystrophin deficiency increased some parameters of disease, however, counter to our hypothesis, quercetin-based cocktails failed to attenuate disease severity.

Previously, we found that 6 months of treatment with quercetin preserved *in vivo* respiratory function, but by 12 months of age respiratory function was similar between quercetin-treated and untreated mdx mice (30). In the present investigation, which used the D2-mdx model, we did not detect a functional improvement in any quercetin-treated group, regardless of duration of treatment. Interestingly, D2-mdx mice treated with the complete cocktail, QNRLisPred, decreased tidal volume and increased frequency of respiration suggesting decreased alveolar ventilation compared to D2-mdx at 8 months and DBA at 10 months of age. Similar to findings using aged mdx mice (30), diaphragm specific force was reduced in D2-mdx at the conclusion of the study, and was not improved following long-term treatment with quercetin. Given the reduction of NAD+ in dystrophic muscle (8, 29), and recent evidence of improved muscle and mitochondrial function in mdx mice following 11-12 weeks of nicotinamide riboside administration (29, 36), we postulated that supplementation with nicotinamide riboside would independently improve respiratory function in dystrophic mice. Furthermore, nicotinamide riboside

could also boost quercetin effectiveness via increased NAD+-mediated SIRT1 activity, which is necessary for quercetin-mediated activation of the PGC-1α pathway. Though long-term quercetin treatment did not decrease histological damage in this study or a previous study (30), despite successfully reducing histological injury following 6 months of quercetin treatment in 8-month-old in mdx mice (19), the use of quercetin in combination with NR may result in an additive or even synergistic therapeutic effect. Contrary to our hypothesis, nicotinamide riboside alone and in combination with quercetin did not improve measures of respiratory function. These data suggest that long-term administration of quercetin does not protect dystrophic diaphragms from damage and muscle weakness even when given in combination with nicotinamide riboside. We cannot rule out the possibility that age of animals at initiation of treatment, duration of treatment, and our selected animal model may have limited the efficacy of nicotinamide riboside (or other drugs/combinations). Indeed, the combination of the severe D2-mdx model coupled with the deliberate selection of a four-month-old start date to allow advanced disease may have made the muscle unresponsive to this intervention. Our rationale was that such a rescue paradigm is necessary to convincingly establish efficacy as onset of treatment begins in DMD patients following diagnosis that is ultimately caused by muscle injury sufficient to impair locomotion. Hence, studies of therapeutics in a model that more closely recapitulates disease severity is important. Further, as patients may be taking drugs for years establishment of long-term efficacy is essential.

Guided by the necessity to treat multiple aspects of DMD disease pathology, Lisinopril was added to the quercetin-based cocktails. While primarily used as a cardioprotective agent, Lisinopril has been shown to reduce histological damage in

skeletal muscle in the mdx/Utrn$^{+/-}$ model (23). In the present investigation, we found that Lisinopril did not decrease fibrosis nor preserve contractile area independently or when given in combination with quercetin, or quercetin, nicotinamide riboside and/or prednisolone. Similarly, respiratory function and diaphragm function were not improved with these interventions. Counter to our findings, Lisinopril administered with aldosterone receptor antagonist, spironolactone, improved function and reduced damage in the mdx/Utrn$^{+/-}$ mouse (28), though not in the mdx model (21). The stage of disease in which treatments were initiated may impact efficacy of treatments such that initiation at 4 weeks of age improved skeletal muscle function and decreased injury, while the same treatment started at 8 weeks failed to improve these parameters (28). Similarly, animal model may also play a role in study outcomes, as demonstrated by the benefits of Lisinopril in mdx/Utrn$^{+/-}$ mice that were not recapitulated in the mdx model (21).

Though C57BL/10-mdx (mdx) mice are conventionally used to model DMD in mice, in this study we employed the DBA/2J-mdx (D2-mdx) mouse model. The mdx mouse generally has a mild phenotype compared to human patients (9), which has hindered translational research. The emerging D2-mdx model has an early onset of disease, a more severe phenotype, and a latent TGF-β-binding protein gene 4 (Ltbp4) genetic modifier contributing to increased fibrosis and inflammation, which has been linked to earlier loss of ambulation in DMD patients (15). Our data demonstrate that fibrotic area was notably increased in D2-mdx mice, which coincided with decreased contractile area. Similarly, in a previous study comparing mdx and D2-mdx mice, muscle fiber damage, evaluated by Evan's blue dye uptake, was increased by approximately 2-fold compared to DBA and also increased over 30% compared to mdx at 8 weeks of age

(11) supporting increased disease severity in the D2-mdx model compared to the mdx model.

Despite decreased diaphragm specific force and advanced histological injury in dystrophic diaphragms compared to healthy, *in vivo* respiratory function was surprisingly similar between D2-mdx and DBA mice. While beyond the scope and capacity of this investigation, it is reasonable to suggest that accessory muscles are likely compensating for the failing diaphragm in D2-mdx. The assistance of accessory muscle results in similar respiratory function, assessed via whole body plethysmography, despite increased diaphragm injury and dysfunction. As DMD is a progressive disease we hypothesized that, despite potential contributions by accessory muscles, respiratory failure may be detected by careful scrutiny of changes occurring during the final phase of our investigation. Indeed, we discovered that in D2-mdx mice parameters of respiratory function declined between 8-10 months of age compared to DBA mice, which suggests that respiratory function is compromised in dystrophin-deficient mice even if the modality of respiration differs dramatically between healthy and dystrophic mice. Specifically, peak expiratory flow, which is ostensibly dependent on the elasticity of the respiratory system, significantly declined while in healthy mice this continued to increase ($p<0.05$). Similarly, tidal volume and minute ventilation also declined between 8-10 months of age in the D2-mdx model compared to DBA ($p<0.05$), while peak inspiratory flow and breath frequency were similar between groups.

In summary, counter to our hypothesis, our data suggest that these quercetin-based cocktails did not protect dystrophic diaphragms from injury nor preserve respiratory function. Based on our collective body of work investigating quercetin, we

suggest that other therapeutic avenues be considered. Importantly, this investigation provides novel data regarding diaphragm and respiratory function in the D2-mdx model, an emerging model of DMD.

Acknowledgements

This work was supported by Project Parent Muscular Dystrophy (01297), Ryan's Quest, and Michael's Cause. Muscle function data were collected by University of Florida Myology Institute Physiological Assessment Core (U54 AR052646).

References

1. **Anhe GF, Okamoto MM, Kinote A, Sollon C, Lellis-Santos C, Anhe FF, Lima GA, Hirabara SM, Velloso LA, Bordin S, and Machado UF**. Quercetin decreases inflammatory response and increases insulin action in skeletal muscle of ob/ob mice and in L6 myotubes. *Eur J Pharmacol* 689: 285-293, 2012.

2. **Ballmann C, Denney T, Beyers RJ, Quindry T, Romero M, Selsby JT, and Quindry JC**. Long term dietary quercetin enrichment as a cardioprotective countermeasure in mdx mice. *Exp Physiol* 2017.

3. **Ballmann C, Denney TS, Beyers RJ, Quindry T, Romero M, Amin R, Selsby JT, and Quindry JC**. Lifelong quercetin enrichment and cardioprotection in Mdx/Utrn+/- mice. *Am J Physiol Heart Circ Physiol* 312: H128-h140, 2017.

4. **Ballmann C, Hollinger K, Selsby JT, Amin R, and Quindry JC**. Histological and biochemical outcomes of cardiac pathology in mdx mice with dietary quercetin enrichment. *Exp Physiol* 100: 12-22, 2015.

5. **Bellinger AM, Reiken S, Carlson C, Mongillo M, Liu X, Rothman L, Matecki S, Lacampagne A, and Marks AR**. Hypernitrosylated ryanodine receptor calcium release channels are leaky in dystrophic muscle. *Nat Med* 15: 325-330, 2009.

6. **Boots AW, Drent M, de Boer VC, Bast A, and Haenen GR**. Quercetin reduces markers of oxidative stress and inflammation in sarcoidosis. *Clin Nutr* 30: 506-512, 2011.

7. **Brooks SV, and Faulkner JA**. Contractile properties of skeletal muscles from young, adult and aged mice. *J Physiol* 404: 71-82, 1988.

8. **Chalkiadaki A, Igarashi M, Nasamu AS, Knezevic J, and Guarente L**. Muscle-specific SIRT1 gain-of-function increases slow-twitch fibers and ameliorates pathophysiology in a mouse model of duchenne muscular dystrophy. *PLoS Genet* 10: e1004490, 2014.

9. **Chamberlain JS, Metzger J, Reyes M, Townsend D, and Faulkner JA**. Dystrophin-deficient mdx mice display a reduced life span and are susceptible to spontaneous rhabdomyosarcoma. *Faseb j* 21: 2195-2204, 2007.

10. **Chan MC, Rowe GC, Raghuram S, Patten IS, Farrell C, and Arany Z**. Post-natal induction of PGC-1alpha protects against severe muscle dystrophy independently of utrophin. *Skelet Muscle* 4: 2, 2014.

11. **Coley WD, Bogdanik L, Vila MC, Yu Q, Van Der Meulen JH, Rayavarapu S, Novak JS, Nearing M, Quinn JL, Saunders A, Dolan C, Andrews W, Lammert C, Austin A, Partridge TA, Cox GA, Lutz C, and Nagaraju K**. Effect of genetic background on the dystrophic phenotype in mdx mice. In: *Hum Mol Genet*2016, p. 130-145.

12. **Dias AS, Porawski M, Alonso M, Marroni N, Collado PS, and Gonzalez-Gallego J**. Quercetin decreases oxidative stress, NF-kappaB activation, and iNOS overexpression in liver of streptozotocin-induced diabetic rats. *J Nutr* 135: 2299-2304, 2005.

13. **Dong J, Zhang X, Zhang L, Bian HX, Xu N, Bao B, and Liu J**. Quercetin reduces obesity-associated ATM infiltration and inflammation in mice: a mechanism including AMPKalpha1/SIRT1. *J Lipid Res* 55: 363-374, 2014.

14. **Eagle M, Baudouin SV, Chandler C, Giddings DR, Bullock R, and Bushby K**. Survival in Duchenne muscular dystrophy: improvements in life expectancy since 1967 and the impact of home nocturnal ventilation. *Neuromuscul Disord* 12: 926-929, 2002.

15. **Flanigan KM, Ceco E, Lamar KM, Kaminoh Y, Dunn DM, Mendell JR, King WM, Pestronk A, Florence JM, Mathews KD, Finkel RS, Swoboda KJ, Gappmaier E, Howard MT, Day JW, McDonald C, McNally EM, and Weiss RB**. LTBP4 genotype predicts age of ambulatory loss in Duchenne muscular dystrophy. *Ann Neurol* 73: 481-488, 2013.

16. **Handschin C, Kobayashi YM, Chin S, Seale P, Campbell KP, and Spiegelman BM**. PGC-1alpha regulates the neuromuscular junction program and ameliorates Duchenne muscular dystrophy. *Genes Dev* 21: 770-783, 2007.

17. **Hollinger K, Gardan-Salmon D, Santana C, Rice D, Snella E, and Selsby JT**. Rescue of dystrophic skeletal muscle by PGC-1 alpha involves restored expression of dystrophin-associated protein complex components and satellite cell signaling. *American Journal of Physiology-Regulatory Integrative and Comparative Physiology* 305: R13-R23, 2013.

18. **Hollinger K, and Selsby JT**. PGC-1alpha gene transfer improves muscle function in dystrophic muscle following prolonged disease progress. *Exp Physiol* 100: 1145-1158, 2015.

19. **Hollinger K, Shanely RA, Quindry JC, and Selsby JT**. Long-term quercetin dietary enrichment decreases muscle injury in mdx mice. *Clin Nutr* 34: 515-522, 2015.

20. **Huang P, Cheng G, Lu H, Aronica M, Ransohoff RM, and Zhou L**. Impaired respiratory function in mdx and mdx/utrn(+/-) mice. *Muscle Nerve* 43: 263-267, 2011.

21. **Janssen PM, Murray JD, Schill KE, Rastogi N, Schultz EJ, Tran T, Raman SV, and Rafael-Fortney JA**. Prednisolone attenuates improvement of cardiac and skeletal contractile function and histopathology by lisinopril and spironolactone in the mdx mouse model of Duchenne muscular dystrophy. *PLoS One* 9: e88360, 2014.

22. **Kuznetsov AV, Winkler K, Wiedemann FR, von Bossanyi P, Dietzmann K, and Kunz WS**. Impaired mitochondrial oxidative phosphorylation in skeletal muscle of the dystrophin-deficient mdx mouse. *Mol Cell Biochem* 183: 87-96, 1998.

23. **Lowe J, Wodarcyk AJ, Floyd KT, Rastogi N, Schultz EJ, Swager SA, Chadwick JA, Tran T, Raman SV, Janssen PM, and Rafael-Fortney JA**. The Angiotensin Converting Enzyme Inhibitor Lisinopril Improves Muscle Histopathology but not Contractile Function in a Mouse Model of Duchenne Muscular Dystrophy. In: *J Neuromuscul Dis*2015, p. 257-268.

24. **Moorwood C, Liu M, Tian Z, and Barton ER**. Isometric and Eccentric Force Generation Assessment of Skeletal Muscles Isolated from Murine Models of Muscular Dystrophies. *J Vis Exp* 2013.

25. **Nemoto S, Fergusson MM, and Finkel T**. SIRT1 functionally interacts with the metabolic regulator and transcriptional coactivator PGC-1{alpha}. *J Biol Chem* 280: 16456-16460, 2005.

26. **Pasternak C, Wong S, and Elson EL**. Mechanical function of dystrophin in muscle cells. *J Cell Biol* 128: 355-361, 1995.

27. **Quindry JC, Ballmann CG, Epstein EE, and Selsby JT**. Plethysmography measurements of respiratory function in conscious unrestrained mice. *J Physiol Sci* 66: 157-164, 2016.

28. **Rafael-Fortney JA, Chimanji NS, Schill KE, Martin CD, Murray JD, Ganguly R, Stangland JE, Tran T, Xu Y, Canan BD, Mays TA, Delfin DA, Janssen PM, and Raman SV**. Early treatment with lisinopril and spironolactone preserves cardiac and skeletal muscle in Duchenne muscular dystrophy mice. *Circulation* 124: 582-588, 2011.

29. **Ryu D, Zhang H, Ropelle ER, Sorrentino V, Mazala DA, Mouchiroud L, Marshall PL, Campbell MD, Ali AS, Knowels GM, Bellemin S, Iyer SR, Wang X, Gariani K, Sauve AA, Canto C, Conley KE, Walter L, Lovering RM, Chin ER, Jasmin BJ, Marcinek DJ, Menzies KJ, and Auwerx J**. NAD+ repletion improves muscle function in muscular dystrophy and counters global PARylation. *Sci Transl Med* 8: 361ra139, 2016.

30. **Selsby JT, Ballmann CG, Spaulding HR, Ross JW, and Quindry JC**. Oral quercetin administration transiently protects respiratory function in dystrophin-deficient mice. *J Physiol* 594: 6037-6053, 2016.

31. **Selsby JT, Morine KJ, Pendrak K, Barton ER, and Sweeney HL**. Rescue of dystrophic skeletal muscle by PGC-1alpha involves a fast to slow fiber type shift in the mdx mouse. *PLoS One* 7: e30063, 2012.

32. **Shimizu-Motohashi Y, Komaki H, Motohashi N, Takeda S, Yokota T, and Aoki Y**. Restoring Dystrophin Expression in Duchenne Muscular Dystrophy: Current Status of Therapeutic Approaches. *J Pers Med* 9: 2019.

33. **Spaulding HR, Ballmann CG, Quindry JC, and Selsby JT**. Long-term quercetin dietary enrichment partially protects dystrophic skeletal muscle. *PLoS One* 11: e0168293, 2016.

34. **Spaulding HR, Kelly EM, Quindry JC, Sheffield JB, Hudson MB, and Selsby JT**. Autophagic dysfunction and autophagosome escape in the mdx mus musculus model of Duchenne muscular dystrophy. *Acta Physiol (Oxf)* 222: 2018.

35. **Spaulding HR, and Selsby JT**. Is exercise the right medicine for dystrophic muscle? *Med Sci Sports Exerc* 50: 1723-1732, 2018.

36. **Zhang H, Ryu D, Wu Y, Gariani K, Wang X, Luan P, D'Amico D, Ropelle ER, Lutolf MP, Aebersold R, Schoonjans K, Menzies KJ, and Auwerx J**. NAD+ repletion improves mitochondrial and stem cell function and enhances life span in mice. *Science* 2016.

Figures

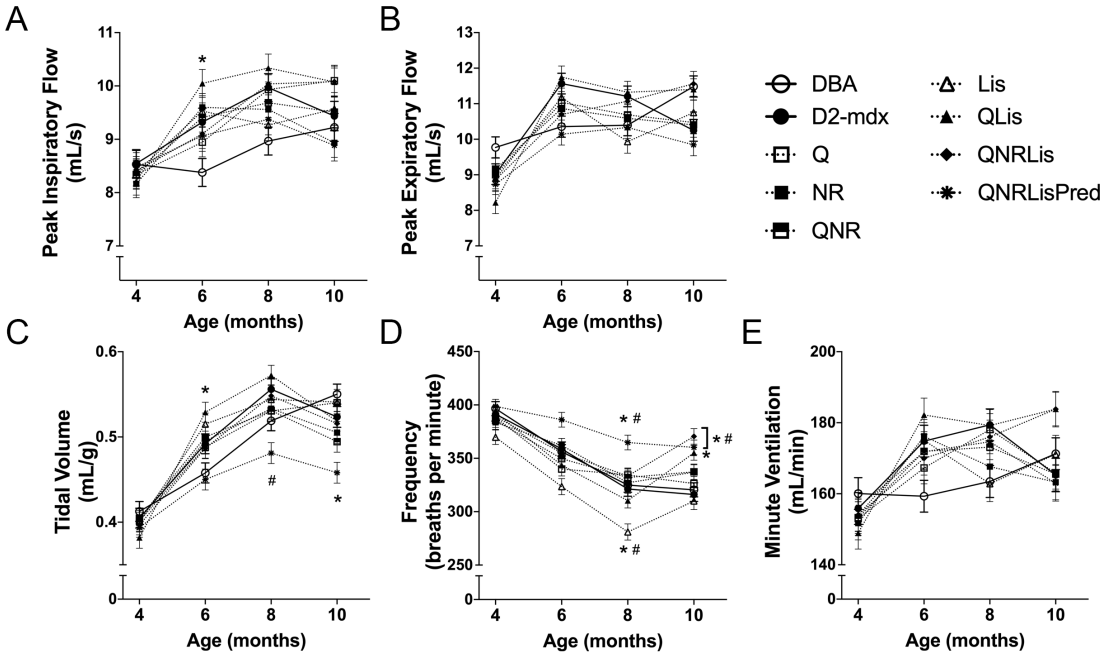

Figure 1: *In vivo* respiratory function. Only statistical differences between all groups compared to DBA and treatment groups compared to D2-mdx are indicated in the figures. Statistically significant difference between treatment groups are included in the results section. A) The main effect of QLis increased peak inspiratory flow compared to DBA and specifically increased peak inspiratory flow at 6 mo of age, but all treatment groups were similar to D2-mdx. B) Peak expiratory flow was not altered at any time point compared to DBA or D2-mdx, regardless of disease or treatment C) QNRLisPred tidal volume was decreased compared to DBA at 10 months and decreased as a main effect of QNRLisPred treatment compared to DBA and D2-mdx. Additionally, tidal volume of QLis treated animals was increased compared to DBA. D) Respiratory rate was increased in QNRLisPred as a main effect of treatment compared to DBA and D2-mdx. Also, at 8 mo, respiratory rate was increased in QNRLisPred compared to DBA and D2-mdx but decreased in Lis treated mice compared to DBA and D2-mdx. Lastly, at 10 mo QNRLisPred breath frequency was still increased compared to DBA and D2-mdx. QNRLis was increased compared to DBA and D2-mdx, and QLis was increased compared to DBA. E) Minute Ventilation was similar between all groups regardless of disease or treatment. DBA (n=10), D2-mdx (n=10), Q (n=9), NR (n=9-10), QNR (n=9-10), Lis (n=7-10), QLis (n=10), QNRLis (n=8-9), and QNRLisPred (n=8). Statistical significance was established at $p<0.05$. * = significantly different from DBA, # = significantly different from D2-mdx.

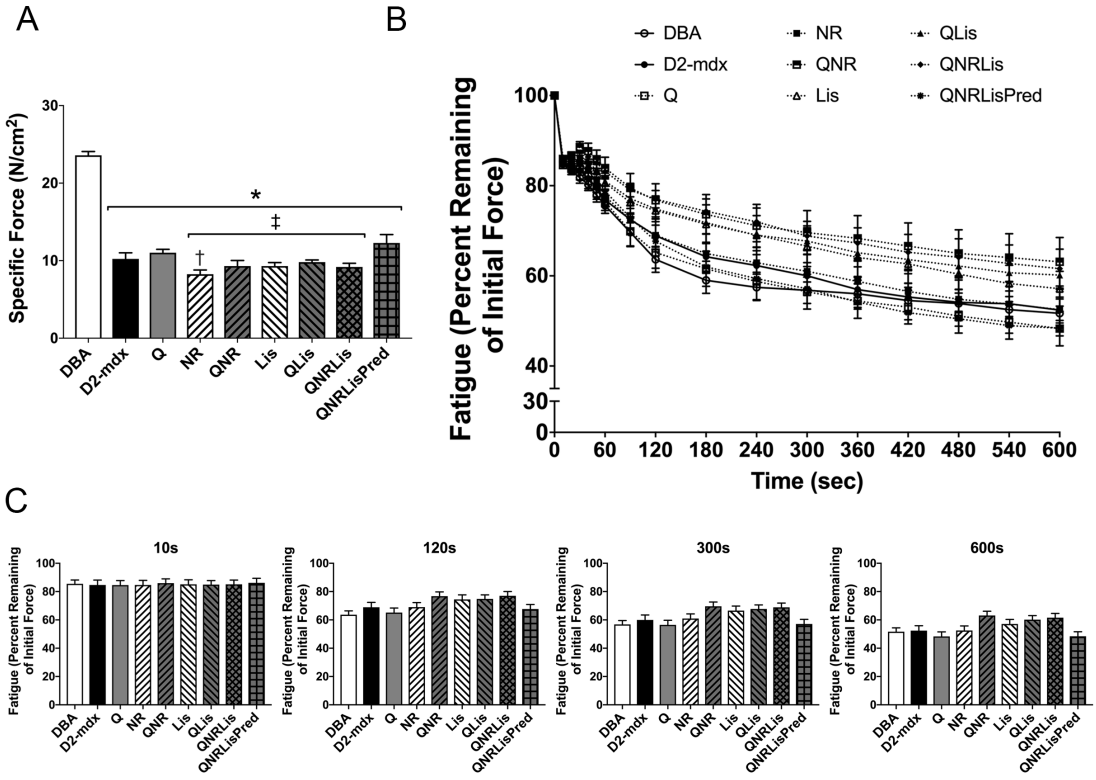

Figure 2: *In vitro* diaphragm function. A) Specific force was decreased in all D2-mdx groups compared to DBA. NR, QNR, Lis, QLis and QNRLis-treated mice were reduced compared to QNRLisPred. B & C) Fatigue resistance was similar between groups at selected time points corresponding to the immediate energy system (10 s), glycolytic system (120 s), and aerobic system (300 s and 600 s). DBA (n=9-10), D2-mdx (n=6-8), Q (n=7-8), NR (n=7-8), QNR (n=8), Lis (n=7), QLis (n=9-10), QNRLis (n=8), and QNRLisPred (n=7-8). Statistical significance was established at $p<0.05$, * = significantly different from DBA, † = significantly different from Q, ‡ = significantly different from QNRLisPred.

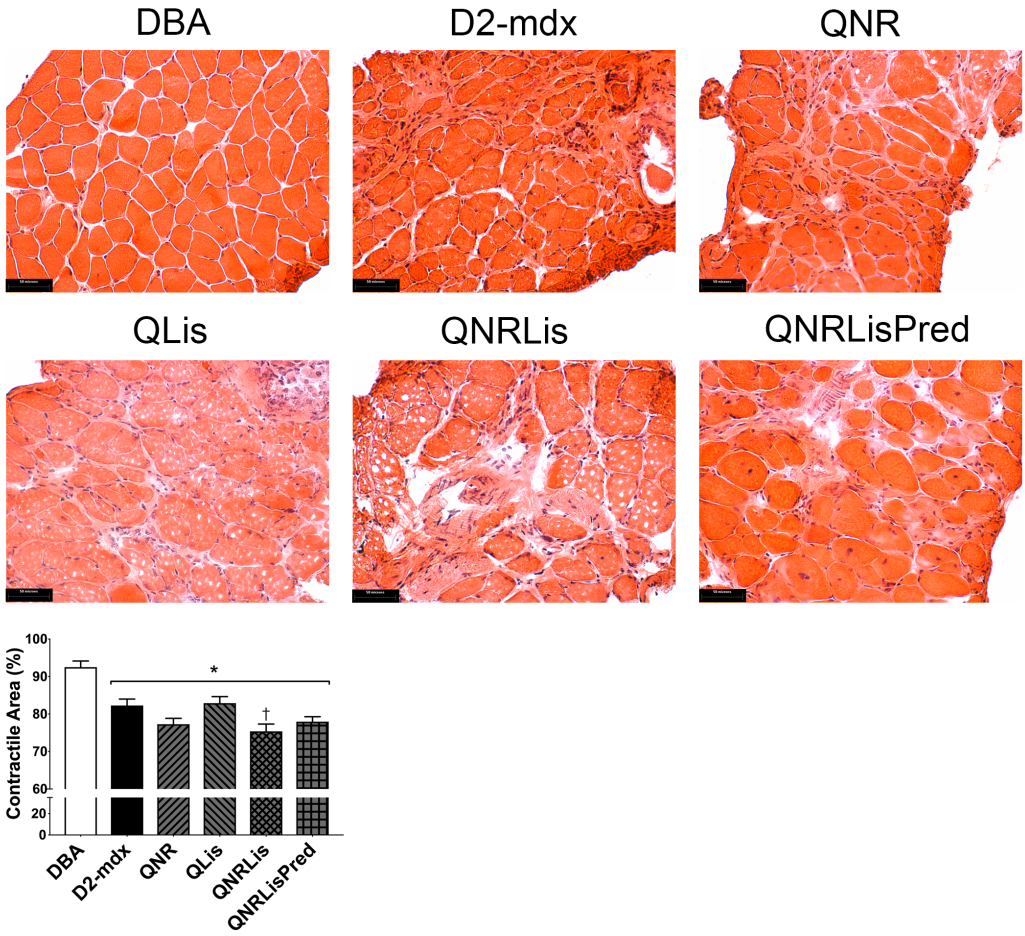

Figure 3: H&E contractile area. Representative H&E images (40x) of diaphragm muscle. Contractile area was decreased in D2-mdx mice, which was not corrected by treatments. DBA (n=6), D2-mdx (n=5), QNR (n=8), QLis (n=10), QNRLis (n=6), and QNRLisPred (n=7). Statistical significance was established at $p<0.05$, * = significantly different from DBA, † = significantly different from QLis.

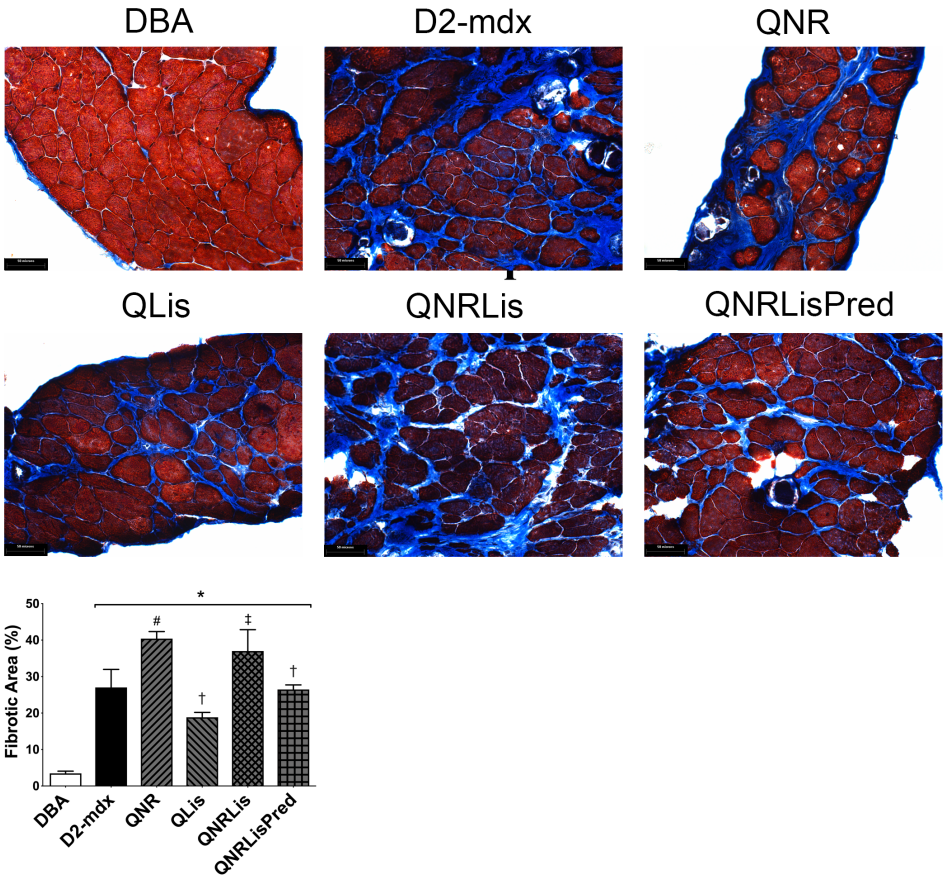

Figure 4: Trichrome fibrotic area. Representative trichrome images (40x) of diaphragm muscle. Fibrotic area was increased in dystrophic muscle, and not attenuated by any treatment. DBA (n=9), D2-mdx (n=8), QLis (n=10), QNRLis (n=8), and QNRLisPred (n=8). Statistical significance was established at $p<0.05$, * = significantly different from DBA, # = significantly different from D2-mdx, † = significantly different from QNR, ‡ = significantly different from QLis.

CHAPTER 6: AUTOPHAGIC DYSFUNCTION AND AUTOPHAGOSOME ESCAPE IN THE MDX *MUS MUSCULUS* MODEL OF DUCHENNE MUSCULAR DYSTROPHY

Hannah R. Spaulding[1], Ellen M. Kelly[2], John C. Quindry[3], Joel B. Sheffield[4], Matthew B. Hudson[5], and Joshua T. Selsby[1]

[1]806 Stange Rd, 2356 Kildee Hall, Department of Animal Science, Iowa State University, Ames, IA

[2]403 Haddon Ave, Coriell Institute for Medical Research, Camden, NJ 08103, USA

[3]101 McGill Hall, Department of Health and Human Performance, University of Montana, Missoula, MT 59812, USA

[4]1900 N. 12th, 311 BioLife, Department of Biology, Temple University, Philadelphia, PA 19122, USA

[5]540 South College Ave, Department of Kinesiology and Applied Physiology, University of Delaware. Newark, DE 19122, USA

Modified from a manuscript published in

Acta Physiologica (Oxf). 2018 Feb;222(2). doi: 10.1111/apha.12944.

Abstract

Aim

Duchenne muscular dystrophy is caused by the absence of functional dystrophin protein and results in a host of secondary effects. Emerging evidence suggests that dystrophic pathology includes decreased pro-autophagic signaling and suppressed autophagic flux in skeletal muscle, but the relationship between autophagy and disease progression is

unknown. The purpose of this investigation was to determine the extent to which basal autophagy changes with disease progression. We hypothesized that autophagy impairment would increase with advanced disease.

Methods

To test this hypothesis, seven week old and 17 month old dystrophic diaphragms were compared to each other and age-matched controls.

Results

Changes in protein markers of autophagy indicate impaired autophagic stimulation through AMPK, however, robust pathway activation in dystrophic muscle, independent of disease severity. Relative protein abundance of p62, an inverse correlate of autophagic degradation, was dramatically elevated with disease regardless of age. Likewise, relative protein abundance of Lamp2, a lysosome marker, was decreased 2-fold at 17 months of age in dystrophic muscle and was confirmed, along with mislocalization, in histological samples, implicating lysosomal dysregulation in this process. In dystrophic muscle autophagosome-sized p62 positive foci were observed in the extracellular space. Moreover, we found that autophagosomes were released from both healthy and dystrophic diaphragms into the extracellular environment, and the occurrence of autophagosome escape was more frequent in dystrophic muscle.

Conclusion

These findings suggest autophagic dysfunction proceeds independent of disease progression, blunted degradation of autophagosomes is due in part to decreased lysosome abundance, and contributes to autophagosomal escape to the extracellular space.

Key words: Autophagy, DMD, dystrophin, extracellular vesicle, lysosome

Introduction

Duchenne muscular dystrophy (DMD) is an X-linked muscle wasting disease in which muscle dysfunction, degeneration, and progressive muscle weakness result from the absence of functional dystrophin protein. Underlying this progression of muscle weakness and injury is mitochondrial dysfunction, oxidative stress, membrane instability, proteolysis, and decreased calcium homeostasis, among other pathologic changes.[1-4] Autophagy has become recognized as a critical process to remove damaged and dysfunctional organelles, proteins aggregates and cellular components promoting cell survival.[5, 6] Further, maintenance of basal autophagy appears to play a vital role in healthful muscle maintenance.[7]

Recent evidence demonstrates increased autophagy in dystrophic muscle could provide therapeutic benefit to patients suffering from DMD. For example, pharmacological activation of AMPK resulted in increased autophagy in mdx mice concomitant with decreased disease-related injury and improved muscle function in dystrophic diaphragms.[8] Interestingly, improved function was due, at least in part, to improved mitochondrial integrity via selective autophagic removal of damaged mitochondria.[8] Further evidence of impaired autophagy is observed by the activation of AKT and mTOR in dystrophic flexor digitorum brevis and diaphragm muscle,[9] as pathway activation of these two molecules inhibit autophagy.[10, 11]

During autophagy, cellular components and organelles are engulfed by autophagosomes, which fuse with lysosomes culminating in degradation. Organelle movement through the autophagic process ultimately results in constituent degradation commonly referred to as ‘autophagic flux’. While evidence of autophagic impairment in

dystrophic muscle exists,[9, 12, 13] the mechanisms and signaling that link this biological process with diminished outcomes are not well understood. Accordingly, the purpose of the present study was to investigate signaling involved in impaired autophagy in dystrophic muscle and determine the relationship between the degree of impairment and disease progression. We hypothesized that increased disease progression would further decrease basal autophagic signaling and suppress autophagic degradation.

Results

Activation of autophagy in dystrophic skeletal muscle.

Damaged organelles and protein aggregates are cleared from cells by autophagosomal packaging and transport to the lysosomes for degradation and is inhibited by mTOR activity, which is increased in dystrophic muscle. In contrast, autophagy is stimulated by AMPK activity, which is equivocally altered in dystrophic muscle. Given these mixed reports[8, 14-16] it was important to clarify the role of AMPK activation in dystrophic skeletal muscle to appreciate its influence on autophagic regulation with disease progression. To address this aim, AMPK protein abundance was measured by Western blot from diaphragms of 7 week and 17 month old dystrophic (mdx) and age-matched control (C57) mice. We found that dystrophin deficiency increased total AMPK 3-5-fold ($p<0.05$), however phosphorylated AMPK at threonine 172 was similar between groups (Figure 1). Alternatively, the pAMPK threonine 172/AMPK ratio was decreased by 3.8-fold in dystrophic muscle ($p<0.05$). In addition, AMPK activation was suppressed 1.4-fold ($p<0.05$) by aging in healthy diaphragms. Phosphorylation of ACC serine 79, another indicator of AMPK activation, was similar between dystrophic and control mice in both young and old mouse diaphragms.

Phosphorylation of ULK1 at serine 555, required for phosphorylation of Beclin-1 at serine 14,[17] was similar between 7 week control and dystrophic diaphragms. In contrast, ULK1 phosphorylation was decreased by 65% in 17 month old diaphragms with advanced disease progression.

Autophagic machinery is increased in dystrophic muscle.

To evaluate the abundances of autophagic machinery, markers of phagosome formation and maturation were evaluated by Western blot. Despite similar pAMPK protein abundance autophagy appeared to be initiated by increased Beclin-1. This latter conclusion is supported by the observation that phosphorylated Beclin-1 and PI3K class III were increased more than 3.5-fold ($p<0.05$) in dystrophic muscle, a finding that was independent of disease severity (Figure 2). Further, Atg12-5 complex formation, indicative of autophagosome formation, was increased over 30-fold ($p<0.05$) in dystrophic diaphragms regardless of age. Protein abundance of Atg7, an E1 activating enzyme that binds Atg5 and 12, was similar between groups. LC3I was increased 3-4-fold in dystrophic diaphragms compared to healthy diaphragms and reached statistical significance in tissues from 7 week old animals ($p<0.05$). The lipidation product, LC3II, which binds to the autophagosome membrane indicating maturation, was significantly increased 2.9-fold ($p<0.05$) in 7 week dystrophic diaphragms, but abundance of LC3II was similar between 17 month dystrophic and control diaphragms.

Autophagic flux markers indicate dysfunction in dystrophic skeletal muscle

Markers of autophagic flux and degradation, including LC3II/LC3I and p62 protein abundance, indicate downstream autophagy is impaired in both 7 week and 17 month dystrophic diaphragms (Figure 3). Specifically, the LC3II/LCI ratio was

numerically decreased 1.4-fold in 7 week and significantly decreased 2.7-fold ($p<0.05$) in 17 month old dystrophic diaphragms compared to respective controls. Similarly, p62, a protein found in autophagosomes trafficked for lysosomal degradation, increased over 5-fold ($p<0.05$) in dystrophic diaphragms from both 7 week and 17 month old animals. Collectively, these findings indicate a substantial impairment in autophagic degradation of autophagosomes. Additionally, the abundance of ubiquitinated proteins was increased 3-fold in dystrophic diaphragms, further supporting decreased autophagic degradation.[18]

Decreased lysosomal content in dystrophic muscle.

Increased autophagic signaling and pathway activation coupled with decreased markers of autophagic degradation suggested a role of lysosomes in this process. During functional autophagy, autophagosomes fuse to lysosomes to form autophagolysosomes, which results in the degradation of autophagosome cargo. Thus, decreased cellular lysosomal content could impair autophagic flux. In 17 month dystrophic diaphragms lysosomal content was decreased 2-fold (Figure 3), as indicated by lysosome-associated membrane protein 2 (Lamp2) protein abundance.

To better understand the role of lysosomes and autophagosomes in dystrophic muscle we next investigated archived diaphragm samples from 14 month old dystrophic and healthy mice by immunohistochemistry, and observed lysosomal content was also decreased in these dystrophic diaphragms (Figure 4). Consistent with hypothesized outcomes, lysosome content, as measured by Lamp2, were localized to muscle cells in healthy muscle. However, in dystrophic diaphragms not only was total Lamp2 decreased but appeared to have localized to the extracellular space around non-fiber nuclei (Figure

4). In addition, we confirmed that p62-positive puncta were largely contained within the presumptive autophagosomal range of 0.5-1.5 microns.[19]

Given that both our Western blot and immunohistochemistry data supported decreased Lamp2 and suggested insufficient intracellular lysosome abundance, we next assessed transcription factor EB (TFEB) localization. Dephosphorylation and translocation of TFEB into the nucleus results in expression of transcripts involved in autophagy and lysosomal biogenesis.[20] We assessed TFEB localization by immunohistochemistry in diaphragm samples from 17 months old dystrophic and healthy mice. In dystrophic muscle, TFEB was notably excluded from centralized nuclei, while it was apparent in peripheral nuclei of healthy muscle (Figure 5A and B). TFEB also appears to be excluded from some extra-muscular nuclei in healthy and dystrophic muscle and likely represents a common sub-population of resident cells.

Skeletal muscle releases autophagosomes into the extracellular environment.

We also noted that p62 positive puncta were apparent outside dystrophic muscle cells but not healthy muscle cells (Figure 4). In most cases p62 was located within Lamp2 positive areas, and ostensibly within immune cells, but we also noted unaccompanied foci. Merged images show p62 puncta within Lamp2 as well as p62 outside the intramuscular space and independent of Lamp2 (Figure 4 and 7A). This finding raised the possibility of autophagosomal migration from the intramuscular space to the extracellular space and escaping lysosomal degradation.

To address this intriguing possibility we first investigated if skeletal muscle cells release vesicles morphologically similar to autophagosomes. We have previously demonstrated that muscles release small lipid vesicles in the 40-150 nm size range

(termed exosomes) into the extracellular space by incubating differentiated myotubes in serum free media and then isolating exosomes from the media via high-speed centrifugation (100,000g).[21, 22] Using the same approach but with a lower centrifugation speed (12,000g) to pellet larger vesicles followed by scanning electron microscopy we identified that skeletal muscle cells release a variety of vesicles including vesicles morphologically similar to autophagosomes (Figure 6).

To determine if dystrophic muscle releases an extracellular vesicle population containing autophagosomes we incubated costal diaphragms from healthy and mdx mice at approximately Lo in an oxygenated Krebs bath and isolated large vesicles using the same centrifugation protocol. Interestingly, flow cytometry analysis revealed that both healthy and dystrophic diaphragms release autophagosomes, but dystrophic diaphragms release nearly 4-fold more autophagosomes (Figure 7B).

Discussion

Duchenne muscular dystrophy is a muscle wasting disease characterized by the absence of functional dystrophin protein that leads to eventual death due to respiratory or cardiac failure. Autophagy functions as a mechanism by which dysfunctional protein, organelles, and cellular components are consumed within the cell. With or without physiologic stress, autophagy is activated by a variety of stimuli including mitochondrial dysfunction and accumulation of dysfunctional organelles or proteins. Indeed, given the potential for these to accumulate in dystrophic muscle we reasoned that autophagy was suppressed in dystrophic muscle. We further reasoned that autophagic signaling would be repressed with advancing disease.

Several investigations have demonstrated decreased AMPK phosphorylation [14, 16] and increased mTOR phosphorylation,[9] both anti-autophagic signals, in dystrophic muscle suggesting impaired autophagic signaling. In recent years autophagic trafficking has been assessed by LC3II/I ratios and p62 accumulation as an indirect metric of suppressed flux.[9, 12, 13] Consistent with previous findings our data indicate AMPK activation was decreased in dystrophic muscle compared to healthy muscle. Further, we report decreased phosphorylation of ULK at serine 555 at 17 months of age, which also suggests suppression of autophagic signaling. Despite this, we found autophagy was strongly induced in dystrophic muscle suggesting that a non-canonical mechanism may initiate this process. Specifically, we noted that Beclin-1 and PI3K class III were markedly increased in dystrophic muscle as was formation of the Atg12-5 complex. This latter point is of high importance because Atg12-5 complex formation results from several protein/protein interactions and is a marker of pathway activation.[23] Despite this activation, and consistent with the findings of others,[9, 12, 13, 24] autophagic degradation appeared to be blunted by dystrophin deficiency as the LC3II/I ratio was decreased and p62 was increased compared to healthy muscle.

Given these data, it is unlikely that autophagy is regulated by upstream AMPK or mTOR signaling in dystrophic muscle. From a therapeutic perspective these data indicate that direct stimulation of autophagy is unlikely to be a successful long-term approach as autophagic machinery is already in place. It is interesting to note that the marked increase in p62 protein abundance promotes mTOR stability [25] and liberates Beclin-1 from Bcl-2 [26] resulting in simultaneous inhibition and stimulation of autophagy. Moreover, mTOR not only inhibits autophagy but also may inhibit degradation of

autophagosomal content by interfering with lysosomal function.[27] These results appeared to be independent of disease severity as autophagic dysfunction was independent of a number of secondary pathologies that may be exacerbated by disease progression (oxidative stress, inflammation, etc.) and instead depend upon lysosomal dysfunction or cytoskeletal derangement. Indeed De Palma et al.[12] also observed stalling of autophagy and suggested that it may be due to signaling but could not exclude other potential mechanisms.

Lysosomal protein abundance was decreased at 17 months of age in dystrophic muscle compared to age matched controls. This finding raised the possibility that stalling of autophagosome degradation in dystrophic muscle is due, at least in part, to a lysosomal insufficiency. If correct, this postulate is likely compounded by a shift in lysosome localization from fibers to the extracellular space, ostensibly to immune cells. Hence, the intrafibrillar lysosomal population is smaller than would be anticipated by Western blot, alone. Moreover, selective exclusion of TFEB, a master regulator of the autophagy-lysosomal pathway,[20] from dystrophic centralized nuclei plays a significant role in this process. Consistent with this rational, TFEB exclusion from nuclei can be driven by increased mTOR activity as is commonly reported in dystrophic muscle.[9, 28, 29] Consistent with our findings a previous report demonstrated decreased lysosome abundance in dystrophic limb muscle compared to controls, as measured by Lamp1 mRNA and protein abundance.[9]

Interestingly, we observed poor colocalization of lysosomes (Lamp2) and autophagosomes (p62) in dystrophic muscle, further supporting impaired autophagosome/lysosome fusion. Similarly, blunted lysosome and autophagosome

colocalization were observed previously in dystrophic limb muscle [9] suggestive of autophagic stalling via impaired autophagolysosome formation.

As a collective response, autophagy appears to be robustly activated in dystrophic muscle, but degradation simultaneously blunted. Accumulation of autophagosomes would be the natural consequence of a 'dystrophic program', however, despite significant prior work in the area, there is no precedent for this outcome occurring in dystrophic muscle. After careful scrutiny of our p62 immunohistochemical images we noted p62 positive foci clustering outside of muscle cells in the extracellular environment as well as in infiltrating immune cells. This led us to consider whether autophagic stalling results in the escape of autophagosomes into the extracellular environment. To address this hypothesis we first imaged vesicles released from healthy myotubes via scanning electron microscopy to determine the feasibility of muscles releasing autophagosome-sized vesicles. Interestingly, in addition to the small exosomes and microvesicles produced by muscle,[21, 22] large vesicles similar in size and morphology to autophagosomes are among the vesicles released from muscle (Figure 6). Remarkably, we observed that healthy diaphragm muscle releases a significant number of autophagosomes into the extracellular environment while dystrophic muscle releases significantly more. Indeed, careful inspection of p62/LC3 images by Pal et al.[9] (Figure 1L, bottom series) supports this novel postulate that dystrophic muscle produce extracellular autophagosomes. While, the physiological mechanisms and biological purpose of muscle released autophagosomes to the extracellular environment are unknown it may occur as a means of removing damaged cellular components in an attempt to maintain intracellular homeostasis. Thus, autophagosome escape in dystrophic muscle may serve as means of cell survival.

Related to this concept, cancer researchers recently found evidence of autophagosome release as Zhou et al [30] identified tumor cell-released autophagosomes (TRAPs), which function in suppression of anti-tumor immunity. Similarly, healthy neurons and neurons affected by stroke conditions release mitochondria in a disease-specific pattern.[31, 32]

In total, these data support previous findings of upstream inhibition of autophagic signaling and impaired flux in dystrophic muscle. However, we found that despite the decreased pro-autophagic signaling and apparent reduction in autophagic degradation, protein abundance of autophagic machinery was increased at both 7 weeks and 17 months of age. Hence, counter to our hypothesis, autophagic dysfunction was independent of disease progression. Moreover, our evidence implicates lysosomal insufficiency as critical to this process. Finally, we discovered compelling new evidence that healthy and dystrophic muscle release autophagosomes to the extracellular environment raising the possibility of a novel paracrine and, given the mass of skeletal muscle, endocrine function of skeletal muscle. Importantly, it seems likely that suppressed autophagic degradation led to increased autophagosome escape in dystrophic muscle. We think it likely that this phenomenon is occurring in other pathologic states that limits autophagy and may contribute to chronic inflammation that accompanies a host of muscle injuries and pathologies.

Methods

Animal Treatment. All animal procedures were approved by the Institutional Animal Care and Use Committee at Iowa State University, Auburn University, or Temple University. Seven week old C57 (n=5) and mdx (n=8) mice along with 17 month old

C57 (n=4) and mdx (n=10) mice were sedated and sacrificed by cervical dislocation. Diaphragms were removed and snap frozen for biochemical analyses.

Immunochemistry. Snap frozen diaphragm tissue was powdered with a steel mortar and pestle then homogenized in 200 µL of whole muscle buffer (10mM Sodium Phosphate buffer, pH 7.0, 2% SDS) using a hand held homogenizer. After homogenization, cellular debris was separated from protein by 15 minutes of centrifugation at 20,000 x g and the supernatant retained. Protein concentration was measured using the Pierce BCA Protein Assay Kit (23225, ThermoScientific, Waltham, MA, USA) and diluted to 2 µg/µL with 2x Laemmli buffer. Following dilution, samples were heated for 5 minutes at 95°C; then 24 µg of protein were separated for 20 minutes at 60 volts followed by 60 minutes at 120 volts using 4-20% gradient gels (Lonza, Basel, Switzerland). Once separated by mass, proteins were transferred to a nitrocellulose membrane (BioRad, Hercules, CA, USA) at 100 volts for 60 minutes. Membranes were blocked for 1 hour in 5% milk, then probed overnight using the following antibodies from Cell Signaling (Danvers, MA, USA), unless otherwise noted: AMPK (Primary (P) 1:1000 5% milk, Secondary (S) 1:1000 1X TBST), phospho (p)AMPK (T172) (P 1:500 5% milk, S 1:1000 5% milk), pACCS79 (Millipore, P 1: 1000 5 % milk, S 1: 2000 5 % milk), pULK (serine 555) (P1:500 1% milk, S 1:500 2.5% milk), PI3K Class III (P 1:1000 5% milk, S 1:2000 5 % milk), Beclin-1 (P 1:500 5% milk, S 1:1000 5% milk), pBeclin-1 (P 1:500 1X TBST, S 1:500 1% milk), ATG12-5 (P 1:750 5% milk, S 1:1500 5% milk), ATG7 (P 1:500 5% milk S 1:1000 5% milk), LC3AB (P 1:500 5% milk, S 1:2000 5% milk), p62 (Abcam, Cambridge, UK, P 1:500 5% milk, S 1:1000 5% milk), Ubiquitin (P 1:1000 1X TBST, S 1:2000 5% milk), and Lamp2 (P 1:2000 5 % milk, S

1:1500 1X TBST). Following primary antibody, membranes were washed in 1X TBST for 10 minutes three times then incubated in anti-rabbit secondary for 1 hour. After antibody incubation, membranes were washed three times for 30 minutes in 1X TBST, then Clarity™ western enhanced chemiluminescence (ECL) blotting substrate (BioRad, Hercules, CA, USA) was applied to the membranes for 7 minutes. Once exposed to ECL, membranes were developed and films were imaged and quantified using Carestream (Carestream Health, Inc. New Haven, CT). All membranes were stained with Ponceau S to verify equal loading.

Immunohistochemistry. To complement protein measures, we performed immunohistochemical measures on archived diaphragm samples from 14 and 17 month old healthy and dystrophic diaphragm muscles. Additional information about these tissues has been previously published.[14, 15] Diaphragm sections were blocked for 1 hour with 5% BSA (Bovine serum albumin). Anti-p62 (1:100, Abcam, rabbit) and anti-Lamp2 (1:100, Abcam, rat) primary antibodies were applied to the 14 month old diaphragm samples at 4°C overnight. At room temperature, sections were washed three times for 10 minutes in 1X PBS (phosphate-buffered saline) then exposed to anti-rabbit AlexaFluor 488 (1:100, Cell Signaling) and goat anti-rat rhodamine secondary antibody (1:200, Thermo) for 1 hour. Sections were washed three times for 10 minutes, then c and confocal images were taken at 63x on a similar Leica microscope. Similarly, diaphragm sections from 17 month old mice were blocked for 45 minutes at room temperature in 5% BSA; then washed as described above. Anti-Transcription Factor EB (TFEB) (1:50, Bethyl) and anti-laminin (1:100, Thermo) primary antibodies and anti-rabbit AlexaFluor 488 (1:500, Cell Signaling) and anti-rat (1:200, Thermo) secondaries were applied to

diaphragm sections as previously described. Total fluorescence of TFEB within the nucleus was measured using ImageJ and normalized to the area of the nucleus and the cellular TFEB intensity.

Cell Culture, Ex Vivo Muscle Preparations, and Extracellular Vesicle Isolation. C2C12 myotubes were grown to full confluence as we have previously described.[21, 22] Briefly, mouse C2C12 myoblasts were cultured in growth medium [DMEM + 10% fetal bovine serum (Atlanta Biologicals, Lawrenceville, GA)] with 1% penicillin-streptomycin (Invitrogen, Carlsbad, CA); all experiments were conducted using cells from passages 3–7. Myoblasts were grown to ~95% confluence and then induced to differentiate into myotubes by replacement of growth medium with differentiation medium (DMEM supplemented with 2% horse serum + 1% penicillin-streptomycin) for 3 days. After 3 days in differentiation medium, cells were washed with serum-free medium and then incubated in serum-free medium. After 6 hours, the medium was collected to isolate large extracellular vesicles. Large extracellular vesicles were isolated from cell culture medium (or tissue bath buffer, described below) via centrifugation. First, medium or buffer was centrifuged at 500 x g for 10 minutes to pellet intact cells and debris, and then supernatant was centrifuged at 12,000 x g to pellet larger vesicles and resuspended in sterile PBS.

A suspension of the large extracellular vesicles taken from myotubes was fixed with an equal volume of 4% paraformaldehyde in 0.08 M phosphate buffer. After 1 hour, 20 µl aliquots were placed on copper tape, which had been attached to standard SEM stubs, and the liquid gradually replaced with graded Ethanol solutions, followed by HMDS (Hexamethyl disilazane), and allowed to air dry. The samples were then sputter

coated with gold, and examined in an Agilent FESEM at 1 kv accelerating voltage, using secondary emission detection.

To follow up cell culture experiments 7 week old C57 and mdx mice were anesthetized with isoflurane before muscle isolation. Whole diaphragms were rapidly excised and prepared in Krebs Ringer solution containing (in mM): 121 NaCl, 5.9 KCl, 2.0 CaCl2, 1.0 MgCl2, 0.6 Na2HPO4, 21 NaHCO3, 0.45 Na2SO4, 11.5 glucose and 10 μM D-tubocurarine. Costal diaphragms were pinned at approximate muscle Lo, and baths were continuously bubbled with 95% O2/5% CO2. After 2 hours, buffer was collected for extracellular vesicle isolation.

Flow Cytometry. Large, muscle-released extracellular vesicles were isolated as described above. Autophagosomes were quantified using the CYTO-ID Autophagy Detection Kit (ENZ-51031; ENZO Life Sciences) that is well established to identify autophagosomes.[34, 35] The kit's instructions were followed with slight modifications in centrifugation speed (all washing/collection steps were performed at 12,000 x g). Samples were analyzed using a MoFlo AstriosEQ (Beckman-Coulter, Inc., Miami, FL), utilizing logarithmic forward scatter (FSC) photomultipliers and various masks to optimize small particle detection and gate of interest and analyzed via a dotplot of Green Fluorescence (513/26 nM) vs. Orange Fluorescence (576/21 nM).

Statistics. Relative protein abundance was compared using two-way ANOVA with a Newman-Keuls post-hoc test where appropriate. Immunohistochemical experiments were analyzed with a Student's T-test and flow cytometry experiments were analyzed with a one-way ANOVA with Newman-Keuls post-hoc test. Significance was established as $p<0.05$, *a priori*. Data are presented as mean ± SEM.

Acknowledgments

This work was supported in part by the Duchenne Alliance and its member foundations (Ryan's Quest, Hope for Gus, Team Joseph, Michael's Cause, Duchenne Now, Zack Heger Foundation, Pietro's Fight, RaceMD, JB's Keys, Romito Foundation, Harrison's Fund, Alex'sWish, and Two Smiles One Hope Foundation) grants 100065 and 100071 to JS and JQ.

References

1. Morris, CA, Selsby, JT, Morris, LD, Pendrak, K, Sweeney, HL: Bowman-Birk inhibitor attenuates dystrophic pathology in mdx mice. *J Appl Physiol,* 109**:** 1492-1499, 2010.

2. Alderton, JM, Steinhardt, RA: Calcium influx through calcium leak channels is responsible for the elevated levels of calcium-dependent proteolysis in dystrophic myotubes. *J Biol Chem,* 275**:** 9452-9460, 2000.

3. Selsby, JT: Increased catalase expression improves muscle function in mdx mice. *Exp Physiol,* 96**:** 194-202, 2011.

4. Godin, R, Daussin, F, Matecki, S, Li, T, Petrof, BJ, Burelle, Y: Peroxisome proliferator-activated receptor γ coactivator 1-α gene transfer restores mitochondrial biomass and improves mitochondrial calcium handling in post-necrotic mdx mouse skeletal muscle. *J Physiol,* 590**:** 5487-5502, 2012.

5. Zhang, J: Teaching the basics of autophagy and mitophagy to redox biologists--mechanisms and experimental approaches. *Redox Biol,* 4**:** 242-259, 2015.

6. Sandri, M, Coletto, L, Grumati, P, Bonaldo, P: Misregulation of autophagy and protein degradation systems in myopathies and muscular dystrophies. *J Cell Sci,* 126**:** 5325-5333, 2013.

7. Grumati, P, Bonaldo, P: Autophagy in skeletal muscle homeostasis and in muscular dystrophies. *Cells,* 1**:** 325-345, 2012.

8. Pauly, M, Daussin, F, Burelle, Y, Li, T, Godin, R, Fauconnier, J, Koechlin-Ramonatxo, C, Hugon, G, Lacampagne, A, Coisy-Quivy, M, Liang, F, Hussain, S, Matecki, S, Petrof, BJ: AMPK activation stimulates autophagy and ameliorates muscular dystrophy in the mdx mouse diaphragm. *Am J Pathol,* 181**:** 583-592, 2012.

9. Pal, R, Palmieri, M, Loehr, JA, Li, S, Abo-Zahrah, R, Monroe, TO, Thakur, PB, Sardiello, M, Rodney, GG: Src-dependent impairment of autophagy by oxidative stress in a mouse model of Duchenne muscular dystrophy. *Nat Commun,* 5**:** 4425, 2014.

10. Kim, J, Kundu, M, Viollet, B, Guan, KL: AMPK and mTOR regulate autophagy through direct phosphorylation of Ulk1. *Nat Cell Biol,* 13**:** 132-141, 2011.

11. Zhao, J, Brault, JJ, Schild, A, Cao, P, Sandri, M, Schiaffino, S, Lecker, SH, Goldberg, AL: FoxO3 coordinately activates protein degradation by the autophagic/lysosomal and proteasomal pathways in atrophying muscle cells. *Cell Metab,* 6**:** 472-483, 2007.

12. De Palma, C, Morisi, F, Cheli, S, Pambianco, S, Cappello, V, Vezzoli, M, Rovere-Querini, P, Moggio, M, Ripolone, M, Francolini, M, Sandri, M, Clementi, E: Autophagy as a new therapeutic target in Duchenne muscular dystrophy. *Cell Death Dis,* 3**:** e418, 2012.

13. Fiacco, E, Castagnetti, F, Bianconi, V, Madaro, L, De Bardi, M, Nazio, F, D'Amico, A, Bertini, E, Cecconi, F, Puri, PL, Latella, L: Autophagy regulates satellite cell ability to regenerate normal and dystrophic muscles. *Cell Death Differ,* 23**:** 1839-1849, 2016.

14. Selsby, JT, Ballmann, CG, Spaulding, HR, Ross, JW, Quindry, JC: Oral quercetin administration transiently protects respiratory function in dystrophin deficient mice. *J Physiol*, 2016.

15. Spaulding, HR, Ballmann, CG, Quindry, JC, Selsby, JT: Long-term quercetin dietary enrichment partially protects dystrophic skeletal muscle. *PLoS One,* 11**:** e0168293, 2016.

16. Ljubicic, V, Khogali, S, Renaud, JM, Jasmin, BJ: Chronic AMPK stimulation attenuates adaptive signaling in dystrophic skeletal muscle. *Am J Physiol Cell Physiol,* 302**:** C110-121, 2012.

17. Nazarko, VY, Zhong, Q: ULK1 targets Beclin-1 in autophagy. In: *Nat Cell Biol.* England, 2013, pp 727-728.

18. Matsumoto, G, Wada, K, Okuno, M, Kurosawa, M, Nukina, N: Serine 403 phosphorylation of p62/SQSTM1 regulates selective autophagic clearance of ubiquitinated proteins. *Mol Cell,* 44**:** 279-289, 2011.

19. Mizushima, N, Ohsumi, Y, Yoshimori, T: Autophagosome formation in mammalian cells. *Cell Struct Funct,* 27**:** 421-429, 2002.

20. Settembre, C, Di Malta, C, Polito, VA, Garcia Arencibia, M, Vetrini, F, Erdin, S, Erdin, SU, Huynh, T, Medina, D, Colella, P, Sardiello, M, Rubinsztein, DC, Ballabio, A: TFEB links autophagy to lysosomal biogenesis. *Science,* 332**:** 1429-1433, 2011.

21. Hudson, MB, Woodworth-Hobbs, ME, Zheng, B, Rahnert, JA, Blount, MA, Gooch, JL, Searles, CD, Price, SR: miR-23a is decreased during muscle atrophy by a mechanism that includes calcineurin signaling and exosome-mediated export. *American journal of physiology Cell physiology,* 306**:** C551-558, 2014.

22. Hudson, MB, Rahnert, JA, Zheng, B, Woodworth-Hobbs, ME, Franch, HA, Price, SR: miR-182 attenuates atrophy-related gene expression by targeting FoxO3 in skeletal muscle. *American journal of physiology Cell physiology,* 307**:** C314-319, 2014.

23. Klionsky, DJ, Abdelmohsen, K, Abe, A, Abedin, MJ, Abeliovich, H, Acevedo Arozena, A, Adachi, H, Adams, CM, Adams, PD, Adeli, K, Adhihetty, PJ, Adler, SG, Agam, G, et al: Guidelines for the use and interpretation of assays for monitoring autophagy (3rd edition). *Autophagy,* 12**:** 1-222, 2016.

24. Bibee, KP, Cheng, YJ, Ching, JK, Marsh, JN, Li, AJ, Keeling, RM, Connolly, AM, Golumbek, PT, Myerson, JW, Hu, G, Chen, J, Shannon, WD, Lanza, GM, Weihl, CC, Wickline, SA: Rapamycin nanoparticles target defective autophagy in muscular dystrophy to enhance both strength and cardiac function. *Faseb j,* 28**:** 2047-2061, 2014.

25. Duran, A, Amanchy, R, Linares, JF, Joshi, J, Abu-Baker, S, Porollo, A, Hansen, M, Moscat, J, Diaz-Meco, MT: p62 is a key regulator of nutrient sensing in the mTORC1 pathway. *Mol Cell,* 44**:** 134-146, 2011.

26. Zhou, L, Wang, H, Ren, H, Chen, D, Gao, F, Hu, Q, Fu, C, Xu, R, Ying, Z, Wang, G: Bcl-2-dependent upregulation of autophagy by sequestosome 1/p62 in vitro. In: *Acta Pharmacol Sin.* 2013, pp 651-656.

27. Zhou, J, Tan, SH, Nicolas, V, Bauvy, C, Yang, ND, Zhang, J, Xue, Y, Codogno, P, Shen, HM: Activation of lysosomal function in the course of autophagy via mTORC1 suppression and autophagosome-lysosome fusion. *Cell Res,* 23**:** 508-523, 2013.

28. Peter, AK, Crosbie, RH: Hypertrophic response of Duchenne and limb-girdle muscular dystrophies is associated with activation of Akt pathway. *Exp Cell Res,* 312**:** 2580-2591, 2006.

29. Dogra, C, Changotra, H, Wergedal, JE, Kumar, A: Regulation of phosphatidylinositol 3-kinase (PI3K)/Akt and nuclear factor-kappa B signaling pathways in dystrophin-deficient skeletal muscle in response to mechanical stretch. *J Cell Physiol,* 208**:** 575-585, 2006.

30. Zhou, M, Wen, Z, Cheng, F, Ma, J, Li, W, Ren, H, Sheng, Y, Dong, H, Lu, L, Hu, HM, Wang, LX: Tumor-released autophagosomes induce IL-10-producing B cells with suppressive activity on T lymphocytes via TLR2-MyD88-NF-kappaB signal pathway. *Oncoimmunology,* 5**:** e1180485, 2016.

31. Hayakawa, K, Esposito, E, Wang, X, Terasaki, Y, Liu, Y, Xing, C, Ji, X, Lo, EH: Transfer of mitochondria from astrocytes to neurons after stroke. *Nature,* 535**:** 551-555, 2016.

32. Davis, CH, Kim, KY, Bushong, EA, Mills, EA, Boassa, D, Shih, T, Kinebuchi, M, Phan, S, Zhou, Y, Bihlmeyer, NA, Nguyen, JV, Jin, Y, Ellisman, MH, Marsh-Armstrong, N: Transcellular degradation of axonal mitochondria. *Proc Natl Acad Sci U S A,* 111**:** 9633-9638, 2014.

33. Hollinger, K, Gardan-Salmon, D, Santana, C, Rice, D, Snella, E, Selsby, JT: Rescue of dystrophic skeletal muscle by PGC-1 alpha involves restored expression of dystrophin-associated protein complex components and satellite cell signaling. *American Journal of Physiology-Regulatory Integrative and Comparative Physiology,* 305**:** R13-R23, 2013.

34. Coleman, J, Xiang, Y, Pande, P, Shen, D, Gatica, D, Patton, WF: A live-cell fluorescence microplate assay suitable for monitoring vacuolation arising from drug or toxic agent treatment. *Journal of biomolecular screening,* 15**:** 398-405, 2010.

35. Mizushima, N, Yoshimori, T, Levine, B: Methods in mammalian autophagy research. *Cell,* 140**:** 313-326, 2010.

Figures

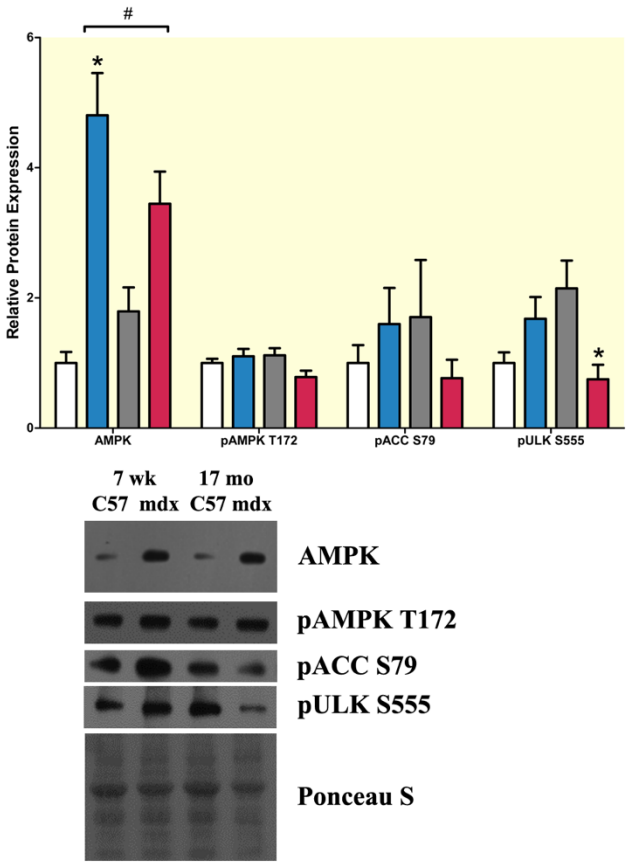

Figure 1. Autophagic regulation. Protein abundance measured by Western blot in 7 week and 17 month old dystrophic (mdx) and control (C57) diaphragms. Significance was established at $p<0.05$. White bars – C57 7 weeks (n=5), blue bars – mdx 7 weeks (n=8), gray bars – C57 17 months (n=4), red bars – mdx 17 months (n=10). * indicates significantly different from age-matched C57 controls, # indicates significant main effect of disease.

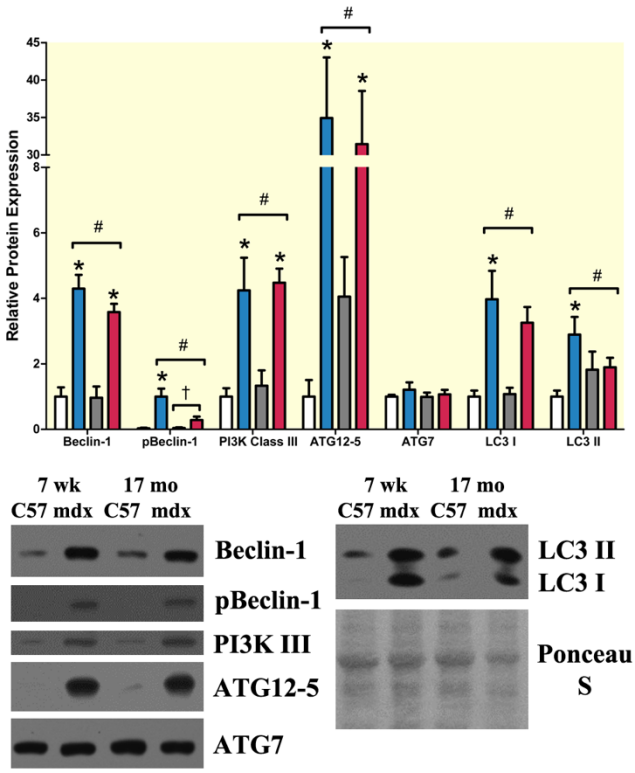

Figure 2. Autophagy initiation and maturation. Protein abundance measured by Western blot in 7 week and 17 month old dystrophic (mdx) and control (C57) diaphragms. Significance was established at $p<0.05$. White bars – C57 7 weeks (n=5), blue bars – mdx 7 weeks (n=8), gray bars – C57 17 months (n=4), red bars – mdx 17 months (n=10). All measures were made relative to C57 7 weeks old controls except pBeclin-1 which was made relative to mdx 7 week old mice. * indicates significantly different from age-matched C57 controls, # indicates significant main effect of disease † = indicates significant main effect of age.

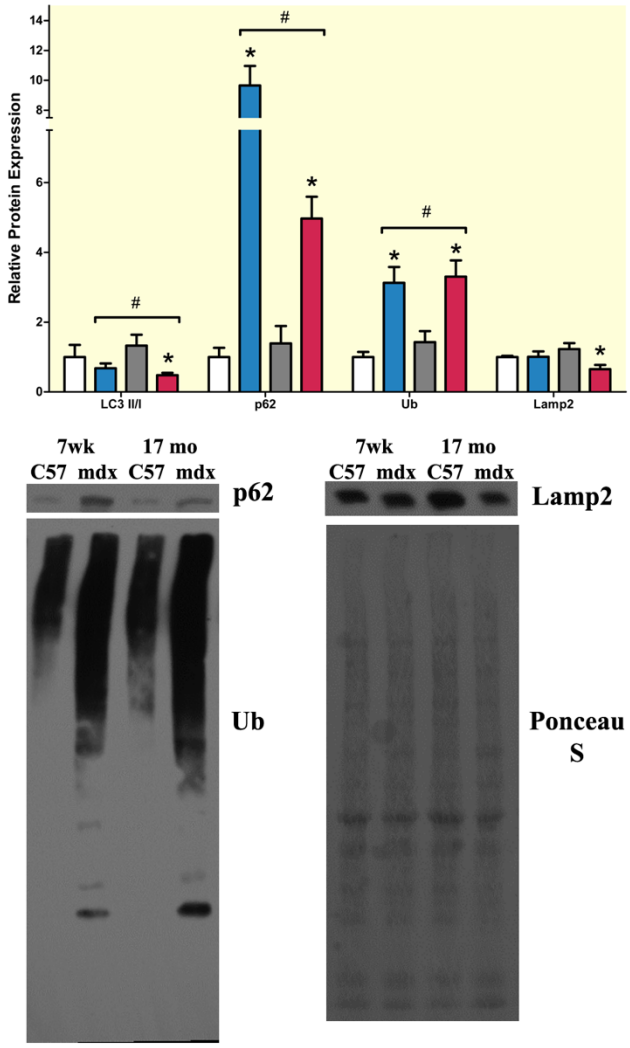

Figure 3. Autophagic degradation. Protein abundance measured by Western blot in 7 week and 17 month old dystrophic (mdx) and control (C57) diaphragms. Significance was established at $p<0.05$. White bars – C57 7 weeks (n=5), blue bars – mdx 7 weeks (n=8), gray bars – C57 17 months (n=4), red bars – mdx 17 months (n=10). * indicates significantly different from age-matched C57 controls, # indicates significant main effect of disease.

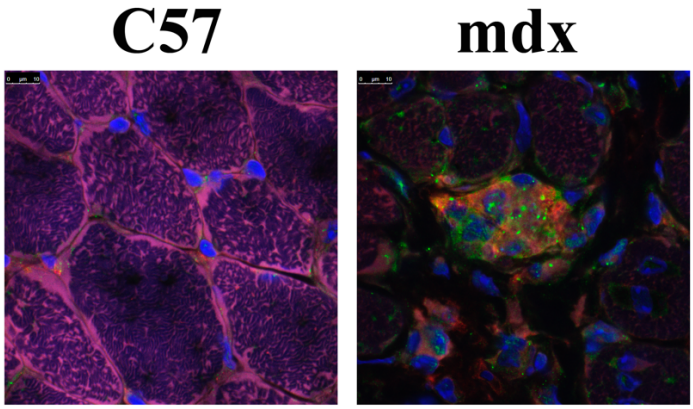

Figure 4. Autophagosome and lysosome colocalization. Confocal images at 63X magnification of DAPI (blue), p62 (green) and Lamp2 (red) from 14 mo old dystrophic and control mice diaphragms.

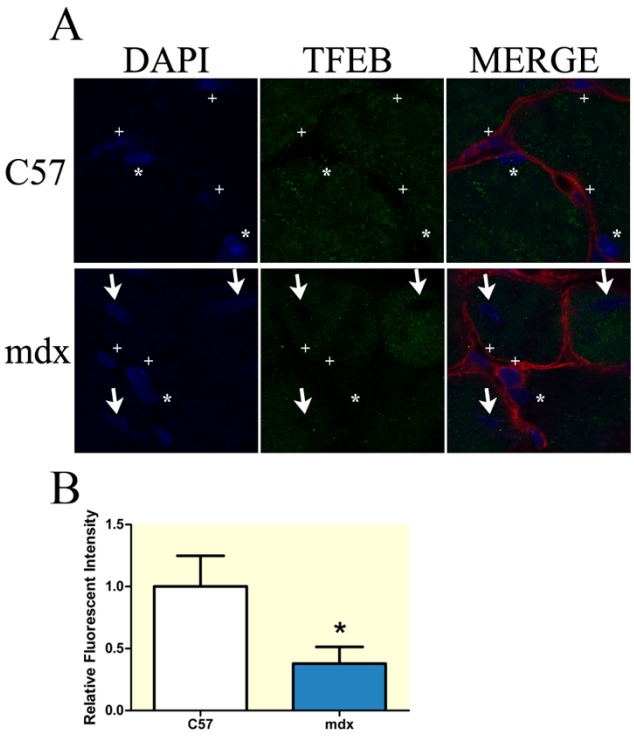

Figure 5. Confocal images of TFEB localization. A) 2X zoomed confocal images (63X images) of immunohistochemistry fluorescence of DAPI (blue), TFEB (green) and laminin (red) from 17 month old dystrophic (mdx) and control (C57) diaphragms. Arrows indicate centralized nuclei in which TFEB is excluded. * indicates peripheral nuclei, + indicates extra-muscular nuclei. B) Quantification of decreased TFEB fluorescent intensity within centralized nuclei of mdx mice compared to nuclei of C57 mice.

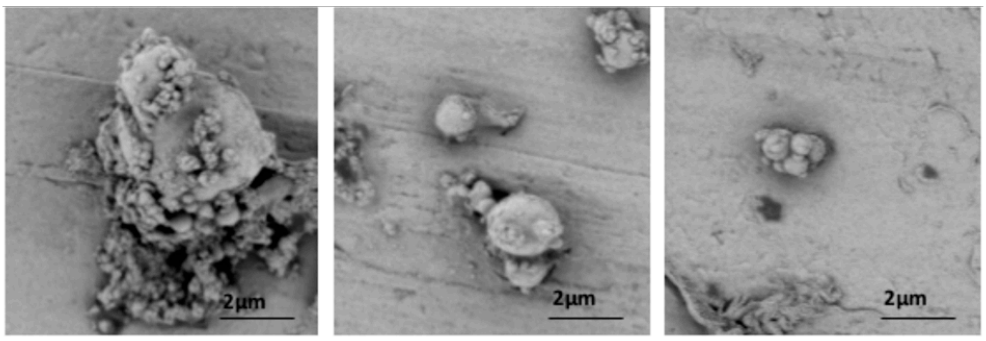

Figure 6. Scanning electron microscopy images of media from C2C12 myotubes demonstrating muscle cells release vesicles of differing size and morphology including round vesicles between 500-2000 nm, consistent with morphology and size of autophagosomes.

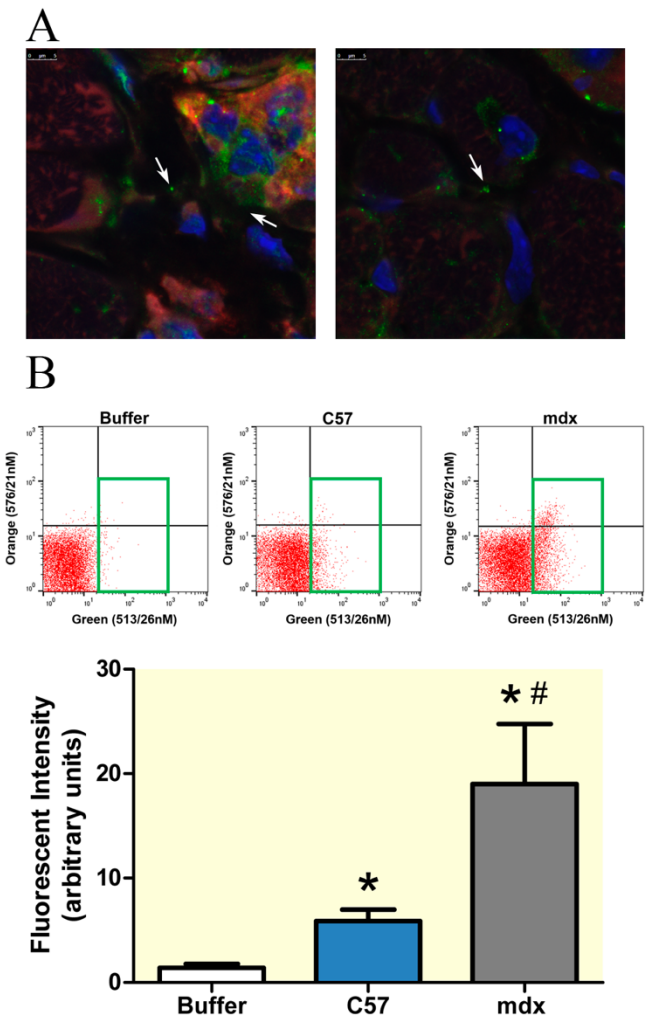

Figure 7. Autophagosome escape from dystrophic and healthy diaphragms. A) 5X zoomed confocal images (63X) of immunohistochemistry fluorescence of DAPI (blue),

p62 (green) and Lamp2 (red) from 14 months old dystrophic diaphragms. Arrows indicate p62 foci independent of Lamp2, which indicates autophagosomes are present in the extracellular space outside muscle cells. B) Autophagosomes were isolated from a bath of intact diaphragms, *ex vivo*, and quantified by flow cytometry. These data verify autophagosomes are released from both healthy and dystrophic diaphragms, with a greater amount of autophagosomes released from dystrophic muscle.

CHAPTER 7: PGC-1α OVEREXPRESSION INCREASED TRANSCRIPTION FACTOR EB NUCLEAR LOCALIZATION AND LYSOSOME ABUNDANCE IN DYSTROPHIC SKELETAL MSUCLE

Hannah R. Spaulding[1], Amanda K. Ludwig[2], Katrin Hollinger[1], Matthew B. Hudson[3], and Joshua T. Selsby[1]

[1]Department of Animal Science, Iowa State University, Ames, IA 50011

[2]Department of Biological Sciences, Purdue University, West Lafayette, IN 47906

[3]Department of Kinesiology and Applied Physiology, University of Delaware, Newark, DE, 19713

Modified from a manuscript in review at

American Journal of Physiology - Regulatory, Integrative and Comparative Physiology

Abstract

Duchenne muscular dystrophy (DMD) is caused by the absence of functional dystrophin protein and results in progressive muscle wasting. Dystrophin deficiency leads to a host of dysfunctional cellular processes including impaired autophagy. Autophagic dysfunction appears to be due, at least in part, to decreased lysosomal abundance mediated by decreased nuclear localization of transcription factor EB (TFEB), a transcription factor responsible for lysosomal biogenesis, among other functions. PGC-1α overexpression decreased disease severity in dystrophin-deficient skeletal muscle and increased PGC-1α has been linked to TFEB activation in healthy muscle. The purpose of this study was to determine the extent to which PGC-1α overexpression increased nuclear

TFEB localization, increased lysosome abundance, and increased autophagosome degradation. We hypothesized that overexpression of PGC-1α would drive TFEB nuclear translocation, increase lysosome biogenesis, and improve autophagosome degradation. To address this hypothesis, we delivered PGC-1α via adeno-associated virus (AAV) vector injected into the right limb of 3-week-old mdx mice and the contralateral limbs received a sham injection. We demonstrated that at 6 weeks of age our approach increased PGC-1α gene expression by 60-fold. This increased TFEB nuclear localization in gastrocnemii from PGC-1α treated limbs by 2-fold compared to contralateral controls. Furthermore, lamp2, a marker of lysosome abundance, was significantly elevated in the muscles from limbs overexpressing PGC-1α. Lastly, increased LC3II and similar p62 in PGC-1α overexpressing-limbs compared to contralateral limbs is supportive of increased degradation of autophagosomes. These data provide mechanistic insight into PGC-1α-mediated benefits to dystrophin-deficient muscle, such that increased TFEB nuclear localization in dystrophin-deficient muscle leads to increased lysosome biogenesis and autophagy.

Introduction

Duchenne muscular dystrophy (DMD) is a devastating muscle wasting disease affecting 1:3,500-5,000 boys (12). This progressive disease is typically diagnosed from 3-5 years of age due to muscle weakness and locomotor dysfunction, advances to wheelchair dependence for mobility by their early teens and culminates in death by cardiac or respiratory failure in their mid to late twenties. DMD is caused by the absence of functional dystrophin protein and results in various cellular dysfunctions such as membrane instability, mitochondrial dysfunction, oxidative stress, calcium mishandling,

and dysregulation of autophagy (1, 2, 5, 8, 18, 28). Autophagy is a process by which cellular components tagged for degradation are collected within autophagosomes, then fused with lysosomes to degrade the autophagosome cargo (16, 22). In dystrophin-deficient skeletal muscle, autophagosome degradation is blunted, resulting in autophagosome accumulation and subsequent escape of autophagosomes into the extracellular space (28). In this same study, lysosome abundance was decreased in dystrophin-deficient skeletal muscle (28), therefore, it seems likely that reduced lysosomal abundance, at least in part, contributes to blunted degradation of autophagosomes.

Lysosome biogenesis is regulated by transcription factor EB (TFEB) (23, 26), which is translocated to the nucleus to promote transcription of lysosomal and autophagy related genes. Nuclear TFEB localization is regulated by phosphorylation in which dephosphorylation of TFEB by calcineurin at Ser142 (15) promotes nuclear translocation. Conversely, phosphorylation by mammalian target of rapamycin (mTOR), protein kinase B (AKT), or extracellular signal-regulated protein kinase (ERK1/2) sequesters TFEB in the cytosol (14, 19, 26). We have previously demonstrated that TFEB nuclear localization is decreased in dystrophin-deficient muscle compared to healthy muscle (28). In healthy muscle TFEB abundance was decreased in peroxisome proliferator-activated receptor-gamma coactivator 1-alpha (PGC-1α) knockout mice (6, 29); conversely, TFEB nuclear localization and transcription were increased with exercise suggesting a PGC-1α-dependent mechanism and indicative of a relationship between PGC-1α and TFEB (6). We and others have previously found that PGC-1α overexpression decreased disease-related injury though protection was largely attributed to increased utrophin expression

associated with a type I fiber shift. The extent to which PGC-1α may also increase TFEB nuclear localization, lysosomal content, and degradation of autophagosomes has not been previously considered in this context. Given that PGC-1α plays a role in TFEB regulation and localization, we hypothesized that overexpression of PGC-1α would increase TFEB nuclear localization and ultimately increase lysosome abundance and restore autophagosome degradation in dystrophin-deficient skeletal muscle.

Methods

Animal Treatment. The Institutional Animal Care and Use Committee at Iowa State University approved all procedures. A detailed description of animal treatments and a demonstration of PGC-1α-mediated rescue of dystrophic soleus muscles has been previously published (10). Briefly, at three-weeks of age, $1x10^{11}$ genome copies of an adeno-associated viral (AAV; serotype 6) vector driving expression of PGC-1α were injected into the right triceps surae group of male and female mdx mice in a single 50 µl dose, while the contralateral limb was injected with an empty capsid (sham) (n=8 mice/group). We have previously used this vector to demonstrate disease prevention and rescue (10, 11, 25). At 6 weeks of age, we sacrificed mice by cervical dislocation and the gastrocnemii were harvested. Gastrocnemii designated for western blotting and qPCR were flash frozen in liquid nitrogen, and gastrocnemii for immunofluorescence were frozen in isopentane and embedded in optimal cutting temperature compound (OCT). Data from these mice have been previously published establishing PGC-1α-mediated histological rescue of treated muscle (10).

qPCR. Quantitative PCR was used to confirm PGC-1α overexpression and was done as previously described (24). Briefly, gastrocnemii were powdered on dry ice and

RNA was extracted using TriZol (15596018, ThermoScientific) and RNeasy purification kit (Qiagen) according to manufacturer instructions. cDNA was reverse transcribed using QuantiTect Reverse Transcriptase Kit (205310, Qiagen), as described by the manufactures except random hexamers (51-0118-01, IDT Premade Primers) were used instead of the RT primer mix provided (Qiagen). The *Ppargc1a* (Pgc-1α) primer set was as follows: Forward – 5'atgtgtcgccttcttgctct-3' Reverse – 5'-atctactgcctggggacctt-3'. *Ppargc1a* was normalized to *18s* (Forward – 5'-ctctagataacctcgggccg-3' Reverse – 5'-gtcgggagtgggtaatttgc-3'). Delta (Δ) CT values were calculated by subtracting the 18s CT value from Ppargc1a CT value. These values were used for statistical comparisons. ΔΔCT was calculated by subtraction of the ΔCT of each sample from the average ΔCT of the mdx-control samples. Data are presented as a fold-change as calculated from ΔΔCT.

Western Blot. Western blotting was performed as previously described (27). Briefly, whole homogenate, nuclear protein fractions and cytoplasmic protein fractions were extracted from powdered gastrocnemius muscles. Total protein was extracted using lysis buffer (1% Triton-x-100, 50mM HEPESS, 150mM NaCl, 10% Glycerol, 50mM NaF, 2mM EDTA, 0.1% SDS, pH 7.5). Additionally, the nuclear protein fraction was separated from the cytoplasmic fraction using a NE-PER™ Nuclear and Cytoplasmic Extraction Reagents (78833, ThermoScientific). Total, nuclear and cytoplasmic protein abundances were measured by Pierce BCA Protein Assay Kit (23225, ThermoScientific) and diluted in 2X Laemmli buffer (161-0737, Bio-Rad). Protein was loaded into 4-20% gels (58545, Lonza), separated by gel electrophoresis and transferred to a nitrocellulose membrane (1620112, Bio-Rad). Membranes were treated with ponceau S (PS) solution to verify equal loading. Membranes were washed in 1X tris buffered saline with 0.2%

Tween20 (1X TBST) and blocked with 5% milk in 1X TBST for 1 hour. Primary antibody was applied to the membrane and rocked overnight at 4ºC. Once primary antibody was removed, the membrane was washed in 1X TBST for 10 minutes, three times. Following washes, anti-rabbit IgG HRP-linked secondary antibody (7074, Cell Signaling) or anti-rat IgG HRP-linked secondary antibody (7077, Cell Signaling) were applied to the membrane for 1 hour at room temperature. After 1 hour the membrane was washed again for 10 minutes, three times. Lastly, Clarity™ Western enhanced chemiluminescence (1705060S, Bio-Rad) was applied to the membrane for 7 minutes, then developed in a dark room. Films were imaged, and protein bands were quantified using densitometry software (Carestream). The primary antibodies used in this study are listed in Table 1.

Immunofluorescence. We performed immunofluorescence as previously described (28). Briefly, muscle sections were blocked for 45 minutes in blocking solution (5% goat serum, 5% bovine serum albumin, 1% DMSO in 2X PBS). We applied primary antibody to the slides and placed the slides at 4ºC overnight, then washed the slides for 10 minutes in 1X phosphate buffered saline (PBS) three times. Corresponding secondary antibody was applied to sections for 1 hour at room temperature in the dark (anti-rabbit IgG AlexaFluor 488 [Cell Signaling, 4412] or goat anti-rat IgG rhodamine conjugated [Thermo Scientific, 31680]) and then slides were washed in 1X PBS for 10 minutes, three times. Finally, sections were treated with SlowFade™ Gold Antifade Mountant with DAPI (S36938, ThermoScientific) and sealed with nail polish. Primary and secondary dilutions can be found in Table 1. Sections were imaged on a QICAM 12-bit Mono Fast

1394 Cooled (QIC-F-M-12-C, QIMAGING) camera attached to a Leica microscope at 40x, and confocal images were taken at 63x on a similar Leica microscope.

Statistics. Data were statistically assessed by paired t-test (PRISM). Data are reported as mean ± SEM. We consider p-values less than or equal to 0.05 to be significant.

Results

PGC-1α overexpression increased nuclear TFEB abundance. Overexpression of *Ppargc1a*, the gene encoding PGC-1α, was confirmed using qPCR (Figure 1). Consistent with our previous experiments (10, 11, 25), *Ppargc1a* was increased approximate 60-fold. Of note, the 60-fold elevation observed in this investigation was greater than the 10-fold elevation observed in soleus muscles obtained from the same mice. It is likely that the differing fiber types of the muscles or that the gastrocnemius likely received a greater content of the injected volume (and hence, viral particles) likely contributed to this difference. PGC-1α gene transfer resulted in an approximate 6 mg reduction ($p<0.05$) in muscle mass compared to control (Control - ~103 ± 4; PGC-1α – 97 ± 4 mg), which we previously reported (10). To assess the effect of PGC-1α overexpression on TFEB abundance, TFEB protein abundance was measured in whole homogenate by Western blot. Total TFEB abundance was similar between groups (Figure 2A). To determine the effect of PGC-1α gene transfer on TFEB nuclear localization, TFEB protein abundance was assessed in nuclear protein fractions. PGC-1α overexpression increased nuclear TFEB abundance 2.2-fold compared to untreated limbs (Figure 2A). In confirmatory experiments using an immunofluorescent approach it was visually apparent that total TFEB was similar between groups, which was further supported by objective

quantification of total fluorescence (Figure 2B&C). Subjective evaluation of confocal images were supportive of nuclear translocation of TFEB in PGC-1α overexpressing limbs compared to contralateral controls (Figure 2D).

PGC-1α overexpression increased lysosome abundance and markers of autophagosome degradation. Given that nuclear TFEB was elevated following PGC-1α overexpression and that TFEB is a transcription factor that promotes lysosomal biogenesis, we next evaluated the effect of PGC-1α gene transfer on lysosome abundance. Using an immunofluorescent approach we discovered that lamp2, a lysosomal marker, was increased by 30% (Figure 3A&B) in PGC-1α overexpressing limbs compared to control limbs. These findings were confirmed by Western blot from whole homogenate (Figure 3C). As our working model is that degradation of autophagosomes in dystrophin-deficient muscle is blunted, as least in part, due to a lysosomal insufficiency we further investigated the effect of increased lysosome abundance on markers of autophagy (Figure 4). Markers of autophagic activation, ULK and pULK (S555), and beclin-1, a marker of autophagosome nucleation, were similar between mdx-PGC-1α and mdx-control muscles. Despite similar total beclin-1 protein abundance in mdx-control compared to mdx-PGC-1α, p-beclin-1 (S93) was numerically increased compared to mdx-control ($p=0.18$). Interestingly, PI3K CIII, a protein involved in autophagosome initiation, was similar between mdx-control and mdx-PGC-1α. Conversely, Atg5/12 was increased numerically ($p=0.16$) but failed to reach significance due to high variability. A marker of autophagosome formation, LC3II, was elevated with PGC-1α overexpression, while p62, a marker of autophagosome degradation was similar between groups. Hence, elevated autophagosome formation paired with similar p62

abundance suggests increased degradation of autophagosomes following PGC-1α overexpression.

Discussion

Duchenne muscular dystrophy is a severe muscle wasting disease in which a host of cellular pathways are altered secondary to a dystrophin protein deficiency. We and others have recently established that autophagic dysfunction is included in the disease sequelae (2, 5, 18, 28). More specifically, our data indicate lysosome abundance is decreased and autophagosome degradation is impaired in dystrophin-deficient skeletal muscle (28). Previous evidence demonstrates that PGC-1α overexpression decreased disease-related injury and preserved muscle function using both prevention and rescue strategies (4, 9, 10, 25). Emerging evidence points to a PGC-1α-mediated activation of TFEB (6) while others have demonstrated a relationship between TFEB and lysosome biogenesis and autophagy (23, 26). We previously established that TFEB nuclear localization is decreased in dystrophin-deficient skeletal muscle as was lysosomal abundance suggesting that decreased lysosomal content is due, at least in part, to dysregulation of TFEB (28). Further, as we and others have demonstrated decreased degradation of autophagosomes in dystrophin-deficient muscle, this dysregulation of TFEB and subsequent blunting of lysosomal content may contribute to impaired degradation of autophagosomes in dystrophin-deficient muscle Given this, we hypothesized that PGC-1α overexpression in dystrophic muscle would drive TFEB nuclear translocation leading to increased lysosome abundance and increased degradation of autophagosomes (28).

While the underlying mechanism governing the relationship between PGC-1α and TFEB is currently unknown, PGC-1α appears to regulate expression of TFEB. For example, PGC-1α overexpression or PGC-1α knockout in healthy muscle results in a parallel effect on TFEB, such that PGC-1α overexpression increased TFEB protein abundance (29) and knockout decreased TFEB transcript and protein abundance (6, 13, 29). Given the relationship between PGC-1α and TFEB and that our previous work hinted of a PGC-1α-mediated change in autophagy (10), continued study of tissues from 3 week old mdx mice treated with PGC-1α provided an opportunity for a probative study regarding TFEB and autophagy in dystrophin-deficient muscle. Contrary to our expectations, in this investigation following 3 weeks of PGC-1α overexpression total TFEB abundance was similar between groups, however, nuclear TFEB was increased by PGC-1α gene transfer. These data indicate regulation of TFEB abundance and/or activity by PGC-1α is more complex than simple transcriptional regulation and likely includes indirect regulation via post-translational modification via a yet-to-be appreciated mechanism(s). Speculatively, as mTOR activity is known to be increased in dystrophin-deficient muscle (18) and that phosphorylation of TFEB by mTOR, AKT or ERK1/2 leads to nuclear exclusion (17, 20, 26), mTOR-mediated inhibition of TFEB and subsequently decreased lysosomal content seems likely. In support of this notion, PGC-1α-mediated inhibition of mTOR signaling has recently been demonstrated (3) providing a plausible and testable mechanism for PGC-1α-mediated regulation of TFEB localization.

PGC-1α overexpression has been known for some time to preserve muscle function and decrease histopathological injury in dystrophin-deficient muscle using

prevention and rescue paradigms (9-11, 25). In addition to histological and functional protection in the dystrophin-deficient soleus, PGC-1α overexpression also altered gene expression suggestive of increased autophagy in the same animals used herein (10). In the present investigation evaluating the gastrocnemius, our data suggest increased autophagosome formation following PGC-1α overexpression (increased LC3II) and increased degradation (similar p62). It seems likely this increased degradation was facilitated by increased lysosomal abundance. Further, given the relationship between PGC-1α and TFEB as well as the role of TFEB in autophagy that mitophagy would also be improved following PGC-1α overexpression. While mitophagy and mitochondrial biogenesis/content was beyond the scope of this investigation, in a previous study using these animals, PGC-1α overexpression numerically increased transcript abundance of BNIP3, a protein which promotes mitophagy, by 50% (10). Similarly, mice treated with AICAR, which stimulates AMPK and ultimately PGC-1α, also increased BNIP3 protein abundance in dystrophin deficient skeletal muscle (21) supporting the notion that PGC-1α overexpression may stimulate mitophagy.

Perspectives and Significance

These data indicate that PGC-1α increased nuclear TFEB localization, lysosomal abundance, and degradation of autophagosomes. We speculate that increased PGC-1α caused, directly or indirectly, increased nuclear TFEB translocation, which in turn, increased lysosome abundance, which allowed for greater degradation of autophagosomes. We temper our conclusions within the limitations of a probative study employing archived samples and encourage future investigations specifically intended to address questions raised herein. In addition to the role of TFEB-mediated elevations in

lysosome abundance, it is important to note that degradation of autophagosomes may be impacted by lysosome function (7) and/or capacity for colocalization due to cytoskeletal derangement or impaired fusion. How these factors may interact and be altered by dystrophin deficiency remains largely unknown.

References

1. **Alderton JM and Steinhardt RA.** Calcium influx through calcium leak channels is responsible for the elevated levels of calcium-dependent proteolysis in dystrophic myotubes. *J Biol Chem* 275: 9452-9460, 2000.

2. **Bibee KP, Cheng YJ, Ching JK, Marsh JN, Li AJ, Keeling RM, Connolly AM, Golumbek PT, Myerson JW, Hu G, Chen J, Shannon WD, Lanza GM, Weihl CC, and Wickline SA.** Rapamycin nanoparticles target defective autophagy in muscular dystrophy to enhance both strength and cardiac function. *Faseb j* 28: 2047-2061, 2014.

3. **Brown EL, Foletta VC, Wright CR, Sepulveda PV, Konstantopoulos N, Sanigorski A, Della Gatta P, Cameron-Smith D, Kralli A, and Russell AP.** PGC-1α and PGC-1β Increase Protein Synthesis via ERRα in C2C12 Myotubes. *Frontiers in physiology* 9, 2018.

4. **Chan MC, Rowe GC, Raghuram S, Patten IS, Farrell C, and Arany Z.** Post-natal induction of PGC-1alpha protects against severe muscle dystrophy independently of utrophin. *Skelet Muscle* 4: 2, 2014.

5. **De Palma C, Morisi F, Cheli S, Pambianco S, Cappello V, Vezzoli M, Rovere-Querini P, Moggio M, Ripolone M, Francolini M, Sandri M, and Clementi E.** Autophagy as a new therapeutic target in Duchenne muscular dystrophy. *Cell Death Dis* 3: e418, 2012.

6. **Erlich AT, Brownlee DM, Beyfuss K, and Hood DA.** Exercise induces TFEB expression and activity in skeletal muscle in a PGC-1alpha-dependent manner. *Am J Physiol Cell Physiol* 314: C62-c72, 2018.

7. **Gelman BB, Davis MH, Morris RE, and Gruenstein E.** Structural changes in lysosomes from cultured human fibroblasts in Duchenne's muscular dystrophy. *J Cell Biol* 88: 329-337, 1981.

8. **Godin R, Daussin F, Matecki S, Li T, Petrof BJ, and Burelle Y.** Peroxisome proliferator-activated receptor γ coactivator 1-α gene transfer restores mitochondrial biomass and improves mitochondrial calcium handling in post-necrotic mdx mouse skeletal muscle. *J Physiol* 590: 5487-5502, 2012.

9. **Handschin C, Kobayashi YM, Chin S, Seale P, Campbell KP, and Spiegelman BM.** PGC-1alpha regulates the neuromuscular junction program and ameliorates Duchenne muscular dystrophy. *Genes Dev* 21: 770-783, 2007.

10. **Hollinger K, Gardan-Salmon D, Santana C, Rice D, Snella E, and Selsby JT.** Rescue of dystrophic skeletal muscle by PGC-1 alpha involves restored expression of dystrophin-associated protein complex components and satellite cell signaling. *American Journal of Physiology-Regulatory Integrative and Comparative Physiology* 305: R13-R23, 2013.

11. **Hollinger K and Selsby JT.** PGC-1alpha gene transfer improves muscle function in dystrophic muscle following prolonged disease progress. *Exp Physiol* 100: 1145-1158, 2015.

12. **Mah JK, Korngut L, Dykeman J, Day L, Pringsheim T, and Jette N.** A systematic review and meta-analysis on the epidemiology of Duchenne and Becker muscular dystrophy. *Neuromuscul Disord* 24: 482-491, 2014.

13. **Mansueto G, Armani A, Viscomi C, D'Orsi L, De Cegli R, Polishchuk EV, Lamperti C, Di Meo I, Romanello V, Marchet S, Saha PK, Zong H, Blaauw B, Solagna F, Tezze C, Grumati P, Bonaldo P, Pessin JE, Zeviani M, Sandri M, and Ballabio A.** Transcription Factor EB Controls Metabolic Flexibility during Exercise. *Cell Metab* 25: 182-196, 2017.

14. **Martina JA, Chen Y, Gucek M, and Puertollano R.** MTORC1 functions as a transcriptional regulator of autophagy by preventing nuclear transport of TFEB. *Autophagy* 8: 903-914, 2012.

15. **Medina DL, Paola SD, Peluso I, Armani A, Stefani DD, Venditti R, Montefusco S, Scotto-Rosato A, Prezioso C, Forrester A, Settembre C, Wang W, Gao Q, Xu H, Sandri M, Rizzuto R, Matteis MAD, and Ballabio A.** Lysosomal calcium signalling regulates autophagy through calcineurin and TFEB. *Nature Cell Biology* 17: 288-299, 2015.

16. **Mizushima N, Ohsumi Y, and Yoshimori T.** Autophagosome formation in mammalian cells. *Cell Struct Funct* 27: 421-429, 2002.

17. **Napolitano G, Esposito A, Choi H, Matarese M, Benedetti V, Di Malta C, Monfregola J, Medina DL, Lippincott-Schwartz J, and Ballabio A.** mTOR-dependent phosphorylation controls TFEB nuclear export. *Nat Commun* 9: 3312, 2018.

18. **Pal R, Palmieri M, Loehr JA, Li S, Abo-Zahrah R, Monroe TO, Thakur PB, Sardiello M, and Rodney GG.** Src-dependent impairment of autophagy by oxidative stress in a mouse model of Duchenne muscular dystrophy. *Nature communications* 5: 4425, 2014.

19. **Palmieri M, Pal R, Nelvagal HR, Lotfi P, Stinnett GR, Seymour ML, Chaudhury A, Bajaj L, Bondar VV, Bremner L, Saleem U, Tse DY, Sanagasetti D, Wu SM, Neilson JR, Pereira FA, Pautler RG, Rodney GG, Cooper JD, and Sardiello M.** mTORC1-independent TFEB activation via Akt inhibition promotes cellular clearance in neurodegenerative storage diseases. *Nat Commun* 8: 14338, 2017.

20. **Palmieri M, Pal R, and Sardiello M.** AKT modulates the autophagy-lysosome pathway via TFEB. In: *Cell Cycle*, 2017, p. 1237-1238.

21. **Pauly M, Daussin F, Burelle Y, Li T, Godin R, Fauconnier J, Koechlin-Ramonatxo C, Hugon G, Lacampagne A, Coisy-Quivy M, Liang F, Hussain S, Matecki S, and Petrof BJ.** AMPK activation stimulates autophagy and ameliorates muscular dystrophy in the mdx mouse diaphragm. *Am J Pathol* 181: 583-592, 2012.

22. **Ryter SW, Cloonan SM, and Choi AM.** Autophagy: a critical regulator of cellular metabolism and homeostasis. *Mol Cells* 36: 7-16, 2013.

23. **Sardiello M, Palmieri M, di Ronza A, Medina DL, Valenza M, Gennarino VA, Di Malta C, Donaudy F, Embrione V, Polishchuk RS, Banfi S, Parenti G, Cattaneo E, and Ballabio A.** A gene network regulating lysosomal biogenesis and function. *Science* 325: 473-477, 2009.

24. **Selsby JT, Ballmann CG, Spaulding HR, Ross JW, and Quindry JC.** Oral quercetin administration transiently protects respiratory function in dystrophin-deficient mice. *J Physiol* 594: 6037-6053, 2016.

25. **Selsby JT, Morine KJ, Pendrak K, Barton ER, and Sweeney HL.** Rescue of dystrophic skeletal muscle by PGC-1alpha involves a fast to slow fiber type shift in the mdx mouse. *PloS one* 7: e30063, 2012.

26. **Settembre C, Di Malta C, Polito VA, Garcia Arencibia M, Vetrini F, Erdin S, Erdin SU, Huynh T, Medina D, Colella P, Sardiello M, Rubinsztein DC, and Ballabio A.** TFEB links autophagy to lysosomal biogenesis. *Science* 332: 1429-1433, 2011.

27. **Spaulding HR, Ballmann CG, Quindry JC, and Selsby JT.** Long-Term Quercetin Dietary Enrichment Partially Protects Dystrophic Skeletal Muscle. *PLoS One* 11: e0168293, 2016.

28. **Spaulding HR, Kelly EM, Quindry JC, Sheffield JB, Hudson MB, and Selsby JT.** Autophagic dysfunction and autophagosome escape in the mdx mus musculus model of Duchenne muscular dystrophy. *Acta Physiol (Oxf)* 222, 2018.

29. **Vainshtein A, Desjardins EM, Armani A, Sandri M, and Hood DA.** PGC-1alpha modulates denervation-induced mitophagy in skeletal muscle. *Skelet Muscle* 5: 9, 2015.

Acknowledgments

Ryan's Quest, Michael's Cause and Project Parent Muscular Dystrophy partially supported HRS, American Physiological Society (UGSRF) supported AKL and NIH 5P20GM113125-03 partially supported MBH.

Figures and Tables

Table 1. Western blot and immunofluorescence antibody details including protein name, primary and secondary dilations, and product number. Secondary antibodies used were specific to the primary antibody host species, which is also indicated in this table alongside the product number. Secondary antibody details can be found in the methods section.

Western blot antibodies			
Protein	**Primary dilution**	**Secondary dilution**	**Company & Product number (host)**
autophagy related (ATG) 5/12	1:1000 1X TBST	1:2000 1X TBST	Cell Signaling 4180 (rabbit)
beclin-1	1:500 5% milk	1:2000 5% milk	Cell Signaling 3495 (rabbit)
phospho (p) beclin-1 (Ser93)	1:1000 5% milk	1:1000 1X TBST	Cell Signaling 14717 (rabbit)
light chain 3 (LC3)	1:500 5% milk	1:2000 5% milk	Cell Signaling 12741 (rabbit)
lysosomal associated membrane protein 2 (lamp2)	1:1000 1X TBST	1:2000 5% milk	Abcam ab13524 (rat)
phosphoinositide 3 kinases (PI3K) class III	1:1000 5% milk	1:2000 5% milk	Cell Signaling 3358 (rabbit)

Western blot antibodies			
Protein	**Primary dilution**	**Secondary dilution**	**Company & Product number (host)**
sequestosome 1 (SQSTM1, p62)	1:500 5% milk	1:1000 5% milk	Abcam ab109012 (rabbit)
transcription factor EB (TFEB)	1:1000 1% milk	1:1000 1X TBST	Bethyl Laboratories A303-673A-M (rabbit)
Unc-51 like autophagy activating kinase 1 (ULK)	1:1000 1X TBST	1:2000 1X TBST	Cell Signaling 8054 (rabbit)
p-ULK (Ser555)	1:500 1X TBST	1:1000 1X TBST	Cell Signaling 5869 (rabbit)
Immunofluorescence antibodies			
Protein	**Primary dilution**	**Secondary dilution**	**Company & Product number (host)**
laminin beta-1	1:100 5% BSA	1:200 5% BSA	ThermoFisher MA5-14657 (rat)
lysosomal associated membrane protein 2 (lamp2)	1:100 5% BSA	1:100 5% BSA	Abcam ab13524 (rat)
transcription factor EB (TFEB)	1:50 5% BSA	1:500 5% BSA	Bethyl Laboratories A303-673A-M (rabbit)

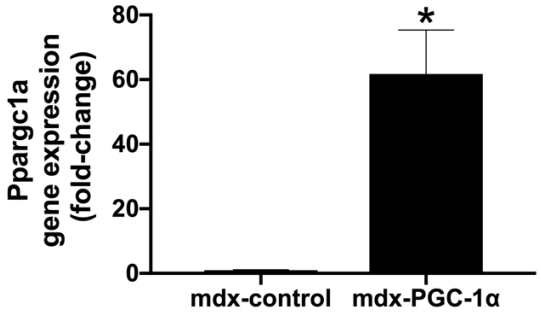

Figure 1. PPARGC1A gene expression increased following AAV injection. PPARGC1A transcript abundance was normalized to 18S and confirmed overexpression of PPARGC1A, which encodes for PGC-1α, in AAV treated gastrocnemii (n=8/group), * = significantly different from mdx-control by paired sample t-test, $p < 0.05$.

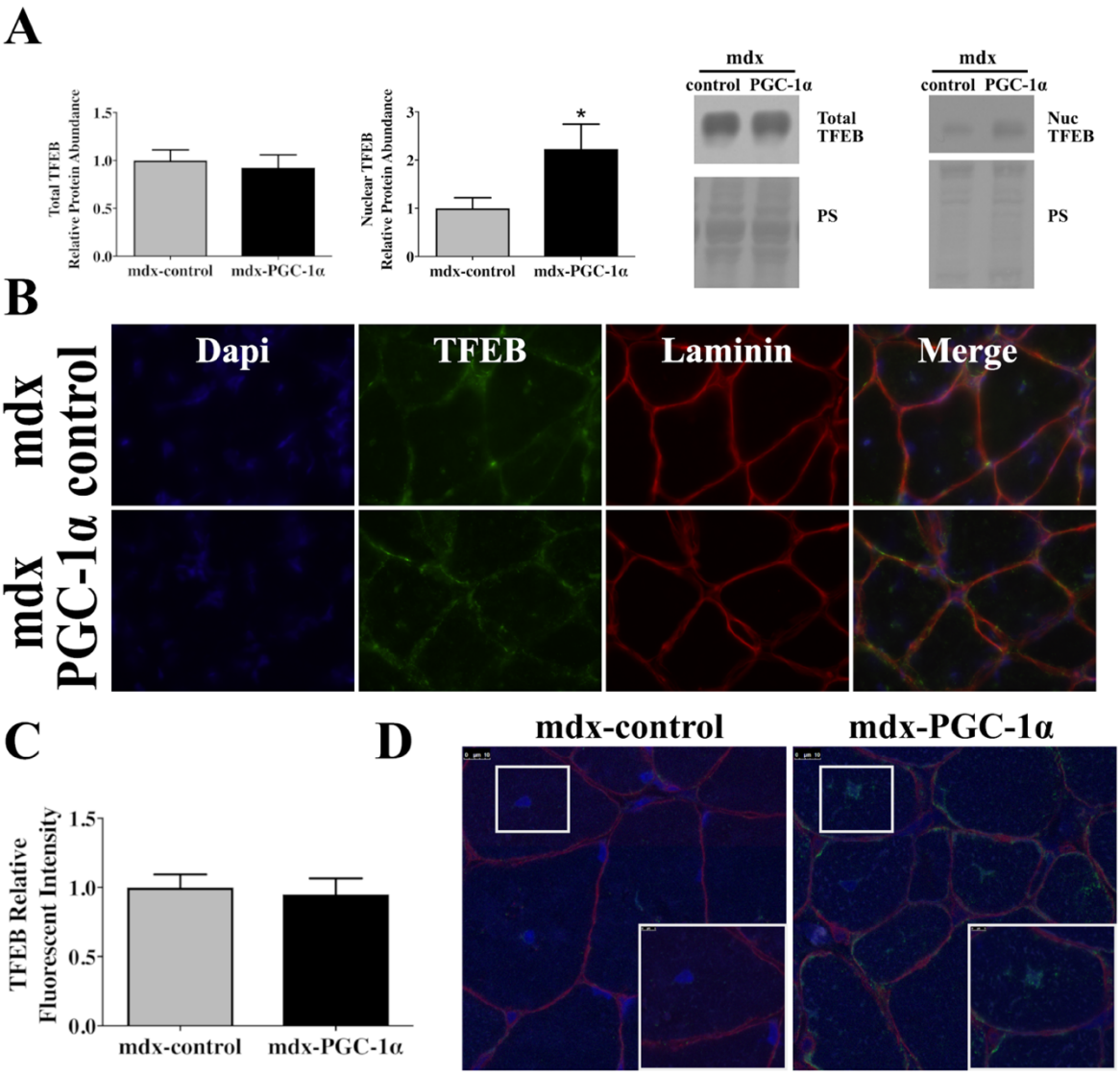

Figure 2. PGC-1α overexpression increased nuclear TFEB. A) Total TFEB protein abundance was similar between groups regardless of treatment, (n=6/group). Nuclear TFEB abundance significantly increased with PGC-1α overexpression, (n=6/group). Ponceau stain (PS) was used as a total protein loading control. B) mdx-control and mdx-PGC-1α overexpressing gastrocnemii were probed for TFEB (green), membrane marker, Laminin (red), and nuclei (dapi, blue) using immunofluorescence. C) Immuno-fluorescence quantification confirms that total TFEB abundance was similar between mdx-control and mdx-PGC-1α, (n=5/group) E) Representative confocal images from C at 63X with 5x zoomed insets showing the increased nuclear localization of TFEB with PGC-1α overexpression. * = significantly different from mdx-control by paired sample t-test, $p<0.05$.

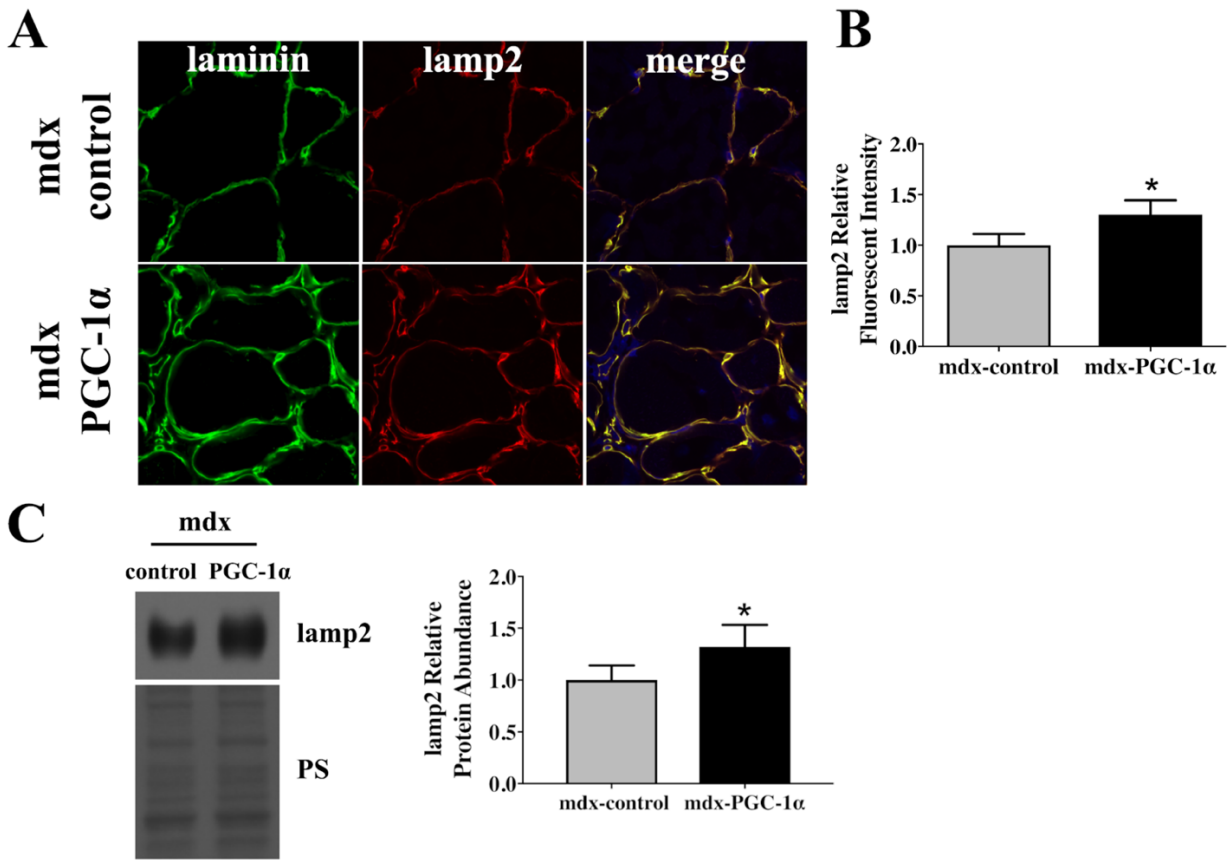

Figure 3. PGC-1α overexpression increased lysosome abundance. A) Mdx-control and mdx-PGC-1α gastrocnemii were probed for lysosome marker, lamp2 (red), using immunofluorescence and nuclei (dapi, blue). B) Quantification of lamp2 (red) fluorescent intensity, (n=5/group). C) Increased lamp2 was confirmed by Western blot, (n=6/group). Ponceau stain (PS) was used as a total protein loading control. * = significantly different from mdx-control by paired sample t-test, $p<0.05$.

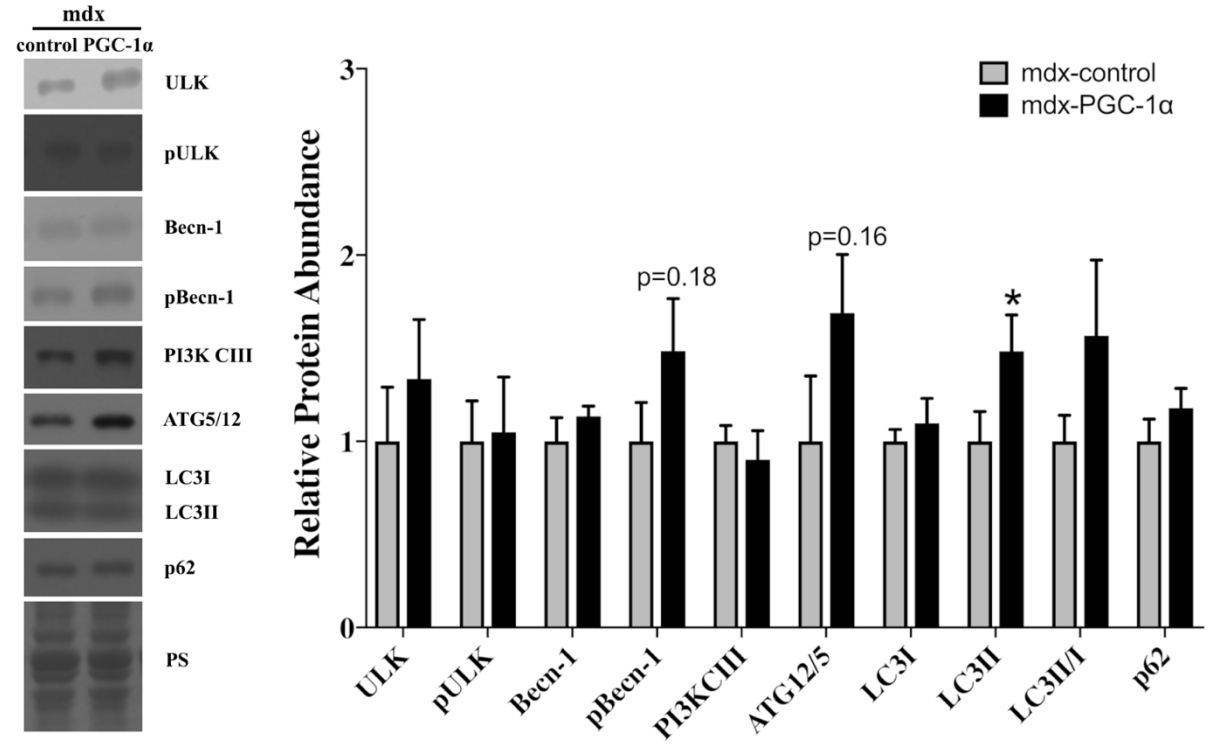

Figure 4. PGC-1α overexpression increased autophagosome degradation. Markers of autophagy related proteins were largely unchanged with PGC-1α overexpression. However, these data suggest increased autophagosome degradation due to increased LC3II with PGC-1α overexpression and similar p62, an inverse correlate of autophagosome degradation. (n=6/group). Ponceau stain (PS) was used as a total protein loading control. * = significantly different from mdx-control by paired sample t-test, $p<0.05$.

CHAPTER 8: GENERAL CONCLUSION

Duchenne muscular dystrophy is a progressive muscle wasting disease for which there is no cure and for which few pharmacological interventions are available. While development of therapeutics to replace dystrophin is ongoing, patients are in need of immediate interventions. In healthy populations, exercise has been shown to alleviate a variety of dystrophin-associated symptoms (2), but the use of traditional exercise is controversial for DMD patients (14). Therefore, exercise mimetics may be a safer means by which to acquire exercise benefits without the detrimental effects of traditional exercise in those with DMD. Previously it has been demonstrated that transcriptional coactivator, PGC-1α, can induce these positive exercise effects in dystrophic muscle (3, 8, 12). In a preliminary study, quercetin, a natural flavonoid which can drive PGC-1α through SIRT1, attenuated disease severity. This suggested that quercetin and quercetin base-cocktails may be therapeutic for DMD patients (10). Our research investigated the extent to which FDA-approved pharmaceuticals and nutraceuticals mitigate disease pathology. Additionally, we probed autophagy to determine the extent to which the autophagy pathway might be manipulated as a therapeutic target for DMD and subsequently the effect of PGC-1α overexpression on autophagy in dystrophic muscle.

In chapter 2, we evaluated the extent to which quercetin attenuated loss of muscle function and reduced muscle damage after 12 months of treatment. Due to the longevity of the disease and need for long-term treatment, our goal was to determine the efficacy of quercetin treatment on dystrophin-deficient skeletal muscle over time. Contrary to our hypothesis, we found that 12 months of quercetin treatment did not preserve muscle function or prevent muscle damage (13). In a companion study from these same animals,

quercetin failed to improve diaphragm function or mitigate muscle damage, but transiently protected respiratory function for 6 months (11). In this same study, SIRT1 deacetylation activity, as measured by abundance of acetylated histone 3 lysine 9, was similar between treated and untreated. Given that SIRT1 is a NAD+ dependent deacetylase and that NAD+ abundance is reduced in dystrophin-deficient skeletal muscle, we hypothesized that supplementation with nicotinamide riboside (NR), an NAD+ precursor, would enhance long-term efficacy of quercetin. Therefore, in chapters 3 and 4, we determined the extent to which quercetin, NR, Lisinopril and prednisolone alone and in combination protected dystrophic muscle. Once again, quercetin did not preserve respiratory function, muscle function, or prevent injury. Similarly, these quercetin-based cocktails did not improve these parameters, suggesting that quercetin is not a suitable therapy for DMD.

When evaluating these quercetin-based cocktails, we utilized an emerging model of DMD, the D2-mdx mice, instead of conventional mdx mice. D2-mdx mice present a more severe phenotype of DMD with increased inflammation and more muscle damage than mdx mice (4). Though a more severe model of DMD is necessary to properly assess potential therapeutics, the D2-mdx mouse may be too severe. For example, at 8 weeks of age, Evan's blue dye uptake was increased in D2-mdx mice compared to both DBA and mdx mice, suggestive of increased muscle fiber damage at 8 weeks. Grip strength was also reduced in D2-mdx mice compared to mdx mice at 9-11 weeks and 22-24 weeks of age (6), likely due to increased muscle damage and subsequent decreased abundance of muscle fibers (6). Furthermore, the self-renewal efficiency of DBA mice was decreased compared to C57, likely contributing to the severity of the D2-mdx model (6). Together,

these data suggest that the D2-mdx model has increased muscle injury, decreased muscle fiber abundance and decreased regenerative efficiency, reducing the viable fibers in which therapeutics can be successful and decreasing regenerative capacity.

Despite the inability of quercetin and these quercetin-cocktails to reduce disease severity, we established in chapter 6 that PGC-1α can improve autophagosome degradation in dystrophic muscle by increasing myonuclear localization of TFEB and the subsequent elevation in lysosome abundance. Before overexpressing PGC-1α in dystrophic muscle, we established that autophagy was impaired in dystrophic skeletal muscle prior to degradation of the autophagosome (chapter 5). This impaired autophagosome degradation could be due to decreased lysosome abundance, an inability of lysosomes and autophagosomes to fuse properly, decreased lysosome function, or a combination of these things. As demonstrated in chapter 6 and its companion study (8), PGC-1α can preserve muscle function, increase TFEB myonuclear localization and ultimately increase autophagosome degradation, improving the impaired pathway.

The precise relationship between PGC-1α and TFEB is unclear. Using PGC-1α knockout and TFEB overexpression models, Erlich et al. (5) identified that TFEB overexpression increased PGC-1α abundance and PGC-1 knockout reduced TFEB abundance. Further exploration of this relationship would be beneficial to the understanding these potential therapeutic targets but given what is currently known about PGC-1α and TFEB, it possible that stimulation of TFEB would result in increased lysosome biogenesis, increased autophagosome degradation and also increased PGC-1α activity. This resulting PGC-1α activity would provide additional therapeutic benefits for

dystrophic muscle, such as increased mitochondrial biogenesis and increased utrophin abundance to protect the sarcolemma (7-9, 12).

Independent of PGC-1α, we discovered that healthy and dystrophic skeletal muscle release autophagosome into the extracellular space, albeit more abundantly in dystrophic muscle. Given the discrepancy between abundance of autophagosomes released from dystrophic and healthy skeletal muscle, the mechanism and purpose of autophagosome release may be of interest. The release of autophagosomes may be a means by which cells can remove excess autophagosomes. Alternatively, the release of autophagosomes may allow autophagosomes, like exosomes (1), to play a role in cell-to-cell communication or endocrine signaling.

In summary, DMD patients are still in need of immediate therapeutic interventions. Quercetin and quercetin-based cocktails failed to attenuate disease pathology in long-term studies, suggesting that these quercetin-based therapies should not be further investigated for DMD. However, increased abundance and activity of PGC-1α continues to show therapeutic promise. In this investigation, we demonstrated that PGC-1α overexpression increased autophagosomes degradation, which was impaired in dystrophic muscle. Additionally, PGC-1α overexpression increased TFEB myonuclear localization, likely contributing to increased lysosome biogenesis and autophagosome degradation. Together, these data suggest that PGC-1α is still a promising therapeutic target and TFEB should be further investigated within the context of DMD.

References

1. **Bang C, and Thum T**. Exosomes: new players in cell-cell communication. *Int J Biochem Cell Biol* 44: 2060-2064, 2012.

2. **Blair SN, Kohl HW, Gordon NF, and Paffenbarger RS, Jr.** How much physical activity is good for health? *Annu Rev Public Health* 13: 99-126, 1992.

3. **Chan MC, Rowe GC, Raghuram S, Patten IS, Farrell C, and Arany Z**. Post-natal induction of PGC-1alpha protects against severe muscle dystrophy independently of utrophin. *Skelet Muscle* 4: 2, 2014.

4. **Coley WD, Bogdanik L, Vila MC, Yu Q, Van Der Meulen JH, Rayavarapu S, Novak JS, Nearing M, Quinn JL, Saunders A, Dolan C, Andrews W, Lammert C, Austin A, Partridge TA, Cox GA, Lutz C, and Nagaraju K**. Effect of genetic background on the dystrophic phenotype in mdx mice. In: *Hum Mol Genet*2016, p. 130-145.

5. **Erlich AT, Brownlee DM, Beyfuss K, and Hood DA**. Exercise induces TFEB expression and activity in skeletal muscle in a PGC-1alpha-dependent manner. *Am J Physiol Cell Physiol* 314: C62-c72, 2018.

6. **Fukada S, Morikawa D, Yamamoto Y, Yoshida T, Sumie N, Yamaguchi M, Ito T, Miyagoe-Suzuki Y, Takeda S, Tsujikawa K, and Yamamoto H**. Genetic background affects properties of satellite cells and mdx phenotypes. *Am J Pathol* 176: 2414-2424, 2010.

7. **Handschin C, Kobayashi YM, Chin S, Seale P, Campbell KP, and Spiegelman BM**. PGC-1alpha regulates the neuromuscular junction program and ameliorates Duchenne muscular dystrophy. *Genes Dev* 21: 770-783, 2007.

8. **Hollinger K, Gardan-Salmon D, Santana C, Rice D, Snella E, and Selsby JT**. Rescue of dystrophic skeletal muscle by PGC-1 alpha involves restored expression of dystrophin-associated protein complex components and satellite cell signaling. *American Journal of Physiology-Regulatory Integrative and Comparative Physiology* 305: R13-R23, 2013.

9. **Hollinger K, and Selsby JT**. PGC-1alpha gene transfer improves muscle function in dystrophic muscle following prolonged disease progress. *Exp Physiol* 100: 1145-1158, 2015.

10. **Hollinger K, Shanely RA, Quindry JC, and Selsby JT**. Long-term quercetin dietary enrichment decreases muscle injury in mdx mice. *Clin Nutr* 34: 515-522, 2015.

11. **Selsby JT, Ballmann CG, Spaulding HR, Ross JW, and Quindry JC**. Oral quercetin administration transiently protects respiratory function in dystrophin-deficient mice. *J Physiol* 594: 6037-6053, 2016.

12. **Selsby JT, Morine KJ, Pendrak K, Barton ER, and Sweeney HL**. Rescue of dystrophic skeletal muscle by PGC-1alpha involves a fast to slow fiber type shift in the mdx mouse. *PLoS One* 7: e30063, 2012.

13. **Spaulding HR, Ballmann CG, Quindry JC, and Selsby JT**. Long-term quercetin dietary enrichment partially protects dystrophic skeletal muscle. *PLoS One* 11: e0168293, 2016.

14. **Spaulding HR, and Selsby JT**. Is exercise the right nedicine for dystrophic muscle? *Med Sci Sports Exerc* 50: 1723-1732, 2018.